

Characterization of the functional and signaling properties of the Intracellular domain of the NG2 proteoglycan

Dissertation zur Erlangung des Grades
Doktor der Naturwissenschaften

am Fachbereich Biologie
der Johannes Gutenberg-Universität Mainz

von
Tanmoyita Nayak
geboren am 17.10.1990 in Kalkutta, Indien

Mainz, 30.10.2018

Table of content

Summary.....	1
List of figures.....	2-3
List of tables.....	4
Abbreviations.....	5-6
1. Introduction	
1.1 Cell types in CNS.....	7
1.2. History of Glia cells.....	7
1.3. Development and types of Glia cells.....	8-9
1.4. Origin and development of NG2-Glia cells	10-15
1.4.1 Development of NG2+ OPCs.....	11-12
1.4.2 Specification of OPCs into matured OLs.....	12-14
1.4.3 Expression of NG2 outside CNS.....	14-15
1.5. Role of glia cells in neuronal synapses.....	15-19
1.5.1. Role of glia in synaptic function.....	16
1.5.2. Role of Neuron-OPC synapse.....	16
1.5.3. Role Astrocytes in neuronal synapse.....	16-17
1.5.4. Role of Microglia in neuronal synapse.....	17
1.5.5. Role of Oligodendroglia and Schwann cells in synapse.....	18-19
1.5.6. Activity-dependent local translation and myelination.....	19
1.6. Cellular functions of NG2 protein	20-23
1.6.1. Role of NG2 in modulating neuronal network.....	20-21
1.6.2. Cell motility.....	21-22
1.6.3. Cell proliferation and survival.....	22
1.6.4. Cytoskeleton reorganization	22-23
1.6.5. Role of NG2 in Glioma.....	23
1.7. Regulated Intramembrane Proteolysis (RIP).....	24

1.7.1. Mechanism of regulated intramembrane proteolysis (RIP).....	24-25
1.7.2. Activity-dependent RIP of neuronal proteins.....	25
1.7.3. Cleavage of NG2	25-28
1.7.4. Structure and function of NG2 ICD.....	28-29
2. Aim of the study.....	30
3. Materials and Methods	
3.1. Equipment and reagents.....	31-38
3.1.1. Equipment.....	32
3.1.2. Materials.....	33-34
3.1.3. Reagents.....	34-36
3.1.4. Antibodies.....	37
3.1.5. Software.....	38
3.2. Cell Biology.....	38-41
3.2.1. Cell culture	
3.2.1.1. Oli- <i>neu</i> Cell Culture.....	38
3.2.1.2. HEK 293T Cell Culture.....	39
3.2.1.3. Primary OPC isolation and maintenance.....	39
3.2.2. Transfection methods	
3.2.2.1. FuGene HD transfection of plasmid DNA.....	39
3.2.2.2. PEI transfection.....	39-40
3.2.2.3. Bio-Rad GenePulser Electroporation.....	40
3.2.2.4. Amaxa Nucleofection of siRNA	40
3.2.3. FACS.....	40-41
3.3. Molecular Biology	
3.3.1. DNA analysis and manipulation.....	42-45
3.3.1.1. Polymerase chain reaction (PCR).....	42-43
3.3.1.2. DNA purification and analysis	43
3.3.1.3. Agarose gel electrophoresis.....	43
3.3.1.4. DNA extraction from agarose gel.....	43

3.3.1.5. Restriction enzyme digestion.....	44
3.3.1.6. Ligation and transformation	44
3.3.1.7. Plasmid preparation.....	44-45
3.3.2. RNA Analysis	
3.3.2.1. Isolation of total RNA from cultured cells	46
3.3.2.2. Reverse transcription cDNA Synthesis	46
3.3.2.3. Quantitative PCR (qPCR).....	47
3.3.2.4. mRNA stability assay.....	47-48
3.4. Protein Biochemistry	
3.4.1. Cell lysis.....	48
3.4.2. SDS-PAGE and Western Blotting.....	48-49
3.4.3. Silver and Coomassie staining of the gel.....	49
3.4.4. Immunoprecipitation (IP).....	50
3.4.5. SUnSET Assay.....	50
3.5. Immunocytochemistry.....	50-51
3.6. Proteomics.....	51-53
3.6.1. Mass Spectrometry based analysis.....	51
3.6.2. Experimental design for Pulsed-SILAC analysis.....	51-53
3.7. Statistical Analysis.....	53
4. Results	
4.1. Subcellular Localization of cleaved NG2 ICD.....	54-60
4.1.1. Generation and functional analysis of NG2 expression constructs.....	55-57
4.1.2. Detection of localization of NG2 ICD by subcellular fractionation assay.....	57-58
4.1.3. Detection of localization of NG2 ICD by confocal microscopy.....	58-60
4.2. Characterization of ICD-interactome.....	61-66
4.2.1. Investigation of ICD-interactome by IP-MS study.....	61-62
4.2.2. Gene Ontology-based analysis of ICD-interactome.....	62-64
4.2.3. NG2 ICD co-precipitates with translation factors.....	65-66

4.3. Translational regulation by released NG2 ICD.....	66-77
4.3.1. NG2 ICD regulates translational rate in cultured cells.....	66-70
4.3.2. NG2 ICD increases translation by modulating mTOR signaling components.....	70-74
4.3.3. NG2 ICD modulates eef2/FMRP signaling pathway.....	74-77
4.4. Characterization of ICD-mediated newly synthesized proteome.....	78-82
4.4.1. pulsed SILAC based proteomic profiling after NG2 ICD overexpression.....	78-81
4.4.2 Validation of NG2 ICD-regulated candidates.....	81-82
4.5. NG2 ICD alters the cell-cycle kinetics.....	82-86
4.5.1. NG2 ICD increases cell population in S-phase.....	82-85
4.5.2. NG2 ICD overexpression is associated with changed nuclear morphology in OPCs.....	85-86
5. Discussion	
5.1. Sub-cellular localization of the NG2 ICD.....	88
5.2. NG2 ICD as a regulator of translation and cell-cycle progression	89-91
5.3. NG2 ICD regulates translation repressor FMRP.....	91-93
5.4. Role of FMRP/eEF2 in synaptic signaling and myelination.....	93-95
5.5. NG2 ICD upregulates proteins involved in differentiation and tumorigenesis.....	95-96
5.6. NG2 ICD signaling in tumours.....	96-97
5.7. Physiological impact of NG2 cleavage.....	97-98
5.8. Future directions.....	99
References	100-121
<u>Appendix</u>	
A. Acknowledgement.....	122-123
B. Curriculum vitae.....	124-125
C. Eidesstattliche Erklärung.....	126

Abstract

The NG2 proteoglycan is a molecular marker of oligodendrocyte precursor cells (OPCs) and is abundantly expressed by a variety of tumours. Published results show that NG2 influences proliferation, migration, and has neuromodulatory effects. Like other type-1 transmembrane proteins, NG2 is subjected to regulated intramembrane proteolysis (RIP), generating a large ectodomain, a C-terminal fragment (CTF) and an intracellular domain (ICD) by the sequential action of α - and γ -secretases. The cleavage of NG2 is constitutive and enhanced by neuronal activity. Functional roles of the NG2 protein domains have so far been shown for the full-length protein, the released ectodomain and CTF, but not for the ICD.

This study characterized the role of the NG2 ICD in a murine OPC cell line (Oli-neu), primary OPCs and human embryonic kidney (HEK) cells. It was found that the cleaved NG2 ICD has a predominantly cytosolic expression including the distal processes of OPCs. A small fraction of the protein exhibits a nuclear localization. Immunoprecipitation coupled with Mass Spectrometric analysis indicated that the NG2 ICD modulates mRNA translation and cell-cycle kinetics. Functional studies showed that ICD overexpression results in an upregulated translation of mRNAs as well as a shift of the cell population towards S-phase. NG2 ICD increases levels of the active (phosphorylated) form of mTOR and modulates downstream signaling cascades. These include increased phosphorylation of p70S6K1 and increased expression of eEF2. Strikingly, levels of FMRP, a translation repressor and RNA-binding protein that is regulated by mTOR/S6K1/eEF2 were decreased upon ICD overexpression. De novo proteomic profiling by pulsed-SILAC method after NG2 ICD overexpression revealed that proteins regulating DNA replication, cell differentiation and apoptosis were highly enriched in the NG2 ICD-overexpressing population.

This study establishes that the NG2 ICD, after release by cleavage, acts as a regulator of translation and cell cycle progression in OPCs by modulating the mTOR pathway, a known global translational regulator. It also influences levels of FMRP, a protein responding to network activity and a well-characterized repressor of translation. Findings from this study additionally help to explain why tumours exhibiting enhanced rates of translation and rapid cell cycle kinetics express high levels of NG2.

List of Figures

1. Introduction

Figure 1-1. Pictorial representation of different glia types in the nervous system.....
Figure 1-2. The lineage of NG2+ OPC.....
Figure 1-3. Summary of NG2 expression.....
Figure 1-4. Diagrammatic representation of an NG2+ OPC-Neuron synapse.....
Figure 1-5. Mechanistic principle of Regulated Intramembrane Proteolysis (RIP).....
Figure 1-6. Diagrammatic representation of NG2 protein.....
Figure 1-7. Schematic cartoon of the NG2 intracellular region.....

3. Materials and Methods

Figure 3-1. Gating strategy for cell-cycle distribution analysis.....
Figure 3-2. Diagrammatic representation of NG2 expression constructs used in the study.....
Figure 3-3. Mechanistic principle of conventional SILAC and pulsed SILAC.....

4. Result

Figure 4-1. General workflow for functional analysis of NG2 expression constructs.....
Figure 4-2. Diagram of used NG2 expression constructs and their expression.....
Figure 4-3. Sub-cellular fractionation assay.....
Figure 4-4. High-resolution imaging of NG2 expression constructs.....
Figure 4-5. Schematic representation of IP-MS workflow.....
Figure 4-6. Pathway analysis of the candidates regulated in NG2 ICD-IP samples.....
Figure 4-7. Validation of IP-MS targets by Co-Immunoprecipitation.....
Figure 4-8. Working principle for SUnSET techniques.....
Figure 4-9. NG2 ICD upregulates translation rate.....
Figure 4-10. Overview of the mTORC1 signaling cascade in translation regulation.....
Figure 4-11. NG2 ICD overexpression regulates mTORC1 signaling components.....

Figure 4-12. NG2 knockdown causes decreased phosphorylation of mTORC1 signaling components.....

Figure 4-13. Role of FMRP/eEF2K/eEF2 pathway in mGluR-LTD regulation.....

Figure 4-14. NG2 ICD regulates expression of eEF2 and FMRP.....

Figure 4-15. Schematic representation of the pSILAC workflow.....

Figure 4-16. Gene-ontology based analysis of pSILAC-MS candidates.....

Figure 4-17. Validation of pSILAC-enriched candidate.....

Figure 4-18. NG2 ICD shifts S-phase population in HEK cells.....

Figure 4-19. NG2 ICD overexpression increases PCNA+ cell numbers in Oli-neu cells.....

Figure 4-20. Altered nuclear morphology in ICD-overexpressing cells.....

5. Discussion

Figure 5-1. Role of mTOR signaling in controlling cellular growth.....

Figure 5-2. Crosstalk between FMRP and mTOR signaling pathways.....

Figure 5-3. Model depicting altered signaling pathways by cleaved NG2 ICD.....

Figure 5-4. Model depicting NG2 cleavage and functions of the cleaved NG2 products in OPC.....

List of tables

1. Introduction

Table 1. Glia cells at a glance.

Table 2. Proteolytic cleavage of neuronal type-1 membrane proteins.....

Table 3. The PDZ-binding partners of the NG2 protein.....

3. Materials and Methods

Table 4. Device and Equipment.....

Table 5. Chemicals and Reagents.....

Table 6. Buffers and Medium.....

Table 7. List of primary antibodies.....

Table 8. List of secondary antibodies.....

Table 9. List of used software.....

Table 10. List of primers and restriction sites used for PCR.....

Table 11. PCR Components.....

Table 12. PCR Cycler Program.....

Table 13. RT-PCR set up.....

Table 14. RT-PCR Program.....

Table 15. Taqman Gene expression assays.....

4. Results

Table 16. List of top 25 interaction partners of cleaved NG2 ICD found by IP-MS study.....

Table 17. List of enriched functional clusters of ICD-interactome.....

Table 18. Summarization of upregulated candidates obtained from pSILAC-MS analysis.....

List of Abbreviations

AMPA	α -amino-3-hydroxy-5-methyl-4-isoxazolepropionic acid receptor
ADAM	A disintegrins and metalloproteinase
ARC	Activity-regulated cytoskeleton-associated protein
BMP	bone morphogenetic protein
BACE	Beta-secretase
BAP	Bacterial alkaline phosphatase
CNS	Central nervous system
CoIP	Co-immunoprecipitation
CTF	C-terminal fragment
CNBP	Cellular nucleic acid-binding protein
CHK1	Cell cycle checkpoint homolog 1
CX3CR1	CX3C chemokine receptor 1
DAPI	4',6-diamidino-2-phenylindole
DBD	DNA-binding domain
ECM	Extracellular matrix
ERK	Extracellular signal-regulated kinase
FMRP	Fragile-X mental retardation protein
FXS	Fragile-X syndrome
GAT	Sodium- and chloride-dependent GABA transporter
GABA	Gamma-aminobutyric acid receptor
GLAST1	Sodium-dependent glutamate/aspartate transporter 1
GRIP	Glutamate receptor-interacting protein 1
GBM	Glioblastoma Multiforme
GTF II-I	General transcription factor II-I
H2B	Histone 2B
IEG	Immediate early genes
iCLiPs	Intramembrane Cleaving Proteases
IP-MS	Immunoprecipitation-Mass spectrometry
LTP	Long term potentiation
LTD	Long term depression
LNS	Laminin G-neurexin-sex hormone binding globulin
MAP1B	Microtubule-associated protein 1B
MEGF10	Multiple epidermal growth factor-like domains protein 10
MERTK	Tyrosine-protein kinase Mer
MELK	Maternal embryonic leucine zipper kinase
mRNP	Messenger ribonucleoprotein
MCM	Mini Chromosome maintenance

mTOR	Mammalian target of rapamycin
mGluR	Metabotropic glutamate receptor
MUPP1	Multiple pdz domain protein
MBP	Myelin Basic Protein
Myrf	Myelin regulatory factor
NMDA	N-methyl-D-aspartate
NPC	Neural precursor cells
NG2	Nerve/Glial antigen 2
OPC	Oligodendrocyte Precursor cells
OL	Oligodendrocyte
PDGFR α	Platelate derived growth factor receptor
PNS	Peripheral nervous system
PKC α	Protein kinase C
PSA-NCAM	Polysialylated-neural cell adhesion molecule
PTGDS	Prostaglandin-H2 D-isomerase synthase
PCR	Polymerase chain reaction
PHF5A	PHD finger-like domain-containing protein 5A
pSILAC	Pulsed SILAC
pMN	Motor neurons progenitor
PND	Postnatal day
Phldb1	Pleckstrin homology-like domain family B member 1
PLP	Proteolipid Protein
PSD95	Post synaptic density protein 95
RIP	Regulated Intramembrane Proteolysis
Sdcbp	Syntenin 1
SuNSET	Surface Sensing of translation
SPARC	Secreted protein, acidic and rich in cysteine
scRNA-Seq	Single-cell RNA sequencing
Shh	Sonic hedgehog
TMD	Transmembrane domain
TSP	Thrombospondin
TNF	Tumor necrosis factor
UTR	Untranslated region
VZ	Ventricular germinal zones
XRCC	X-ray repair cross-complementing protein

1. Introduction

1.1 Cell types in CNS

The central nervous system (CNS) is composed of neurons and glia cells that work together in a highly coordinated fashion to elicit a various neural response. Neurons are responsible for receiving, processing, integration and propagation of information via synapses. While neurons play the pivotal role as an information processor, glial cells have long been known for their role as a supporting system for neurons in the CNS. Their major functions discussed for quite a time involves providing protection, nutritional support, anchoring and facilitate neuronal conduction. However, detailed research on glial cells, especially in the last 20 years shed light on glial functions extending beyond a mere support system in CNS. These findings revealed that glial cells are essential for neuronal development, axon guidance, synaptic transmission, and neurotransmitter release. These cells are an essential part of the neuronal network and intriguing topic of neuro-research.

1.2. History of glia cells

The history of glia cells goes back to the mid-1800's where a pathologist, Rudolf Virchow, coined the term 'neuro-glia' in his book published in 1856 and the same year another eminent scientist, Henrich Müller, made the first drawings and description of glial cells (today known as Müller glia cells in the retina). In 1871, Camileo Golgi described oligodendrocytes and astrocytes in his book and in 1893, Michael Von Lenhossek coined the term for 'astrocytes' describing it as a star-shaped cell. Robert Remak first observed and described the 'medullated fibers' in PNS which were later termed as 'myelin' by Rudolf Virchow in 1854. Pio del Rio-Hortega, in 1919, separated two other cell types and named one as oligodendroglia (first described by Robertson, 1899) in 1921 and he also proposed that oligodendrocytes produce myelin, but this theory took a long time to be established and was fully accepted in 1962 after the published work of Richard Bunge where he showed by electron microscope pictures that oligodendrocytes produce myelin sheath and wrap axons.

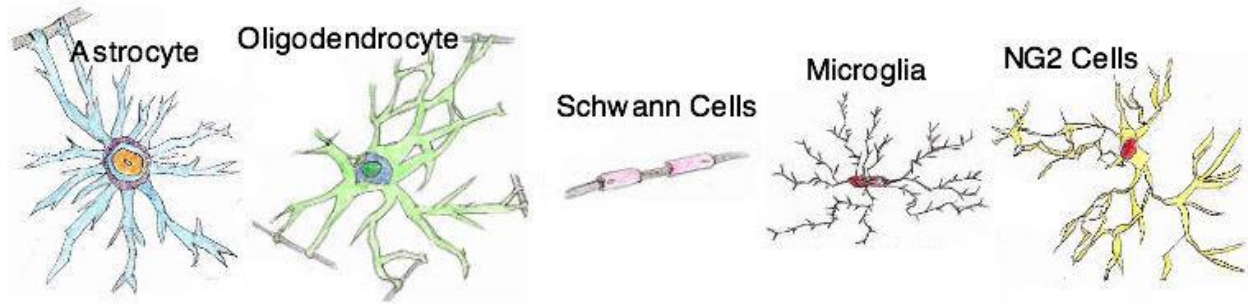


Fig.1.1. Pictorial representation of different glia types in the nervous system (Source: Google images).

1.3. Development of glia cells

Owing to their ‘stem-cell-like’ property, the development of glial cells itself is a fascinating topic. By using different models and *in vitro* systems, the origin of oligodendrocytes and Schwann cells can be traced, and other cell types also can be distinguished based on their molecular markers. Neuronal and glial cell types of the mature CNS originate initially from neural precursors (NPCs) in the embryonic neural tube. The differentiation of NPCs into neurons and glial cells is highly controlled in a spatiotemporal manner in response to surrounding signaling cues which includes soluble morphogens like Sonic hedgehog (Shh) and bone morphogenetic protein (BMP). After fate switching from NPCs to glia, different kinds of glial cells can be distinguished by their morphology and expression of molecular markers. The table below represents a summary of the origin, molecular marker and main functions of main glia types.

Table 1. Glia cells at a glance

Cell type	Developmental area and time point	Identifying markers	Main functions
<i>Astrocytes</i>	Neural Stem cells (NSCs) transitions from neurogenesis to gliogenesis in the Ventricular Zone (VZ), in the spinal cord, this switching happens at E12.5 and in the cortex at E16-18 in rodents.	Astrocyte Precursor Marker: Glast, FABP7, FGFR Mature Astrocyte Markers: GFAP, S100B, AldoC, Glt1	<ol style="list-style-type: none"> 1. Neurotransmitter release and clearance. 2. Shaping extracellular space surrounding neurons. 3. Pre and post-synaptic assembly of excitatory synapses during early postnatal development.
<i>Oligodendrocytes</i>	Detected in Sub-ventricular zone (SVZ) of the brain and spinal cord during mid-gestation in rodents.	OPC stage: NG2, PDGFR Mature OL: MBP, PLP, MAG.	<ol style="list-style-type: none"> 1. Myelination. 2. Neuronal protection. 3. Metabolic support to neurons
<i>Microglia</i>	Microglia, unlike other glia cells, are of myeloid origin, and they developed from yolk sac (YS) primitive macrophages during E7-E10.	TMEM119, Iba1	<ol style="list-style-type: none"> 1. Neuronal survival and death 2. Synaptogenesis and synapse pruning. 3. Cross-talk with the periphery.
<i>Schwann Cells</i>	Schwann cell precursors originate from neural crest at around E12-13 and subsequently produce immature Schwann cells at E16-18 in rodents.	Precursor stage: BFABP, Connexin 29, PMP22 Myelinating Schwann cells: S100, Sox 10, EGR2	<ol style="list-style-type: none"> 1. Myelination in PNS. 2. Response to nerve injury and maintenance. 3. Nerve fasciculation.

1.4. Lineage plasticity of NG2-glia cells

Nerve/Glial antigen 2 (NG2) is a member of the chondroitin sulfate proteoglycan family, and NG2+ glial cells are found in high abundance in both grey and white matter, comprising around 5-8% of the total population in CNS. (Pringle et al., 1992, Dawson, 2003). The history of NG2-Glia started nearly thirty years ago, when a group of neural progenitors cells, called O-2A progenitors, found to express prominent molecular markers, NG2 and PDGFR α . Developmentally, O-2A cells originate from the germinal ventricular zone of embryonic brain and spinal cord and later proliferate and migrate through developing CNS forming an even distribution throughout gray and white matter (Richardson et al., 2006, Miller, 1996). The progeny type of O-2A cells remained debatable for a decade where some research data revealed that besides producing a large pool of myelinating oligodendrocytes, they could also give rise to so-called type-2 astrocyte cells *in vitro* (Raff et al., 1983). Matthias et al., in 2003, by using a transgenic mouse model also showed the presence of two distinct cell populations where one was positive for both NG2 and S100 β (astrocytic marker) and the other was only positive for NG2 but not for S100 β , suggesting the existence of shared Oligodendrocyte/astrocyte lineage. It has been proposed and shown that during development the fate of NG2+ cells are not restricted to oligodendrocyte (OL) lineage, rather they contribute to 40% of protoplasmic astrocytes in the grey matter of the ventral forebrain (Zhu et al., 2008, 2011, Huang et al., 2014, Nishiyama et al., 2014), although this astrogliogenic property of NG2+ cells is lost shortly after birth.

There are also evidences that reactive astrocytes at sites of CNS injury are generated by the NG2+ cells (Leoni et al., 2009, Alonso et al., 2005), although Tripathi et al., in 2010, in their EAE model of demyelinating disease, showed that in adult mouse spinal cord, NG2+ cells generate a major population of oligodendrocyte (OL) lineage cells, including mature and differentiated OLs, with a very few astrocytes or neurons. There are also some publications reporting that NG2+ cells can generate a fewer numbers of neurons during adulthood (Rivers et al., 2008, Guo et al., 2010, Robins et al., 2013),

although this topic remains highly controversial as other reports provide no evidence for neurogenesis from NG2+ glia cells (Dimou et al., 2008, Zhu et al., 2011).

The ambiguous nature of the experimental data to prove that NG2+ glia can give rise to both oligodendrocytes and astrocytes, put a question on the terminology of 'O-2A' cells which gradually replaced by the name of Oligodendrocyte Precursor cells or OPCs as these cells are, so far, the exclusive and well-established source of mature OLs generation. OPCs can be distinguished from the other glial cell types by the expression of molecular markers PDGFR-alpha and NG2.

The major distinguishable features of NG2+ OPCs lie in their ability to maintain a resident population of undifferentiated cells by self-renewal while continuously producing mature oligodendrocytes throughout adulthood. However, OPC proliferation and differentiation are different in the grey and white matter, where white matter NG2+ OPCs show a stronger proliferative response to PDGF-AA than those in grey matter (Hill et al., 2013). Another intriguing characteristic of OPCs which separates them from astrocytes is their robust migratory nature which involves both radial and tangential migration (Tsai et al., 2012, Bayraktar et al., 2015). Moreover, NG2+ OPCs have been shown to form a synapse with neurons and serve as a post-synaptic compartment which makes them exclusive in this context (Bergles et al., 2010, Sakry et al., 2014, reviewed in Steinhäuser and Dietrich, 2015). As NG2+ OPCs are endowed with a distinct molecular pattern and functional properties, they are postulated as the fourth glia cell type in the CNS.

1.4.1 Development of NG2+ OPC

Oligodendrocytes (OL), the myelin-producing cells of the Central Nervous System (CNS), develop from Oligodendrocyte precursor cells (OPCs). NG2+ OPCs are also known as polydendrocytes because of their branched morphology. The intriguing features of OPCs are that they retain self-renewing capability and can differentiate into OLs in the adult CNS. These features allow them to regenerate myelin by producing myelin-forming mature OLs in the case of age-dependent and injury-related myelin loss.

OPCs are identifiable in CNS by the markers NG2 and PDGFR-alpha. Neural precursors that produce oligodendrocyte lineage cells are first detected by E12-14 in rodents by the expression of PDGFR mRNA (Pringles et al., 1992, Pringles and Richardson, 1993) in ventricular germinal zones (VZ) in the brain and spinal cord. The position of OPCs corresponds to motor neurons progenitor (pMN) domain, which just before OPC production, give rise to motor neurons (Rivers et al., 2008, Richardson et al., 1997). After their appearance, the ventrally derived OPCs proliferate and migrate to populate other CNS regions so that by E17, there is even distribution of NG2+ PDGFR+ cells throughout spinal cord, hindbrain and basal forebrain (Nishiyama et al, 1996).

After the first wave of OPC production from the pMN domain in VZ, a second wave produce more OPCs in the dorsal cord at around E15.5 in mice. Dorsally derived OPCs do not migrate as much as ventrally derived ones and they comprise approximately 20% of total OPC population.

At around E18.5 in mice, some OPCs in the spinal cord start differentiating into mature OLs with an expression of Myelin Basic Protein (MBP) and Proteolipid Protein (PLP). They first appear in developing white matter where they start myelinating surrounding axons and OL production reaches its peak ~2-4 week postnatal in mice throughout the white and grey matter.

1.4.2 Specification of OPC into matured OLs

Differentiation of OPCs into matured OLs is tightly controlled by a milieu of transcription factors and diffusible morphogens. In the precursor of Motor Neurons (pMN) domain, the specification of OPCs is triggered by Sonic Hedgehog (Shh) signal which acts via the downstream mediator Gli proteins, which in turn, activate lineage-determining genes. Shh also collaborates with Notch pathway which plays a key role in neuron-glia fate switching; activated notch promotes neurogenesis over gliogenesis during the first wave of OPC production in pMN domain.

Development of the OLs also depends on Sox transcription factors. While Sox9 promotes oligodendrocyte specification, Sox10 regulates terminal differentiation of OLs. Sox10-deficient neural stem cells cannot produce myelin when transplanted into a wild-

type host establishing a direct cell-autonomous role of Sox10 for myelin production (Stolt et al., 2004, Woodruff et al., 2001).

The most important and well-studied transcription factors for OPC differentiation are the Olig genes. Shh activates the transcription factor, Olig2, which is an absolute requirement for the sequential production of motor neurons and OPCs from the pMN domain (Lu et al., 2002, Zhou and Anderson, 2002). Olig1 is structurally very similar to Olig2 and expressed coordinately, but studies found that it is not required for OPC specification in the spinal cord and is not expressed until ~E18.5 in mice (Fu et al., 2009).

Olig2 and Sox10 share a common target to drive the expression of another transcription factor called myelin regulatory factor (*Myrf*), which is strongly induced during the early onset of OL differentiation (Hornig et al., 2013) and promotes OL maturation and myelination (Review by Ben Emery and Q. Richard Lu., 2015, Emery et al., 2009, Bujalka et al., 2013). Recently, another less well-known transcription factor YY1 came out to be one of the regulators of OPC specification. Reduced YY1 causes arrested OPC specification and halted maturation. (He et al., 2007).

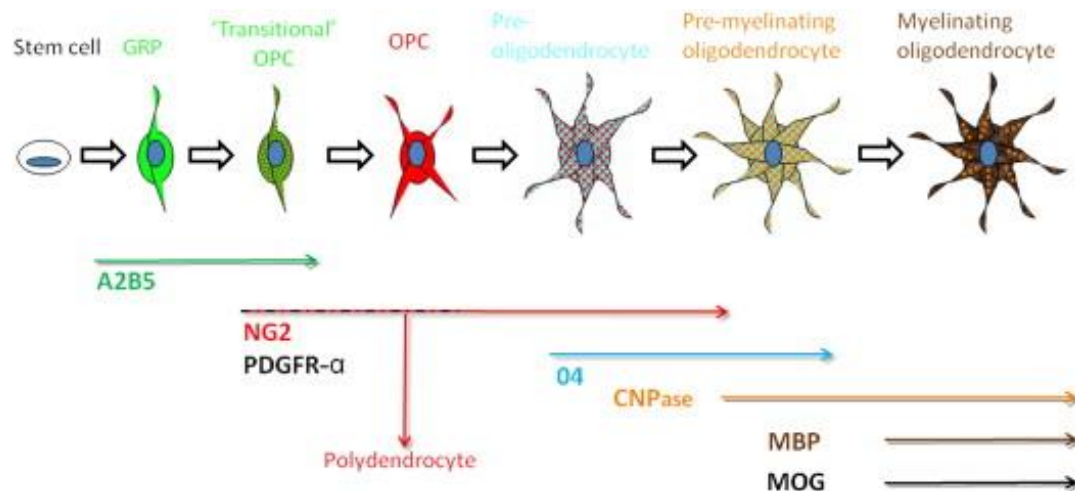


Fig 1.2. The lineage of NG2+ OPCs (Taken from Girolamo et al., 2011)

As OPCs start to differentiate into matured OLs, they gradually lose the expression of NG2+ PDGFR+ antigenic profile and enter an intermediate pro-oligodendrocyte stage which is recognized by O4-immunoreactivity (Sommer and Schachner, 1981, Bansal and Pfeiffer, 1989). The gradual progression of NG2+ PDGFR+ to NG2+O4+ and finally to O4+MBP+ stage takes around P9-P20 in mice (Polito A and Reynolds R, 2005). Mallon et al. (2002) using a transgenic mouse model where the EGFP protein was expressed under the PLP promoter, proposed that there is two distinct types of NG2+ cells during the development of the neocortex where one population was NG2+/EGFP+, and another one was NG2+/EGFP-. The advent of single-cell RNA sequencing (scRNA-Seq) now present a solid platform to trace OL-lineage cells and subtypes in an extensive manner and already provides information on the heterogeneity of OL cells in a spatiotemporal manner (Bruggen et al., 2017, Marques et al., 2017).

1.4.3 Expression of NG2 outside CNS

Although NG2 was originally described and most-discussed in the context of CNS, the protein is also expressed by other various cell-types, mostly those in a precursor state. In the developing rodent limb, NG2 is expressed by immature chondroblasts (Nishiyama et al., 1991, Fukushi et al., 2003) and a similar pattern of NG2 appearance and disappearance was detected in osteoblast to osteocyte transition in maturing bone (Fukushi et al., 2003).

Keratinocyte stem cells produce keratinocyte precursor cells which also express NG2+, and they have a range of progenies (Legg et al., 2003, Ghali et al., 2004, Kadoya et al., 2008). NG2 expression is also prominent and well-established in the developing vascular system. Beside cardiomyocytes expressing NG2, smooth muscle cells in the macrovasculature and pericytes in the microvasculature express NG2 (Grako et al., 1995, Schlingemann et al., 1991, Ozerdem et al., 2002).



Fig.1.3. Summary of NG2 expression (Credit: Human Protein Atlas)

1.5. Role of glia cells in neuronal synapses

The primary place of intercellular information flow in the nervous system occurs at the junctions between neurons, known as synapses. Till the end of the 1990s, synapses were envisioned as a two-compartment system (classical bi-partite synapse), composed of one pre-synaptic element releasing neurotransmitters in the synaptic cleft and one post-synaptic element receiving the information through activation of invariant number and type of receptors. (Choquet et al., 2013). However, last 20 years of research tells

us a different story with the concept of emerging and well-established participation of glia cells in synaptic functions.

1.5.1. Role of glia in synaptic functions

Extensive recent studies on the role of glia cells in synaptic biology revealed that glia could modulate neuronal synapse formation, synaptic strength and the removal of synapses (e.g., by synaptic pruning), challenging the common notion that synapses are solely modulated by neurons and the neuronal network. ((Ullian et al., 2001, Bergles et al., 2010, Wu et al., 2007, Garrett et al., 2009).

1.5.2. Role of Neuron-OPC synapse

Interestingly, recent discoveries revealed an intriguing relationship between the progenitor cells of OLs (Known as Oligodendrocyte Precursor Cells or OPCs) and neurons. It has been found that these cells form their own glutamatergic synapses with axons (Bergles et al., 2000, Lin et al., 2005), serving as a post-synaptic compartment, and harbors a wide array of GABA and glutamate receptors (Maldonado et al., 2011). To date, OPC are the only glial cell population that are known to form chemical synapse with neurons directly. It has also been shown that activity influence OPC proliferation (Mangin et al., 2012) and OPC can cross-talk with the neuronal network as well (Sakry et al., 2014, Sakry, et al., 2015) making these cells extremely interesting to study further.

1.5.3. Role of Astrocytes in synapse

Astrocytes are the most numerous constituents of the CNS and play a critical role in brain functions. Due to their proximity to neurons, astrocytes sense synaptic modulation efficiently and can control synaptic behavior. Astrocytes harbor many neurotransmitter receptors and thus respond to synaptic information produced by the neuronal activity. Studies have found that addition of astrocytes or astrocyte-derived medium in RGC neurons promote formation of excitatory synapses (Ullian et al., 2001) and research on the underlying molecular mechanism behind this phenomenon revealed that astrocytic release of apolipoprotein A bound to cholesterol (Goritz et al, 2005), TSP-1 and 2 (Christopherson et al., 2005), glycoprotein hevin and SPARC (Kucukdereli et al, 2011)

facilitates synapse formation and pre-synaptic release. Hevin and SPARC are also reported to induce post-synaptic membrane insertion of Glu1-A containing AMPAR (α -amino-3-hydroxy-5-methyl-4-isoxazolepropionic acid receptor (Allen et al, 2012).

During development, it is essential to fine-tune synapse formation and elimination for a mature brain-circuit and astrocytes play a key role in synapse loss too. It has been found that astrocytes express phagocytic genes and engulf synapses throughout adulthood via MEGF10 and MERTK pathways (Chung et al., 2013).

Astrocytes are also involved in regulating neuronal-activity by potassium and calcium buffering and uptake of neurotransmitters, Glutamate (by GLT-1, GLAST) and GABA (by GAT-1) and thus they are necessary for synaptic plasticity and maintenance (Zhang et al., 2017, Poskanzer et al., 2016, Thrane et al, 2013, Tanaka et al., 1997).

1.5.4. Role of Microglia in synapse

Microglia are the resident macrophages and phagocytes in the CNS, comprising 10% of the total glia population in human and around 20% in the rodent brain (Kettenmann et al., 2011). Microglia is largely known for regulating neuroinflammatory procedure, but they also play a key role in maintaining synapse architecture using their motile processes interacting with boutons and spines. Direct interaction between microglia and synaptic elements is already established by EM pictures (Tremblay et al., 2010).

Phagocytic microglia engulf pre and post-synaptic elements in the hippocampus and retinogeniculate system (RGS) during the first weeks after birth (Paolicelli et al., 2011, Schafer et al., 2012). This procedure is largely controlled by the CX3CR1 receptors in hippocampus and CR3 in the thalamus, expressed by microglia. CX3CR1-knockout mice show impaired social behavior, presumably caused by delayed electrophysiological properties of synapses during development (Paolicelli et al., 2011). There is also reference that microglia modulate synaptic plasticity by TNF-alpha mediated LTP and LTD induction in developing CNS (Wang et al., 2004, Stellwagen et al., 2006).

1.5.5. Role of Oligodendroglia and Schwann cells in synapse

The well-established role of myelin-producing oligodendrocytes and schwann cells is to ensheath axons to enable saltatory neuronal conduction in the CNS and PNS respectively. But more recent studies on myelin biology demonstrate another crucial role of myelin in CNS: it contributes to cognition and learning by modulating synaptic plasticity (Hoz et al., 2014, Scholz et al., 2009). The underlying molecular mechanism involves myelin protein and their ability to suppress axon sprouting and synaptogenesis (Schlegel et al., 2012). Early studies showed that transection of the developing optic nerves of the developing mice significantly reduced OPC proliferation rate (Barres and Raff, 1993) and produced thinner myelin sheath (Demerens et al., 1996). Neural impulse activity has been shown to inhibit PNS myelination via changing membrane properties of axons and releasing signaling molecules (Stevens et al., 1998) and on the other hand myelin sheath formation by individual OLs was increased by neuronal stimulation of synaptic vesicles (Reviewed in Forbes and Gallo, 2017, Mensch et al., 2015). Activity-dependent release of Adenosine appears to play a dual role in myelination, as in CNS, Adenosine is an active axon-glia transmitter promoting myelination and in PNS, it has been shown to inhibit myelination (Stevens and Fields, 2000, Stevens et al., 2007). Cellular studies on myelination have found that this process can be influenced by action potential firing in axons (Shrager et al., 1995, Stevens et al., 1998, Wake et al., 2011). Elevated neuronal activity in premotor areas has been shown to influence myelin patterning in callosal projections (Gibson et al., 2014) and recently, Etxeberria et al., in 2016, showed in their study that experience-dependent activity can change the length of myelin internodes and thus results in altered action potential conduction velocity.

Recent discoveries suggest that oligodendrocytes and axons are metabolically coupled as glycolytic oligodendrocytes provide lactate to neurons for aerobic ATP generation (Fünfschilling et al., 2012, Lee et al., 2012) and ensheathing glia provide trophic support to metabolically isolated neurons (Nave, 2010). Oligodendroglia are also reported to provide supportive biomolecules to neurons via exosome upon receiving neuronal signals. (Frühbeis et al., 2013). Micu et al., in 2016, showed that axonal activity triggers

NMDA receptor (N-methyl-D-aspartate)-mediated calcium response in myelin-producing oligodendrocytes (Micu et al., 2016).

1.5.6. Activity-dependent local translation and myelination

Neuronal activity induces a plethora of structural and functional changes in the post-synaptic compartment of a given synapse. The activity-driven alterations include rapid local translation, trafficking to and from the postsynaptic membrane, receptor expression, and internalization and altered intracellular signaling pathways. Most of these influenced synaptic events finally control synaptic strength, dendritic spine outgrowth and potentially mediate retrograde signaling (Kopec et al., 2007, Tanaka et al., 2008, Yang et al., 2008). The molecular events occurring during synaptic transmission are rapid and well-coordinated, and growing evidence suggests that stimuli-induced local translation lay the foundation of synaptic plasticity. Synaptic modulation within the neuronal network provides a mechanism for learning and memory, proper cognitive functions and stabilization of the neuronal network itself (Trinidad et al., 2013). Many of the neuronal mRNAs are actively transported via motor proteins in a form of mRNP (messenger ribonucleoprotein) granule to localize in dendrites or distal processes where they generally remained in a translationally repressed stage and later translated upon receiving external stimuli (Martin et al., 2009, reviewed in Sutton and Schuman, 2006, Wang et al., 2010), for example, In OLS, MBP mRNA has been shown to be transported into the distal processes where myelination takes place (Ainger et al., 1997, Smith et al., 2004). One of the most well-studied and emerging case in this context is Fragile-X syndrome (FXS), an intellectual disorder caused by mutation of an activity-dependent neuronal protein, FMRP, mutation of which leads to exaggerated translation and impaired synapses. Strikingly, FMRP has been reported to translationally repress MBP mRNA (Darnell et al., 2011, Li et al., 2001) and FXS patients often display myelin abnormalities (Hass et al., 2009, Hoefft et al., 2010).

1.6. Cellular functions of NG2 protein

1.6.1. Role of NG2 in modulating neuronal network

NG2 has long been considered mainly as a cell surface anchor or adhesion molecule due to the well-established interaction with Collagen V and VI and integrin complex (Burg et al., 1996, Tillet et al., 2002). Although, ECM remodeling is an important event in synapse formation, supporting data for the role of NG2 in the neuronal network was limited until the 2000's. Bergles et al., in their work in 2000, demonstrated that NG2+ OPCs could receive synaptic input from neurons and focus on NG2's role in this context has gained massive attention since then. Sakry et al., in 2014, revealed that the two LNS domains in the cleaved NG2 extracellular domain modulated neuronal synaptic AMPAR currents and kinetics of pyramidal neurons in somatosensory cortex in rodents most likely by influencing the AMPAR subunit composition. Moreover, NG2-Knockout mice (NG2-KO) displayed reduced NMDAR-induced LTP and impaired sensory input-related behavioral differences compared to wildtype (Sakry et al., 2014). NG2+ OPCs serve as a post-synaptic compartment as NG2-KO mice show post-synaptic phenotype changes by LNS domain while pre-synaptic changes remain unaltered. NG2 cleavage is also increased by neuronal activity and the cleaved product has been shown to exert neuromodulator effects by regulating the expression level of PTGDS, a known neuromodulator (Sakry et al., 2015) (Fig 1.4).

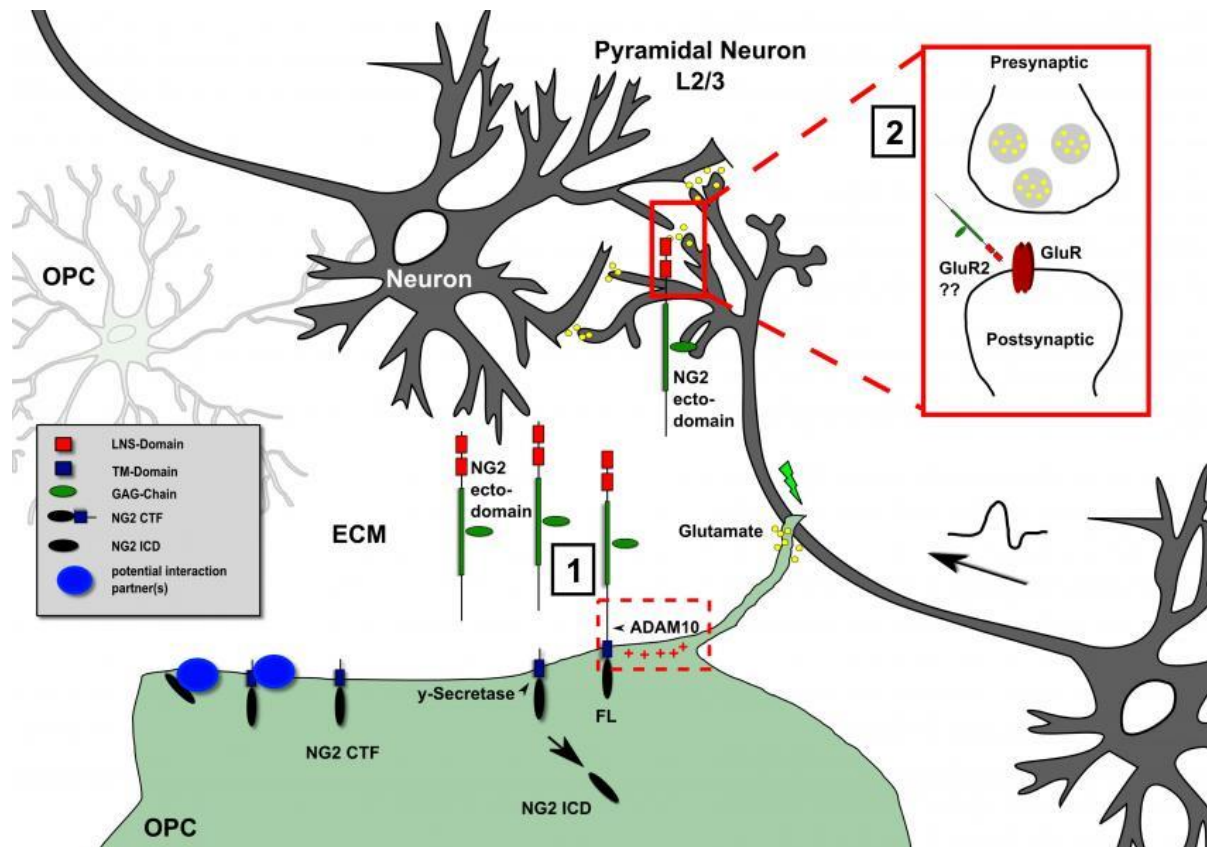


Fig 1.4. Diagrammatic representation of an NG2+ OPC-Neuron synapse (Taken from Sakry et al., 2014)

1.6.2. Cell motility

OPCs are highly motile as they migrate through the developing CNS and NG2 plays a crucial role in the regulation of adhesion and migration. NG2 facilitates cell motility by binding collagen VI through the extracellular central D2 domain (Burg et al., 1996). Moreover, NG2 has been shown to increase motility in vascular endothelial cells by interacting with galectin3/ $\alpha 3\beta 1$ integrin complex in trans on the endothelial cell surface (Fukushi, 2004). Investigation of the underlying molecular mechanism behind this event revealed that PKC α -dependent phosphorylation at the Thr2256 residue of the intracellular part of NG2 was required for the increased cell motility (Mackagiansar et al., 2004, 2007) and this phosphorylated epitope colocalized with integrin at the broad lamellipodia at the leading edges of motile cells (Stallcup et al., 2008). A study by

Biname et al. has reported that NG2 tightly controls directional OPC migration and cell polarity (Biname et al., 2013) by stimulating RhoA activity at the cell periphery via interaction with Syx1/Mupp1 signaling. It is also reported that NG2+ glia responds to soluble chemotactic factors like Netrin 1 and class 3 semaphorins (Spaskey et al., 2002). PSA-NCAM and N-cadherin also regulate NG2-mediated cell motility effect in vitro (Zhang et al., 2004, Schnadelbach et al., 2000).

1.6.3. Cell proliferation and survival

To obtain even distribution throughout the major areas of the CNS, OPCs rely on their proliferative ability as well as migration and PDGF-AA and FGF are essential for OPC proliferation (Goretzki et al., 1999). The core protein of NG2 contains binding sites for these receptors scattered through D2 and D3 domain of extracellular region. It has also been shown that treatment with NG2 antibody reduces OPC proliferation in response to PDGF (Nishiyama et al., 1996). Phosphorylation by ERK at the Thr-2314 residue in the intracellular domain of NG2 also plays a role in proliferation (Makagiansar et al., 2007).

Interestingly, the NG2-dependent effect on the $\alpha3\beta1$ integrin signaling cascade activates PI3K/Akt signaling which plays an important role in cell survival (Downward et al., 2003, Joy et al., 2003). The NG2-transfected U251 glioma cell line was reported to be more resistant to treatment with TNF- α and other chemotherapeutic drugs than the parental ones (Chekenya et al., 2008) and NG2-knockdown is also effective in triggering apoptosis in gliomas endogenously expressing NG2. Recent findings by Maus et al., in 2015, revealed that NG2 also binds a protease, OMI/Htra2 via the intracellular PDZ-binding domain, and by sequestering this protein, it exerts a protective role in OPCs.

1.6.4. Cytoskeleton reorganization

Since the contribution of NG2 in cell migration and polarity formation is already well-established by separate groups, it was anticipated that NG2 elicits these changes by modulating the composition of underlying cytoskeleton framework. The intracellular part of NG2 is particularly important in this context as it interacts with several scaffolding proteins like MUPP1 (Stegmuller et al., 2003) and GRIP (Barritt et al., 2000) via its PDZ domain. It has also been reported that NG2 intracellular region interacts with Syntenin-1

which mediates cytoskeletal rearrangements at the plasma membrane (Chatterjee et al., 2008). There is also evidence of stimuli-dependent NG2 interaction with two distinct subdomains of the actin cytoskeleton (Lin et al., 1996).

1.6.5 Role of NG2 in Glioma

Glioblastoma Multiforme (GBM) is the most prominent and aggressive type of brain tumours with patients having a median life expectancy of only 14 months and less than 25% of patients surviving 24 months (Stupp et al., 2005). The source of glioma, being heterogeneous, includes neural stem cells, astrocytes, and glial progenitor cells. The involvement of glial progenitors, in this context, inevitably comes with their molecular signatures like NG2, PDGFR and Olig2 as these are highly abundant in tumour cells (Chekenya et al., 2002, Bouvier et al., 2003, Shoshan et al., 1999).

Several studies on the role of the NG2 proteoglycan in tumours suggest that the expression of NG2 can be correlated with the degree of malignancy (Chekenya et al., 2002, Schrappe et al., 1991). Owing to the fact that NG2+OPCs are surprisingly abundant in the CNS (more than 70% of the cycling progenitors) (Goldman et al., 2005, Dawson et al., 2003), they are likely to constitute a major cell population in which accumulating mutations can lead to tumourigenesis.

The main functions of NG2 include rapid cell proliferation, increased cell survival, and migration which are also highly beneficial for tumour survival and progression. This may explain high expression of NG2 in glioma and other type of tumours. NG2 knock-down has been reported to slow down tumour progression (Chekenya et al., 2008) and overexpression of it in melanoma has been demonstrated to increase tumour growth (Burg et al., 1998).

Due to the high expression level of NG2 by tumours, it has been chosen as a cancer therapeutic target and treatment with monoclonal antibody, siRNA or shRNA-mediated knockdown has been shown to reduce tumour proliferation and increased tumour necrosis in murine models of melanoma (Wang et al., 2011, Wang et al., 2010).

1.7. Regulated intramembrane proteolysis (RIP)

1.7.1 Mechanism of regulated intramembrane proteolysis (RIP)

Regulated Intramembrane Proteolysis (RIP) is a cellular process that links external cues with intracellular events. RIP is a highly regulated proteolytic event where a transmembrane protein (type 1 or type 2) is cleaved by a group of proteases (iCLiPs, Intramembrane Cleaving Proteases), either constitutively or in response to ligand binding, yielding a soluble intracellular fragment called intracellular domain (ICD).

iCLiPs are multi-span, integral membrane proteins, the active sites of which are exposed to the hydrophobic environment, typically embedded in the predicted transmembrane domain (TMD) region. For the most studied cases, optimal action of iCLiPs requires substrate priming where members of disintegrins and metalloproteinase (ADAM family), matrix metalloproteases or BACE family (BACE1 and BACE 2) proteases cleave off the extracellular domain at the transmembrane domain (TMD), an event known as 'Shedding'. The released ectodomain is released either in the vesicular lumen or the extracellular matrix and often exhibits unique biological properties. The shedding results in generation of a membrane-bound stub (also known as C-terminal fragment or CTF) which is then subjected to a second cleavage event within its transmembrane domain releasing a shorter peptide secreted in the extracellular milieu and an intracellular domain which is released into the cytosol. The intracellular domains sometimes act as signaling molecules and often have a defined biological role. (Lal et al., 2010., Lichtenthaler et al., 2011) (Fig 1.5).

In case of type-1 transmembrane proteins, intracellular proteolysis is catalyzed by the γ -secretase complex. The γ -secretase is comprised of minimal four proteins that are essential for its proteolytic activity (De Strooper et al., 2003). While Presenilin 1 or presenilin 2 (PS1 and PS2) is the core catalytic unit of the γ -secretase complex, Nicastrin (NCT), anterior pharynx defective 1 (APH-1), and presenilin enhancer 2 (PEN-2) are the three other cofactors for active γ -secretase-mediated proteolysis (Goutte et al., 2002, Kimberly et al., 2003, Edbauer et al., 2003). The four proteins stabilize each other post-assembly and are required for proper trafficking of the mature complex to the cell surface or to the endocytic compartments where the γ -secretase exerts its effect.

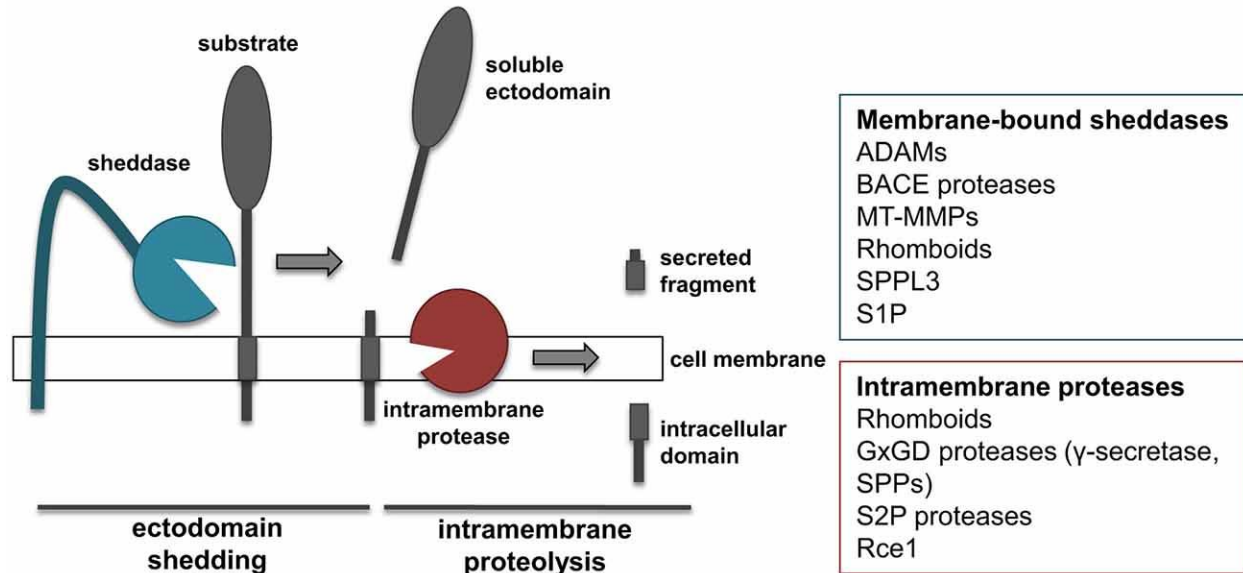


Fig 1.5. Mechanistic principle of Regulated Intramembrane Proteolysis (RIP) (Taken from Müller et al., 2016)

1.7.2. Activity-dependent cleavage of neuronal proteins

Regulated intramembrane proteolysis is an elegant cellular mechanism for fine-tuning extracellular cues with intracellular signal transduction, and thus could be an excellent mechanism of choice when it comes to activity-dependent information transmission. There is growing evidence of RIP occurring in the nervous system, and often the released ICDs play a significant role in gene regulation, cell maturation, apoptosis and synapse formation in CNS. The following table (Table 1.2) contains a list of emerging and characterized neuronal proteins that undergo RIP. Their ICDs has been found to play a predominant role in controlling and orchestrating cellular processes in the brain.

1.7.3. NG2 is a type-1 transmembrane protein that undergoes proteolytic cleavage

NG2 (*CSPG4*) is a type-1 transmembrane protein (300 kD MW), belonging to the chondroitin sulfate proteoglycan protein family with a large extracellular region (290 kD, consisting of 2200 aa) and a very short intracellular domain (8.5 kD, composed of 77 aa). It was first discovered in the rat nervous system (Stallcup, 1977) and has reported homologs in mouse (Niehaus et al., 1999; Schneider et al., 2001; Stegmüller et al.,

2002), human (Pluschke et al., 1996) and Drosophila (Estrada et al., 2007; Schnorrer et al., 2007).

Table 2. Proteolytic cleavage of neuronal type-1 membrane proteins

Name of the Protein	The function of released ICDs	References
Notch	<ol style="list-style-type: none"> 1. Involved in nuclear signaling 2. Inhibits neurogenesis and promotes gliogenesis. 	Zhou et al., 2010, Andersson et al., 2011.
APP	<ol style="list-style-type: none"> 1. Exerts transcriptional activity. 2. Regulates cytoskeleton reorganization. 3. Regulates neuronal growth, and apoptosis. 	Kawasumi et al., 2004, Raychaudhuri and Mukhopadhyay, 2011, Muller et al., 2008.
Neuregulin 1	<ol style="list-style-type: none"> 1. Prevents neuronal apoptosis. 2. Positively regulates neuronal survival. 	Bao et al., 2003, Wolpowitz et al., 2000.
p75NTR	<ol style="list-style-type: none"> 1. Facilitates TrkA-dependent neurite outgrowth. 2. Crosstalk with Erk1/2 signaling. 	Forsyth et al., et al., 2014 Ceni et al., 2010.
L1CAM	<ol style="list-style-type: none"> 1. Downregulates PTEN and p53, causing increased neuritogenesis. 2. Regulates gene expression of Cathepsin, integrins, and HOXA9. 	Wang et al., 2015., Riedle S et al., 2009.
ErbB4	<ol style="list-style-type: none"> 1. Together with TAB2 and N-CoR, ErbB4-ICD represses expression of genes associated with neuronal precursor cell differentiation. 2. Plays a role in NRG1-induced oligodendrocyte maturation and cell death. 	Lal M et al., 2011, Sardi et al., 2006.
N-cadherin	<ol style="list-style-type: none"> 1. Nuclear translocation along with bound catenin and upregulates EMT effector genes such as catenin or cyclin D1. 	Marambaud et al., 2003 VR Rao et al., 2003

The extracellular region of NG2 is heavily glycosylated and contains one confirmed glycosaminoglycan (GAG) chain with several predicted N-glycosylation motifs (Nishiyama et al., 1991). The extracellular part also harbors two conserved Laminin Neurexin Sex-hormone binding (LNS) domain N-terminally, which show similarity with the LNS domain of neuronal synaptic adhesion proteins, the Neurexins. No interaction partner for the NG2 LNS domain has been reported so far. (Sakry et al., 2015). (Fig 1.6)

The large extracellular domain of NG2 protein includes cleavage site proximal to the membrane (Nishiyama, 2009) and undergoes sequential cleavage mediated by α -secretase and γ -secretase resembling a common cellular event known as Regulated Intramembrane Proteolysis (RIP). It has been shown that ADAM10 is the major catalyzing α -secretase for NG2 ectodomain shedding, similar to the cleavage pattern of Notch, generating a 290 kD ectodomain and a 12 kD membrane-bound C-terminal fragment (CTF), the latter is found in a higher level in membrane fractions. It has been demonstrated by inhibiting γ -secretase function that the NG2 CTF is subjected to constitutive cleavage by the γ -secretase yielding an intracellular fragment of the NG2 protein (Sakry et al., 2014). NG2 ICD is defined as a proteolytically cleaved and released intracellular part of the NG2 protein in analogy to the ICDs of NOTCH or APP. This peptide-sequence is an element of the intracellular region of the full-length protein or the CTF.

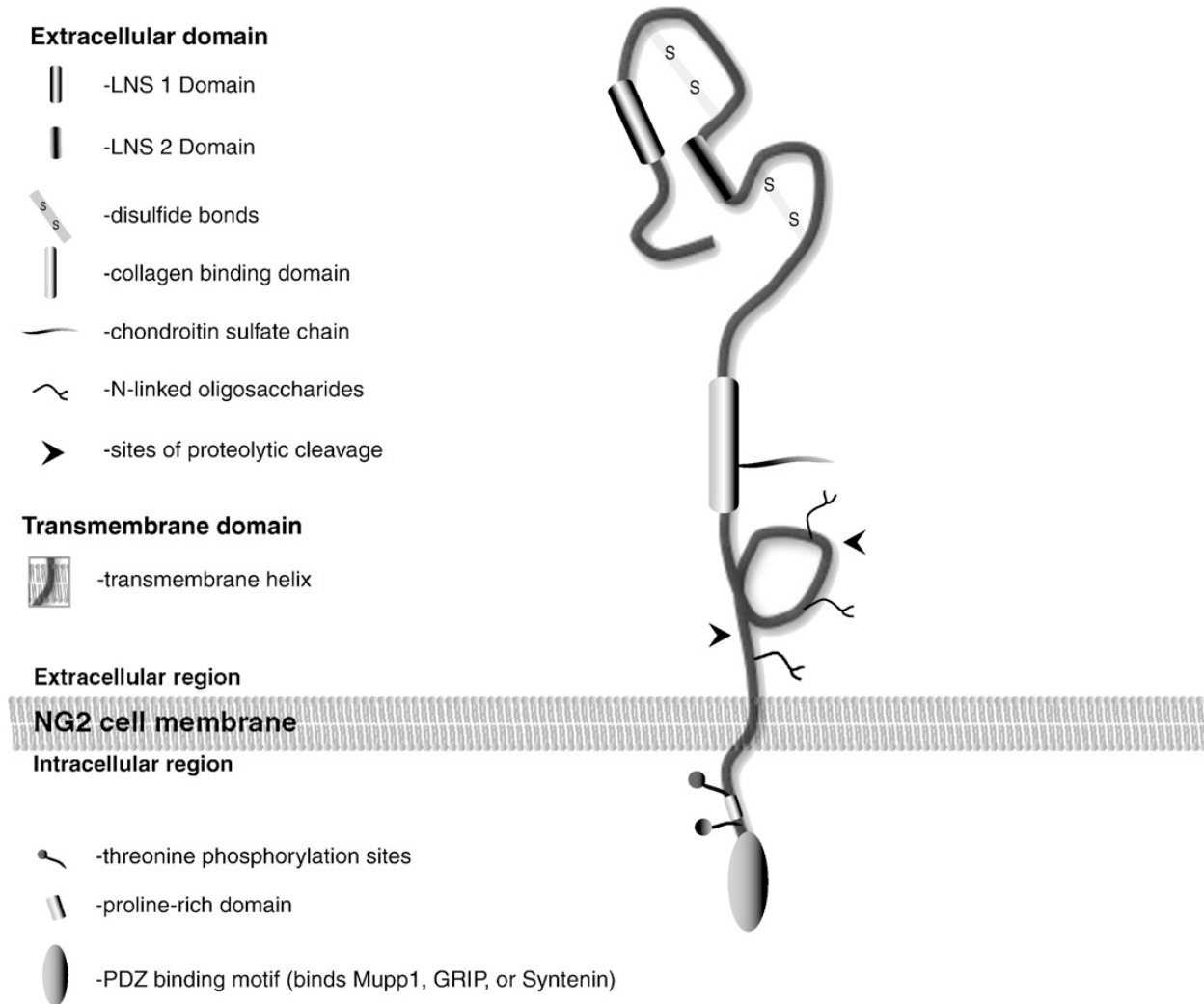


Fig 1.6. Diagrammatic representation of NG2 protein (Taken from Trotter et al., 2010)

1.7.4. Structure and function of NG2 ICD

The small C-terminal part of the NG2 protein consists of 77 amino acids and 8.5 kD (MW). This intracellular domain (ICD) is a product of γ -secretase action on full-length NG2 and it harbors several predicted protein binding motifs (ELM database) including MAPK binding motif (6-14 aa), WW4 motif (62-67 aa), PDZ2 binding motif (72-77 aa), PTB-Phospho domain-binding motif (69-75 aa) and two monopartite classical Nuclear localization signals (NLS; 1-7 aa). To date, the study of phosphorylation in the intracellular region of the NG2 protein and the identification of intracellular binding

partners of NG2 has been done mainly on membrane-bound CTF of NG2 (table 1.3). However, it is still not known if NG2 intracellular domain exerts any distinct functional properties of its own after its release into the cytosol.

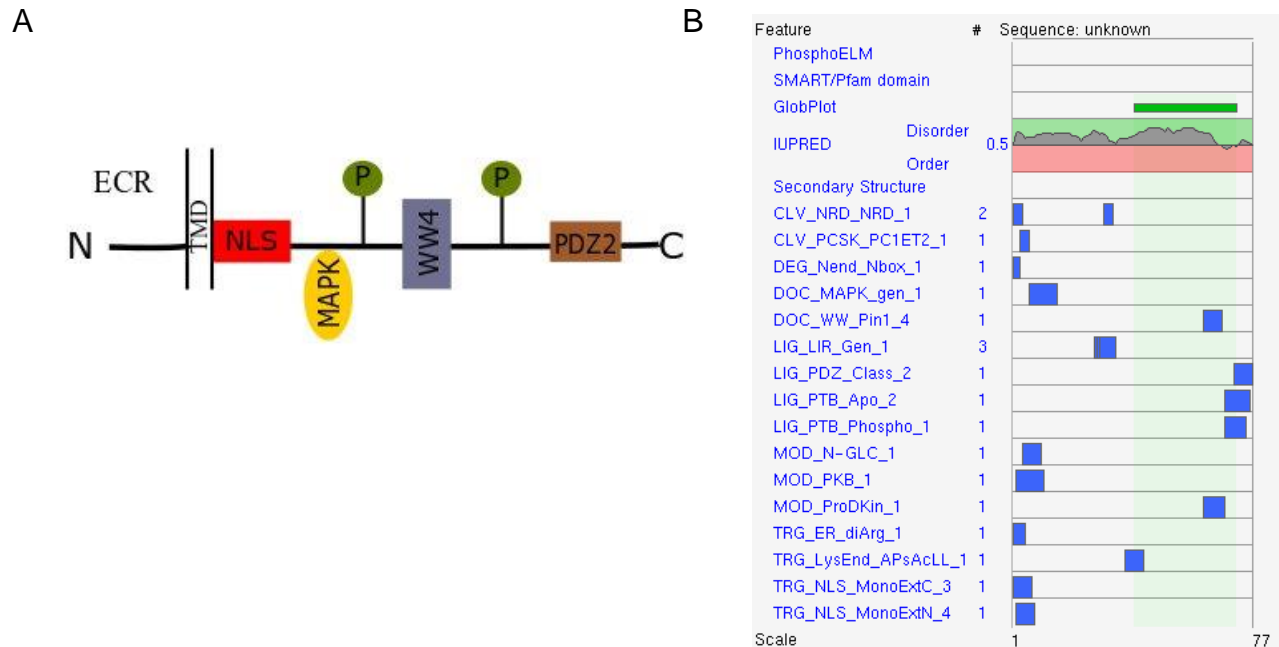


Fig 1.7. (A) Schematic cartoon of the NG2 intracellular region along with predicted motifs. B) predicted motifs found in the NG2 intracellular region by ELM motif search database (<http://elm.eu.org/>).

Table 3. The intracellular PDZ-binding partners of the NG2 protein

Name of the Protein	Function	Reference
Syntenin-1	Serves as an adapter molecule that connects NG2 to its downstream signaling components and especially required for cytoskeleton reorganization and migration.	Chatterjee et al., 2008, JBC.
MUPP1	Scaffolding protein associated with the formation of multimeric structural and signaling complex.	Barritt et al., 2000, JCB.
GRIP1	Act as a scaffolding protein and cluster protein complexes at the cell surface and serves as a direct molecular link between AMPA receptor and NG2 proteoglycan in OPCs.	Stegmüller et al., 2003, JBC.
OMI/Htra2	A serine protease that acts as a chaperone but in stress conditions, induce apoptosis. NG2 exerts a protective effect on OPCs by binding and sequestering OPCs.	Maus et al., 2015, PLOS One.

2. Aim of the study

As previously discussed, growing evidence suggests the involvement of RIP in regulating neuronal network function and architecture. Since NG2 also undergoes RIP and releases an intracellular cleavage product, it is important to characterize the cleaved product and potential intracellular binding partners in order to clarify a possible biological role. This project aimed to investigate the subcellular localization pattern and function of cleaved NG2 ICD after its release into the cytosol. With a combination of various NG2 expression constructs and Mass-spectrometry based proteomics study along with high-resolution microscopy and molecular biology tools, the questions mentioned above have been addressed in this study.

Materials and Methods

3. Materials and Methods

3.1.1. Equipment

Table 4. Device and Equipment

Device Type	Manufacturer
Cell culture Equipments	
Sterile working bench	The Baker Company
CO2 incubator	Labotect, Sanyo
Centrifuge Megafuge® 1.0R	Heraeus
Inverted microscope	Leica
Water bath	Hermle
Microscope	
DM6000	Leica, Wetzler
TCS SP5	Leica, Wetzler
DMLB	Leica, Wetzler
Transfection device	
AMAXA Nucleofactor II	Lonza
GenePulser Xcell	BioRad, München
PCR machine	
Real-Time PCR System	Applied Biosciences
PCR Thermocycler	Biometra
Other lab equipments	
Bacteria incubator	Noctua
Luminometer (Infinite M200 Pro)	Tecan
Tabletop Biofuge® fresco	Heraeus
Magnetic separation device	Invitrogen
Heating thermomixer	HLC, Bovenden
NuPAGE western blotting system	Invitrogen
NanoDrop 1000 Spectrophotometer	Peqlab
Optimax Type TR X-Ray Film processor	MS Laborgeräte
Scanner	Epson

3.1.2. Materials

Table 5. Chemicals and Reagents

Name	Cat. No	Source
96-well Plates white (Luminescence)	#236105	Nunc
anti-flag M2 dynabeads	#M8823	Sigma
Anisomycin	#A9789	Sigma
Agarose (low melt)	#6351.2	Roth
BrdU (5-Bromo-2'-Deoxyuridine)	#B23151	Life Technologies
Benzonase, Purity>90%	#70746-4	Merck Millipore
BSA Nuclease-free 10%	#126615	Calbiochem
Chloroform	#3313.1	Roth
DAPI	#D9542	Sigma Aldrich
DMEM	#D5796	Sigma
Dynabeads Protein G	#10004D	Life Technologies
EDTA	#8040.2	Roth
Ethanol	#9065.4	Roth
FuGENE HD transfection reagent	#E2311	Promega
H2O Ultrapure	#W4502	Sigma Aldrich
Halt Protease Inhibitor Cocktail	#1860932	Thermo Fisher
Ivermectin	#I8898	Sigma
MG-132, proteasome inhibitor, ≥90% (HPLC)	#M7449	Sigma
Magnesium chloride	#M2670	Sigma Aldrich
MicroAmp® 48-Well Optical Adhesive Film	#4375323	Life Technologies
MicroAmp® Fast Optical 48-Well Reaction Plate	#4375816	Life Technologies
Mowiol 4-88 reagent	#475904	Calbiochem
NE-PER Nuclear/Cytoplasmic Extraction Kit	#78833	Pierce
Nonidet™ P 40 Substitute	#74385	Fluka
NuPAGE® LDS Sample Buffer (4x)	#NP0007	Life technologies
Invitrogen NuPAGE® MES SDS Running Buffer (20X)	#NP0002	Life technologies
NuPAGE® MOPS SDS Running Buffer (20X)	#NP0001	Life technologies
NuPAGE® Novex® 4-12% Bis-Tris Protein Gels	#NP0335BOX	Life technologies
O'GeneRuler 1kb DNA Ladder	#SM1163	Thermo Scientific
PFU Turbo DNA Polymerase	#600250	Stratagene
Puromycin dihydrochloride	#P8833	Sigma
Propidium iodide	#P4176	Sigma
Ponceau S solution	#P7170	Sigma
Propanol ROTIPURAN®	#6752.2	Roth
QIAzol Lysis Reagent	#79306	Qiagen

RNase A	#12091-039	Invitrogen
RNase-free DNase Set	#79254	Qiagen
RNaseZAP	#R2020	Sigma Aldrich
RNasin® Plus RNase Inhibitor	#N2611	Promega
Roti®-Histofix	#P087.3	Roth
Sodium butyrate	#30341-0	Sigma Aldrich
Sodium chloride	#S3014	Sigma Aldrich
TaqMan® Gene Expression Master Mix	#4369016	Life Technologies
Tris	#4855.1	Roth
Triton X-100	#3.051	Roth
Tween 20	#9127.2	Roth
Kit name	Cat No	Manufacturer
PureLink HiPure Plasmid Miniprep kit	#K210011	Invitrogen
PureLink HiPure Plasmid Maxiprep kit	#K2100-07	Invitrogen
QIAquick Gel Extraction Kit	#28706	Qiagen
QIAquick PCR Purification Kit	#28106	Qiagen
Basic Primary neurons Nucleofector kit	#VPI-1003	Lonza
Transcriptor First Strand cDNA Synthesis Kit	#04896866001	Roche
BCA Protein Assay Kit	Merck Millipore	71285-3
Direct-zol™ RNA MiniPrep Plus	Zymo Research	R2070
TaqMan® Universal Master Mix II, with UNG	Life Technologies (Thermo Scientific™)	4440042
SensiFAST Probe Hi-ROX Kit (Lot.B018180)	Bioline	BIO-82002/S

3.1.3 Reagents

Table 6. Buffers and Medium

Buffer/Medium/Solution	Composition
10 x Poly-L-Lysine (PLL)	0.1 % PLL (Sigma, #P1524) in ddH ₂ O
Sato 1.0-1.5 % HS (Oli-neu culture medium)	13.4 g/l DMEM (Invitrogen, #52100-039), 2 g/l NaHCO ₃ , 0.01 g/l transferrin, 100 µg/l insulin, 100 µM putrescine 200 nM progesterone, 500 nM TIT, 220 nM Sodium-selenite, 520 mM L-thyroxine, 1.0-1.5% (v/v) horse serum
SILAC light medium (modified SATO)	SILAC-DMEM (Life technologies, 89985), 2 g/l NaHCO ₃ , 0.01 g/l transferrin, 100 µg/l insulin, 100 µM putrescine, 200 nM progesterone, 500 nM TIT, 220 nM Sodium-selenite, 520 mM L-thyroxine, 4 mM L-Glutamine, 1% (v/v) horse serum, 146 mg/ml Lysine-0 (Sigma-

	Aldrich L8662), 84 mg/ml L-Arginine-0 (Sigma-Aldrich, A6969)
SILAC Medium-heavy medium (modified SATO)	SILAC-DMEM (Life technologies, 89985), 2 g/l NaHCO ₃ , 0.01 g/l transferrin, 100 µg/l insulin, 100 µM putrescine, 200 nM progesterone, 500 nM TIT, 220 nM Sodium-selenite, 520 mM L-thyroxine, 4 mM L-Glutamine, 1% (v/v) horse serum, 146 mg/ml Lysine-4 (Cambridge Isotope laboratories, DLM-2640-PK), 84 mg/ml L-Arginine-6 (Cambridge Isotope laboratories, CLM-2265-H-1)
SILAC heavy medium (modified SATO)	SILAC-DMEM (Life technologies, 89985), 2 g/l NaHCO ₃ , 0.01 g/l transferrin, 100 µg/l insulin, 100 µM putrescine, 200 nM progesterone, 500 nM TIT, 220 nM Sodium-selenite, 520 mM L-thyroxine, 4 mM L-Glutamine, 1% (v/v) horse serum, 146 mg/ml Lysine-8 (Cambridge Isotope laboratories, CNLM-291-H-1), 84 mg/ml L-Arginine-6 (Cambridge Isotope laboratories, CNLM-539-H-1)
HEK Culture medium	Dulbecco's Modified Eagle's Medium - high glucose (Sigma, D5796), 10% FCS, 1% sodium pyruvate
DMEM-SILAC light medium	SILAC-DMEM (Life technologies, 89985), 10% Dialyzed FBS (Sigma-aldrich, F0392), 1% Penicillin/Streptomycin, 146 mg/ml Lysine-0 (Sigma-Aldrich L8662), 84 mg/ml L-Arginine-0 (Sigma-Aldrich, A6969)
DMEM-SILAC Medium-heavy medium	SILAC-DMEM (Life technologies, 89985), 10% Dialyzed FBS (Sigma-aldrich, F0392), 1% Penicillin/Streptomycin, 146 mg/ml Lysine-4 (Cambridge Isotope laboratories, DLM-2640-PK), 84 mg/ml L-Arginine-6 (CIL, CLM-2265-H-1)
DMEM-SILAC Heavy medium	SILAC-DMEM (Life technologies, 89985), 10% Dialyzed FBS (Sigma-aldrich, F0392), 1% Penicillin/Streptomycin, 146 mg/ml Lysine-8 (CIL, CNLM-291-H-1), 84 mg/ml L-Arginine-6 (CIL, CNLM-539-H-1)
Trypsin/EDTA „low“	0.01% trypsin, 0.02% EDTA in HBSS
Freezing medium	20% (v/v) FCS, 10% (v/v) DMSO in RPMI 1640
LB medium	10 g trypton, 5 g yeast extract, 10 g NaCl, fill to 1000 ml with ddH ₂ O, pH=7.4
LB agar	4.5 g agar-agar in 300 ml LB medium

SDS running buffer for electrophoresis (5x)	125 mM Tris, 1.25 M glycine, 0.5 % (w/v) SDS, pH=8.3
Western blot transfer buffer	24 mM Tris, 192 mM glycine, 20% ethanol in dH2O
WB blocking buffer	4 % (w/v) dry milk/BSA powder in PBST
PBS	150 mM NaCl, 8 mM Na2HPO4, 1.7 mM NaH2PO4, pH=7.2
PBST	0.1% (v/v) Tween 20 in PBS
Homemade ECL solution	Solution A: 50 mg luminol in 200 ml 0.1 M Tris-HCl pH=8.6, Solution B: 11 mg para-hydroxy coumaric acid in 10 ml DMSO (dark), ECL solution: combine 1 ml solution A + 100 µl solution B + 0.3 µl H2O2
DAPI stain	1 µg/µl DAPI (#D9542, Sigma) in PBS
Mounting medium	2.4 g moviol 4-88, 6 g glycerol, 6 ml ddH2O, 12 ml 0.2 M Tris pH=8.5
4x sample buffer	200 mM Tris-HCL, pH=6.8, 10% (w/v) SDS, 0.4% (w/v) bromphenol blue, 40% (v/v) glycerol, 400 mM DTT
Post-nuclear cell lysis buffer	1X PBS, 1% Tx-100, 1X Protease inhibitor cocktail.
Nuclear lysis buffer	20 mM Tris-HCl (pH 7.4), 150 mM NaCl, 10 mM MgCl2, 1% TX-100, 2.5 mM Beta-glycerophosphate, 1 mM NaF, 1 mM DTT, 2mM EDTA, 10% glycerol 10 unit of Benzonase, 1X Protease inhibitor cocktail.
Permeabilization buffer	1X PBS, 0.1%-0.5% TX-100
Fixation solution	1x PBS, 4% paraformaldehyde or 1:1 acetone:methanol
Blocking solution	1X PBS, 10% Horse serum.

3.1.4. Antibodies

Table 7. List of primary antibodies (IB: Immunoblot, IF: Immunofluorescence, FC: Flow cytometry)

<i>Antigen</i>	<i>Cat No</i>	<i>Host species</i>	<i>Application with dilution</i>	<i>Manufacturer</i>
<i>Flag M2</i>	F1804	Mouse	IB (1:1000), IF (1:400)	Sigma
<i>Flag-FITC M2</i>	F4049	Mouse	FC (1: 200)	Sigma
<i>Lamin B</i>	ab16048	rabbit	IB (1:1000), IF (1:500)	Abcam
<i>Eef2</i>	ab40812	rabbit	IB (1:1000)	Abcam
<i>Eif4b</i>	3592 T	rabbit	IB (1:1000)	NEB(CST)
<i>FMRP</i>	F4055	rabbit	IB (1:1000)	Sigma
<i>Cofilin</i>	#612144	Mouse	IB (1:1000)	BD Transduction
<i>GAPDH</i>	A-300-641A	rabbit	IB (1:5000)	Biomol
<i>Tubulin</i>	T9026	mouse	IB (1:5000)	Sigma
<i>PCNA</i>	13110T	rabbit	IF (1:250)	NEB(CST)
<i>p70S6K1</i>	9202S	rabbit	IB (1: 1000)	NEB(CST)
<i>mTOR substrate antibody sampler kit</i>	9862T	rabbit	IB (1:1000)	NEB(CST)
<i>phospho-eif4b (Ser422)</i>	3591T	rabbit	IB (1:800)	NEB(CST)
<i>ADNP2</i>	WA-AP13981	rabbit	IB (1:1000)	Biomol
<i>AGAP2</i>	NBP2-24498	rabbit	IB (1: 1000)	Novus Biological
<i>Puromycin</i>	MABE343	Mouse	IB (1:1000)	Merck Millipore
<i>Cyclin E</i>	SC-377100	Mouse	IB (1:400)	Santa Cruz
<i>NG2</i>		Rat	IB (1:200), IF(1:100)	Hybridoma Culture supernatant
<i>NG2-Cyto</i>		Rabbit	IB (1:200)	AG Trotter

Table 8. List of secondary antibodies

Host species	Target species	Conjugation	Application	Manufacturer
goat	mouse	HRP	1:10000	Dianova
goat	rat	HRP	1:10000	Dianova
goat	rabbit	HRP	1:10000	Dianova
goat	mouse	Alexa488	1:400	Invitrogen
goat	rabbit	Cy3	1:800	Dianova
donkey	mouse	Alexa546	1:400	Invitrogen

3.1.5 Software

Table 9. List of used software

Software	Resource
<i>Microsoft Office 2013</i>	Microsfot
<i>FunRich proteomics analysis tool</i>	FunRich
<i>Pathways analysis by ontology</i>	DAVID (NIH)
<i>StepOne Software 2.2.2</i>	Applied Biosystem
<i>Endnote X5</i>	Thomson Reuters
<i>ImageJ</i>	Open source, NIH
<i>Clone Manager 9 Professional</i>	Sci-Ed Software
<i>LAS AF Microscope Software</i>	Leica
<i>GraphPad</i>	Prism
<i>Flowjo</i>	BD company
<i>MaxQuant</i>	Max Planck Institute of Biochemistry

3.2. Cell biology

3.2.1. Cell culture

3.2.1.1. Oli-*neu* Cell Culture

The oligodendrocyte precursor cell line Oli-*neu* was generated from primary mouse OPCs by transferring the t-*neu* oncogene using replication deficient retroviruses. t-*neu* is expressed under the control of the thymidine kinase promoter in Oli-*neu* cells and maintains the proliferative state of the cells (Jung et al., 1995). Oli-*neu* cells were cultured on 1X PLL coated culture dishes in Sato + 1.5 % HS medium with 8% CO₂. For passaging, cells were detached after incubation with pre-warmed trypsin/EDTA for 2 min. Reaction was stopped by adding the same amount of PBS + 10 % HS (4 °C) and cells were centrifuged at 800 rpm at 4 °C for 10 min. To freeze cells for long-term storage, cell pellet was resuspended in freezing medium at – 80 °C and stored in liquid nitrogen.

3.2.1.2. HEK293T Cell Culture

HEK293T cells derive from human embryonic kidney cells and were cultured in DMEM + 10 % FCS in non-coated culture dishes with 5% CO₂. Passaging and freezing procedure was like the protocol used for *Oli-neu* cells.

3.2.1.3. Primary OPCs isolation and maintenance

For primary OPC (pOPC), single cell suspensions were obtained from total brains of the Postnatal day (P) P6-9 of C57Bl/6N mice using the NTDK-P Kit (Miltenyi Biotec). Magnetic isolation (MACS) was performed as described previously (Diers-Fenger et al., 2001). 300,000 cells were plated in each well of a PLL-coated dish (6-well format) and cultured in OPC proliferation medium. OPC proliferation medium consists of NeuroMACS medium (Miltenyi) supplemented with 1:50 of NeuroBrew Miltenyi, 1:100 of L-Glutamine, 1:100 Pen-strep and 1:1000 of stock conc. of each of Forskolin (4.2 mg/ml), CNTF (10 µg/ml), PDGF (10 µg/ml) and NT-3 (1µg/ml). pOPCs were maintained at 37°C with 8%CO

3.2.2 Transfection methods

3.2.2.1. FuGENE HD transfection of plasmid DNA

Oli-neu cells were transfected with plasmid DNA chemically by FuGENE HD (Promega) according to the manufacturer's instructions. Generally, 90-100 x 10³ cells were seeded into 6-well plate the day before transfection. 2 µg of DNA were diluted in 100 µl pre-warmed DMEM (without serum) and combined with 6 µl FuGENE HD (1:3 ratio). Transfection complexes were mixed and incubated for 10 mins before applying to the cells. Cells were analyzed 24-72 hours after transfection. The amount of plasmid DNA and FuGENE reagent were scaled up according to the used cell-culture dish diameter and cell number with a constant transfection ratio.

3.2.2.2. PEI transfection

HEK293 cells were transfected chemically using PEI reagent. One day prior transfection, 0.5×10⁶ cells were seeded in 6-well plate format. For transfecting cells in a 3 cm dish, in a sterile tube, 2 µg of plasmid DNA was diluted with serum-free, pre-

warmed DMEM and 6 μ l of PEI (1 μ g/ μ l) and mixed immediately. After 15 mins incubation at RT, the mixture was applied to cells and after 48 hours of transfection, cells were analyzed. 12 hours after transfection, cells were checked and if needed, the medium was replaced with fresh batch.

3.2.2.3. Bio-Rad GenePulser electroporation

Cells were transfected with plasmids using the Bio-Rad GenePulser Xcell. 1.5 – 2.0 x 10⁶ cells in 600 μ l were transferred to a 4 mm electroporation cuvette containing 8 μ g DNA followed by thorough mixing. The cuvette containing the cells was attached to the GenePulser device for pulsing (exponential decay program; 220 V, 950 μ F) followed by an incubation time of 5 min at RT. Cells were plated on a 6cm culture dish. After 4 – 6 h medium was changed with fresh batch of medium.

3.2.2.4. Amaxa nucleofection of siRNA

RNAi was used to knockdown expression of selected target genes from Oli-*neu* cells using the Amaxa Basic Nucleofector® Kit for Primary Neurons according to the manufacturers' instructions. 1 x 10⁶ Oli-*neu* cells were pelleted at 100 g at room temperature, resuspended in 100 μ l AMAXA solution and combined with 160 pmol of siRNA. Electroporation was carried out using program O-005 in the AMAXA Nucleofector II device, the cell suspension in the electroporation cuvette was immediately combined with the warm, CO₂-equilibrated plating medium and then carefully seeded in PLL-coated cell culture dishes. Culture medium was exchanged 4-5 hours post nucleofection and cells were analyzed 24-72 hours later.

3.2.3. FACS

Cells were plated in 100 mm dishes and chemically transfected with flag-tagged constructs (BAP-Flag and ICD-Flag) one day after plating. After 48 hours post-transfection, cells were trypsinized and pelleted down (800 rpm, 10 mins). Cells were washed with PBS two times to remove residual medium and resuspended in PBS for counting. Equal number of cells were taken into a glass tube from each condition and

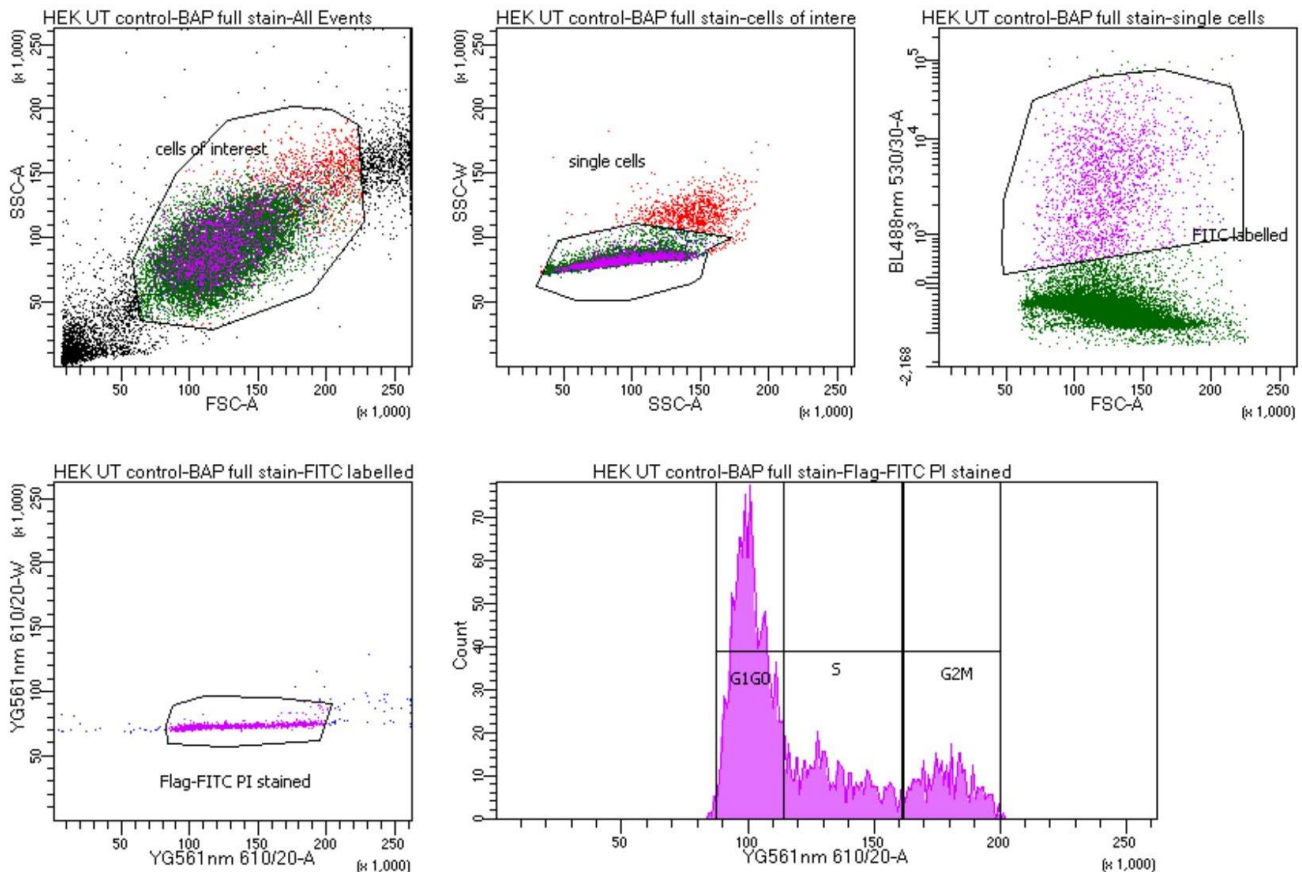


Fig 3.1. Gating strategy for cell-cycle distribution analysis in FITC+ cells only

cells were fixed with pre-chilled 80% ethanol (1:3 volume ratio) in a dropwise manner while low-vortexing the tubes and put on ice for 30 minutes. Fixed cells were washed two times with PBS and then permeabilized with permeabilization buffer (1XPBS, 0.1% TX-100) for 15 minutes at RT. Primary antibody (Flag-FITC, 1 μ g of antibody taken for 1 million cells) was diluted in permeabilization buffer and cells were incubated with primary antibody solution for 2 hours at RT in dark. Afterwards, cells were washed two times with PBST and RNase A (final conc; 10 μ g/mL) was immediately added. Propidium Iodide (PI) was added for staining DNA at a final concentration of 50 μ g/mL and the cells were incubated in dark for 30 mins on ice. Untransfected cells were taken as a negative control for assessing Flag-FITC background staining and incubated in similar fashion with PI and RNase A before subjecting to FACS analysis. BD FACSAria and LSRFortessa were used for cell sorting and cell-cycle analysis. The gating strategy was chosen in a manner so that only Flag-transfectants were sorted for DNA content analysis.

3.3. Molecular Biology

3.3.1. DNA analysis and manipulation

3.3.1.1. Polymerase chain reaction (PCR)

Polymerase chain reaction (PCR) was used to amplify DNA fragments from plasmid DNA according to the following PCR set-up program below. Recognition sequences specific to restriction enzymes were included into designed primer pairs and are summarized in table X. Reaction conditions mainly varied in annealing temperature (primer-dependent) or the duration of elongation step (depends on amplicon's length).

Table 10. List of primers and restriction sites used for PCR

Target sequence	Forward primer	Reverse primer	Used Restriction enzyme
NG2 DEL	ATATCTAGAATGCTTCTCGGCCCGGGACA	ATAGGATCCCCCACCAGTACT	XbaI(Fwd), BamHI(Rev)
NG2 ICD (2251-2327 aa)	ATATCTAGAATGCTCCGCAAACGCAACAAG AC	ATAGGATCCCCCACCAGTAC	XbaI(Fwd), BamHI(Rev)
NG2ICDΔNL S (2259-2327 aa)	ATAGAATTCATGCACGATGTCCAGGT	GCTTTCTAGATCCCACCAGTA CT	EcoRI(Fwd), XbaI(Rev)

Table 11. PCR Components

Component	Amount
DNA template	50 ng
Forward Primer (10 μM)	2 μl
Reverse PRIMER (10 μM)	2 μl
DNTPs mix	4 μl
reaction buffer (10X)	5 μl
Pfu polymerase	1 μl
nuclease free DDH2O	fill to 50 μl

Table 12. PCR Cycler Program

Function	Temperature	Time	Step
Initial denaturation	95°C	1-2 min	1
Denaturation	95°C	30 secs	2
Primer annealing	60-65°C	30 secs	3
Extension	72°C	1 min / kb	4, go to Step 2 (19x- 35x)
Final extension	72°C	10 min	5

After final extension of 10 min, samples were cooled to 4°C and subsequently analyzed or stored at -20°C for further use.

3.3.1.2. DNA purification and analysis

The QIAquick® PCR Purification Kit (Qiagen) was used according to manufacturer's protocol and DNA was eluted with nuclease-free H₂O. Concentration of the eluted DNA samples were determined with the Nanodrop® 1000 photospectrometer (Thermo Scientific) and subsequently PCR products were analyzed by agarose gel electrophoresis.

3.3.1.3. Agarose gel electrophoresis

According to the DNA product size, 1-2% Agarose gels were prepared fresh in 1x TAE Buffer by dissolving the agarose in a microwave. After cooling it down, 0.01% Ethidium Bromide was added, and the gel was poured into a horizontal gel chamber to solidify. The samples were mixed with 6x Loading dye (Fermentas), loaded on the gels and ran together in 1X TAE buffer with the Gene ruler 1 kb DNA ladder (Fermentas) until desired separation was achieved. Afterwards, images of the gels were taken and printed with a UV-based gel documentation system.

3.3.1.4. DNA extraction from agarose gel

The corresponding DNA fragments were excised from the gel with a clean razor blade and the DNA was isolated using the *QIAquick Gel Extraction Kit* (Qiagen) according to the manufacturer's instructions.

3.3.1.5. Restriction enzyme digestion

Restriction enzyme digestion (purchased from NEB) were done according to Manufacturer's protocol. Volume and amounts were varied depending on whether a single or double digestion was being performed. The total volume was finally filled with ddH₂O up to 50µl.

3.3.1.6. Ligation and transformation

Ligation of DNA inserts with the chosen vector backbone was carried out using the T4 DNA Ligase (Promega) according to the manufacturer's instruction. Ligation products were amplified in transformation competent TOP10F' Escherichia coli cells (Invitrogen). For transformation of TOP10F' cells, after thawing, 50 µl cell suspension was taken and mixed with 10 µl of ligation product. The mixture was kept on ice for 30 min and subjected to heat-shock at 42°C for one minute. After adding 500 µl of pre-warmed, antibiotic-free LB medium, cells were incubated for 30 min at 37°C before an appropriate volume was spread on antibiotic-containing LB-Agar plates. The agar plates were incubated overnight at 37°C in a bacterial incubator and single colonies were selected for plasmid amplification and preparation.

3.3.1.7. Plasmid preparation

For Miniprep cultures, individual bacterial colonies from the agar plates were picked and incubated in 4 ml LB medium containing selected antibiotics on a shaker at 37°C for overnight. Plasmid preparation from transformed bacteria cultures was performed using the PureLink™ Quick Plasmid Miniprep Kit (Invitrogen). Pelleted plasmid was extracted from the column with 30 µl of ddH₂O.

To set up Maxiprep cultures, 100 µl of Miniprep culture or a filter tip covered with bacterial glycerol stocks were added to 300 ml of LB medium containing suitable antibiotics. Cultures were incubated overnight at 37°C in a shaking bacterial incubator. Plasmid DNA was extracted using PureLink™ HiPure Plasmid Maxiprep Kit (Invitrogen) according the manufacturers' protocols. Plasmid DNA was eluted with 200 µl ddH₂O and concentration was measured using Nanodrop and afterwards stored in -20°C for

further use. The following NG2 expression constructs were created with the p3X-Flag-CMV-14 (Sigma) vector backbone.

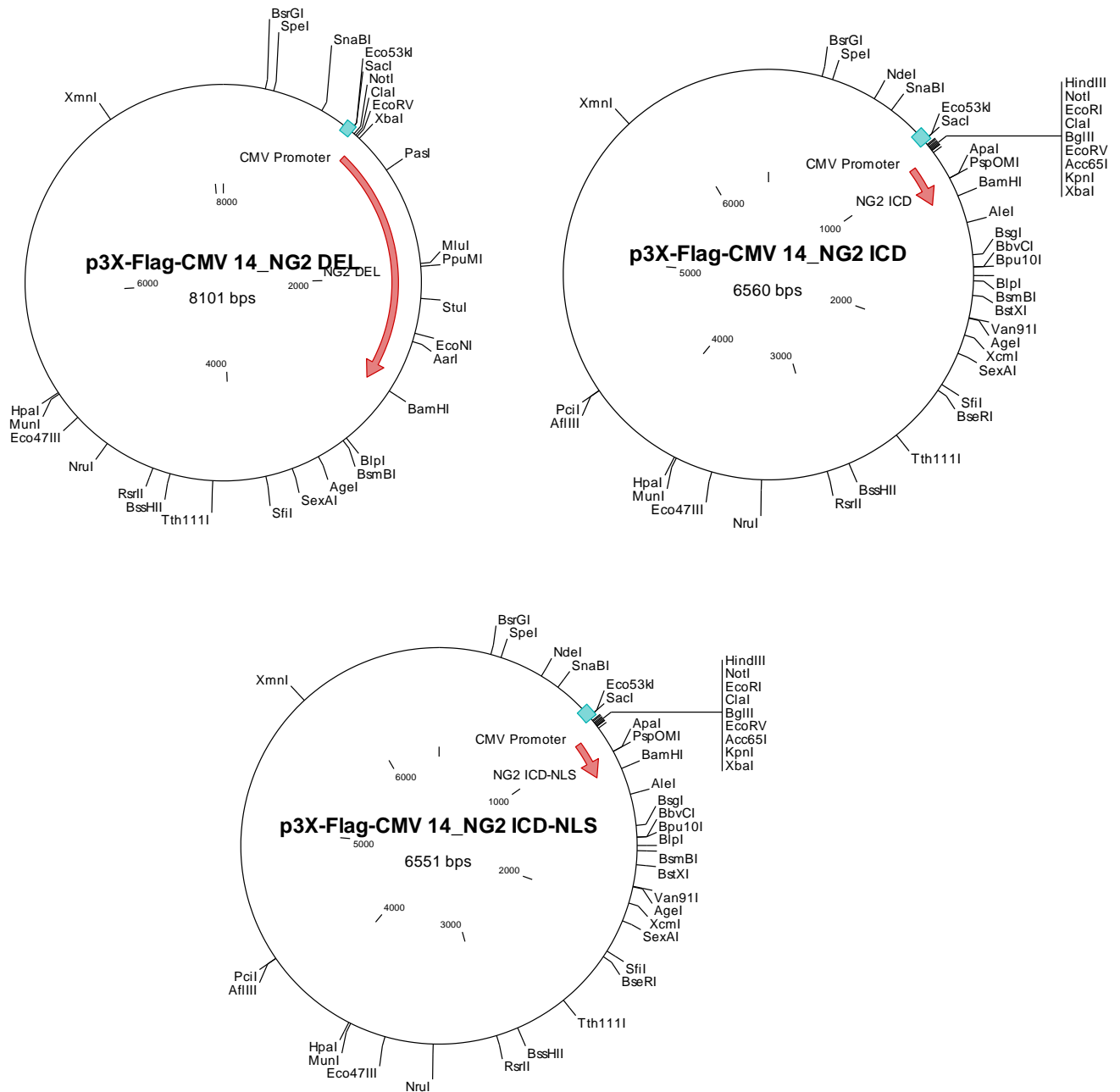


Fig 3.2. Diagrammatic representation of NG2 expression constructs used in the study

3.3.2. RNA analysis

3.3.2.1. Isolation of total RNA from cultured cells

Oli-*neu* cells were washed with cold PBS and directly lysed with 700 μ l QIAzol Lysis reagent, vortexed for 15 seconds and stored at -80°C . Total RNA was extracted with the miRNeasy® Mini Kit (Qiagen) according to the manufacturer's instructions, including DNase digestion using the RNase-free DNase Kit (Qiagen). 30 μ l of nuclease-free water was used to elute RNA from the column, concentration was determined using Nanodrop® 1000 and samples were stored at -80°C immediately or used for cDNA synthesis.

3.3.2.2. Reverse transcription cDNA synthesis

cDNA was synthesized by using the Transcriptor First Strand cDNA Synthesis Kit (Roche) according to the manufacturer's instructions with minor modifications. Initially, 100 ng of RNA and 2 μ l of random hexamer primers were mixed and heated for 10 min at 65°C and immediately placed on ice. The RT master mix, including 5U of Transcriptor Reverse Transcriptase was added and RT reaction was performed according to Table 13 in a thermal cycler, yielding cDNA libraries directly used in quantitative real time PCR or normal PCR reactions.

Table 13. RT-PCR set up

Component	Amount
RNA template	100 ng
RT master mix	4 μ l
dNTP mix	2 μ l
Reverse Transcriptase	0.5 μ l
RNAasin	0.5 μ l
Random hexamer primers	2 μ l
nuclease free ddH ₂ O	fill upto 20 μ l

3.3.2.3. Quantitative PCR (qPCR)

The cDNA libraries were analyzed with gene specific Taqman® Gene Expression Assays (Table 15) using the Taqman® Gene Expression Master Mix (Applied Biosystems) according to the manufactures' instructions and a total reaction volume of 10 µl. In each reaction, 1.0 µl cDNA was used and samples were run in duplicate or triplicate on a StepOne™ Real-Time PCR system following the mentioned cyclers program. In no template-controls (NTC) cDNA was replaced by nuclease-free water. Relative gene expression was calculated by the $\Delta\Delta C_t$ method with the StepOne Software 2.2.2 using *Pgk1* or *Gapdh* as a reference gene.

Table 14. RT-PCR Program

Step	Temperature	Time
Annealing	25°C	10 min
Reverse Transcription	55°C	30 min
RT Enzyme deactivation	85°C	5 min
Storage	4°C	End

Table 15. Taqman Gene expression assays

Target gene	Catalogue number	Source
Eef2	Mm01171435_gH	Applied Biosystems
Fmr1	Mm01339582_m1	Applied Biosystems
Mbp	Mm01262037_m1	Applied Biosystems
Pgk1	Mm00435617_m1	Applied Biosystems
Dlg4 (PSD-95)	Mm00492193_m1	Applied Biosystems
Gapdh	Mm99999915_g1	Applied Biosystems

3.3.2.4. mRNA stability assay

For studying mRNA stability, Oli-*neu* cells were grown in 6 cm culture dishes one day prior transfection. 48 hours post-transfection with NG2 ICD and control expression constructs, cells were treated with a transcription blocker, DRB (5,6 Dichlorobenzimidazole 1-β-D ribofuranoside). DRB was dissolved in ethanol and used at a final concentration of 100µM. The optimal timepoint of DRB treatment was first

established and subsequently cells were harvested and collected for RNA extraction and analysis followed by qPCR as described above.

3.4. Protein Biochemistry

3.4.1. Cell lysis

For preparing post-nuclear (PN) lysate, cells were washed twice with cold 1x PBS before being scraped off on ice in cold triton lysis buffer (4 °C) containing Complete Protease Inhibitor Cocktail (Roche) using a rubber policeman. Lysates were incubated on a rotor at 4 °C for 20-30 min and subsequently centrifuged (1000 x g, 4 °C, 10 min) to remove cellular debris and nuclei. Lysates were immediately used or stored at – 20 °C. If needed, protein concentrations were determined with BCA protein Assay Kit (Novagen) according to the “Enhanced Assay” protocol.

For subcellular fractionation assay, cells were washed (1X PBS) and scraped off with a rubber policeman on ice and directly lysed on dish with ice-cold cytosolic lysis buffer (1X PBS+ 1% NP-40, 1X Protease inhibitor cocktail). Lysates were incubated on a rotor at 4 °C for 20-30 min and subsequently centrifuged (2000 x g, 4 °C, 10 min). Supernatants enriched with cytosolic fraction was collected and the pelleted nuclei was digested with nuclear lysis buffer (20 mM Tris-HCl (pH 7.4), 150 mM NaCl, 10 mM MgCl₂, 1% TX-100, 2.5 mM Beta-glycerophosphate, 1 mM NaF, 1 mM DTT, 2mM EDTA, 10% glycerol 10 unit of Benzonase, 1X Protease inhibitor cocktail.) for 1 hour on rotor at 4 °C for 40-60 min with occasional mixing. Samples were centrifuged at 7000 g for 10 mins and supernatant was collected which comprises of nuclear proteins.

3.4.2. SDS-PAGE and Western blotting

Proteins were separated according to size by Sodium Dodecyl Sulfate Polyacrylamide Gel Electrophoresis (SDS-PAGE). Novex® NuPAGE® SDS-PAGE Gel system (Invitrogen) using 4-12% Bis-Tris gradient gels with MOPS or MES running buffer was used for this purpose. Protein lysates were diluted in appropriate volumes of 4X sample buffer and heated to 90°C for 5 minutes prior loading into the gel wells next to 5-10 µl of the Precision Plus Protein Standard (Bio-Rad). Electrophoresis was performed at constant 150V until the desired separation achieved. Proteins were transferred from the

gel on a polyvinylidene fluoride (PVDF) membrane (Immobilon-P transfer membrane, 0.45 µm pore size, Millipore) for 3 hours at 200mA with transfer buffer (see buffer recipe table).

After blotting, membranes were briefly washed in dH₂O and incubated in blocking solution for at least 30 min to block unspecific antibody binding to the membrane. Primary antibodies were applied in blocking solution over night at 4 °C on a shaker. Before applying secondary antibodies coupled to horse radish peroxidase (HRP) diluted in blocking solution, the membrane was washed three times with PBST for 10 min each. After a 30 min incubation time, secondary antibodies were removed, and membrane was again washed three times for 10 min each using PBST. Afterwards, proteins were visualized on X-Ray films by enhanced chemiluminescence (ECL) reaction using a OptiMax X-Ray film processor and subjected to quantitative analysis using the ImageJ software. Membranes were dried and kept at – 20 °C for long-term storage.

For studying the phosphorylated mTOR cascade, for each experiment, same cell lysate was used, and the experiment was repeated independently more than three times. Two western blots were run in each experiment, one is for the non-phosphorylated protein level (example, mTOR) and another is for studying the phospho-specific level (example; p-mTOR) as they run on the same molecular weight. First, every studied protein (mTOR and p-mTOR) level was normalized to its corresponding loading control (Example; GAPDH/tubulin) and then the normalized phospho-protein was divided by normalized non-phosphorylated protein level to get the fold-change only specific for the phospho-epitope.

3.4.3. Silver and Coomassie staining of the gel

Before transferring the separated protein on to a blot, gel was stained with Silverquest Kit (Invitrogen, LC6070) according to manufacturer's protocol or with Coomassie BrilliantBlue G-250 (SERVA) staining solution according to the instructions. Gel was washed with dH₂O until the background stain was completely removed and image was taken using the Epsilon scanner.

3.4.4. Immunoprecipitation (IP)

Cells were transfected with NG2 ICD-Flag or with a positive control protein; Bacterial Alkaline phosphatase (BAP)-flag for Flag-pull down assay. After 48 hours of transfection, cells were washed, lysed (1x PBS+ 1% TX-100+ 1x protease inhibitor), scraped off and incubated on a rotor at 4 °C. Afterwards, cells were centrifuged (3000 g, 10 mins) and supernatant, enriched with cytosolic proteins were collected. Prior IP, protein concentration of the control and ICD-transfected lysate was measured by using BCA assay. Generally, 1-1.5 mg of protein was taken for doing IP. Magnetic, pre-conjugated anti-flag dyna beads (Sigma, M8823) were equilibrated with 1X TBS prior use and 60 µl of beads was incubated with pre-cleared (10,000 g, 10 mins, 4 °C) protein lysate for 2 hours on a rotor at 4 °C. Afterwards, the beads were washed three times (5 mins, each wash) with wash buffer (1X TBS, 0.3% Triton-X) by using a magnetic rack (Dynamag, Invitrogen) and the immunocomplex was eluted with 80 µl of 2X LDS buffer and heated at 80°C for 10 mins. The bead was discarded after separation with magnetic rack and the separated lysate containing the immunocomplex was taken in a clean eppendorf tube. IP samples were later used in various experiments including CoIP and Mass spectrometry-based analysis.

3.4.5. SUnSET Assay

HEK293 and *Oli-neu* cells were plated 1 day before transfection with different NG2 expression constructs. 48 hours post-transfection, cells were incubated with puromycin (10 µg/mL, diluted in ddH₂O) for 15-20 mins in culture medium and immediately lysed afterwards directly on culture dish with ice-cold lysis buffer (PBS + 0.5% TX-100 + 1X PI). Lysates were run on a 4-12% gradient gel and subjected to western blot analysis. Puromycin incorporation was investigated with anti-puromycin antibody. Anisomycin was used as a translation blocker (40 µM final conc.) to specify puromycin incorporation takes place only in growing nascent polypeptide chains.

3.5. Immunocytochemistry

For immunostaining, transfected cells, after reaching desired density, were washed three times with 1X PBS to remove residual medium and cell debris and fixed with either Roti Histofix 4% paraformaldehyde solution for 15 mins at RT or with pre-chilled

100% methanol at -20°C for 10 mins (for PCNA staining). After washing 3 times with PBS, cells were transferred into a humidified chamber and permeabilized with 0.1%-0.5% TX-100 in 1X PBS. After 5 mins, cells were washed again twice with PBS and incubated for 30 mins with blocking solution (1X PBS+ 10% HS) to prevent unspecific binding. Primary antibodies were diluted in blocking solution and cells were incubated with primary antibody according to antibody data sheet. After three times washing step with PBS, fluorescently labelled secondary antibodies diluted in blocking buffer were applied for 30 min and cells were washed again with PBS for three times. For nuclei staining, 4'6- diamidino-2-phenylindole (DAPI) was used for 2 min followed by two additional washing steps. Finally, coverslips were briefly submerged in ddH₂O for the removal of residual buffer salts and mounted in moviol on object slides.

3.6. Proteomics

3.6.1. Mass Spectrometry (MS) based analysis

The IPed samples as described previously was subjected to Mass spectrometry-based analysis with the Proteomics core facility from IMB, Mainz. 30µl of sample/IP was needed for labelling peptides with Dimethyl (DML method) and after running both forward and reverse experiment, the output was analyzed by MaxQuant Software including removal of potential common contaminants and reverse database entries. Only identified proteins with at least two peptides were allowed. The threshold was set to a default value of 2x enriched on a log₂ scale.

3.6.2. Pulsed-SILAC (pSILAC) protocol

SILAC is an invaluable tool for studying protein synthesis and turnover in response to stimuli. Furthermore, protein abundance can be monitored in a temporal fashion with the SILAC method by using a different isotopic version of an amino acid for each time point whereas pSILAC (pulsed SILAC) can quantitate the relative levels of newly synthesized proteins in one experiment and for two conditions in a given time as well as the relative levels of remaining preexisting proteins by means of a three-channel labelling.

In this experiment, SILAC-DMEM medium along with three different isotopic version of Lysine and Arginine and dialyzed FBS were purchased from IMB, Proteomics core facility.

First, SILAC-Light medium was prepared (DMEM, Lys-0, Arg-0, 10% dialyzed FBS) and cells were plated and cultured in Light medium until they reach 70% confluency. For Oli-neu cells, Modified SATO-SILAC medium was used in each case (See recipe). The next day after plating, cells were transfected with control or NG2 ICD-construct by FuGENE reagent and cells were incubated in Light medium. After 16-18 hours post-transfection, SILAC Light medium was discarded, cells were washed with pre-warmed PBS for three times. Transfected cells were replaced with 'SILAC-Medium-heavy' medium (DMEM, Lys-4, Arg-6, 10% dialyzed FBS) in one condition (e.g. for control) and 'SILAC-heavy' medium (DMEM, Lys-8, Arg-10, 10% dialyzed FBS) in another condition (e.g. for ICD). Parallely, in a same but separate experiment, transfected cells were reverse-labelled (e.g; control with 'Heavy' and ICD-TF with 'Medium-heavy'). After 18-20 hours post-incubation, mediums were discarded, cells were washed and trypsinized with TE-Low and pelleted down (800 rpm, 10 mins). Cells were resuspended in PBS and counted with a hemocytometer. Equal number of cells were taken from each experimental condition and mixed in a 1:1 ratio. Cells were immediately lysed with lysis buffer (PBS, 1% TX-100, 1X PI) on ice and protein concentration was measured by BCA method. Desired amount of lysate from forward and reverse-labelled conditions were sent to IMB proteomics core facility, Mainz for quantitative MS analysis.

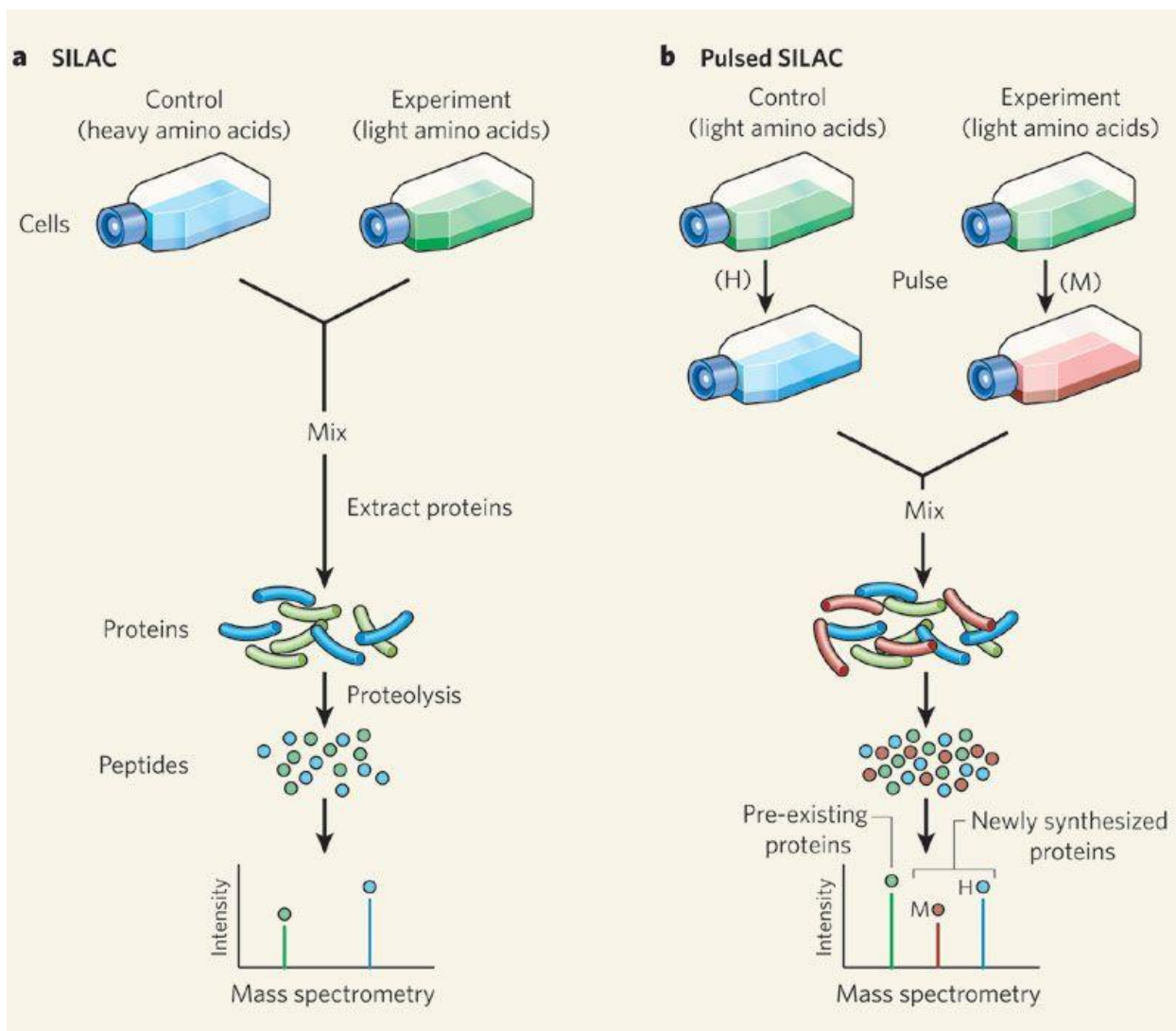


Fig 3.3. Mechanistic principle of conventional SILAC and pulsed SILAC (Taken from Zissimos Mourelatos, Nature, 2008)

Statistical analysis

Each experiment was repeated independently at least three or more times. The numerical data of multiple experiments is expressed as mean \pm standard error of the mean (SEM). Statistical analysis was done using Excel and Graph Pad Prism. For significance analysis, normal distribution was tested by the Shapiro-Wilk Normality test. For parametric distributed datasets two tailed *t*-test was applied: In the case of non-parametric distribution, Mann-Whitney or Wilcoxon Signed rank test was used. Significance was classified as follows: *, $p \leq 0.05$; **, $p < 0.01$; ***, $p < 0.001$; n.s. $p > 0.05$.

Results

4.Results

In this thesis, the cellular localization of the NG2 ICD after cleavage of NG2 was addressed. This also includes the role of the predicted NLS sequences. Furthermore, as most of the ICDs liberated by RIP is involved in regulating gene expression, cell signaling pathways and cellular processes, function of NG2 ICD released after cleavage was addressed.

4.1.1. Generation and functional analysis of NG2 expression constructs

To address the localization and function of released NG2 ICD, different NG2 expression constructs were derived from pRK5 constructs used in the study by Sakry et al., in 2015, by PCR amplification and sub-cloned into a Flag-tagged vector backbone (p3X-Flag CMV14 expression vector, c-terminally tagged (Fig 4.1). NG2 DEL expresses a short recombinant version of full-length NG2 (consisting the signal sequence, one-fourth of the extracellular portion including two laminin G-type motifs, a transmembrane domain, and intracellular region).

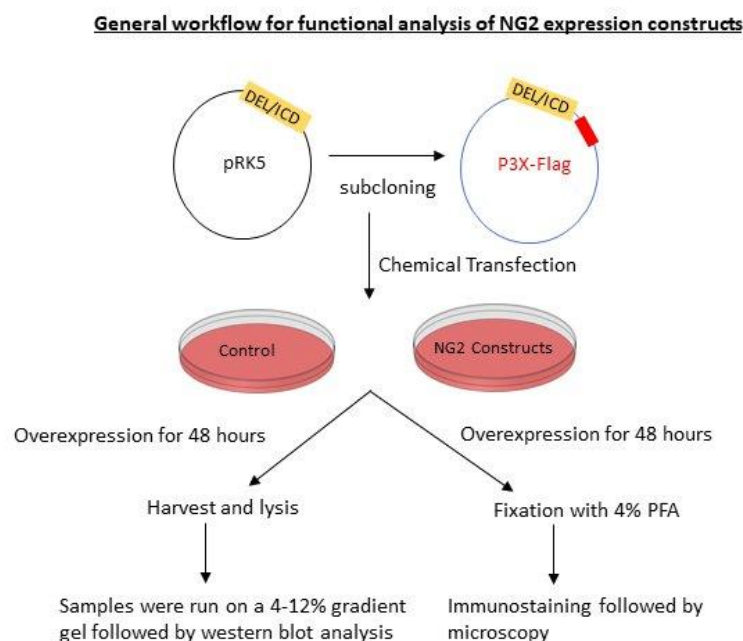


Fig 4.1. General workflow for functional analysis of NG2 expression constructs

Two other constructs, expressing only the intracellular domain (NG2 ICD, AA 2251-2327 (UniProt: Q8VHY0) and without the predicted Nuclear Localization Signal (NLS) of ICD (NG2 ICD Δ NLS, AA 2259-2327) were generated as well.

For studying the expression of the generated flag-tagged constructs, OPC were transfected, and 48 hours post-transfection, lysates were prepared and analyzed by western blot (WB) analysis. Fig.4.2. shows that NG2 DEL generates two distinguishable fragments, one at 65 kD indicating the full-length (FL) protein and another at 14 kD corresponding to the membrane-bound CTF. NG2-ICD runs at ~10 kD and owing to the deletion of predicted NLS motif (2251-2259 bases of ICD sequence), NG2 ICD Δ NLS runs (~9 kD) just below ICD. In this experiment, Na-butyrate was used to enhance the protein expression *in vitro* as ICD Δ NLS, being small-sized and truncated construct, was unstable and hard to detect in WB with NG2-cyto specific antibody. The expression of the flag epitope was also checked by probing the membrane with an anti-flag antibody.

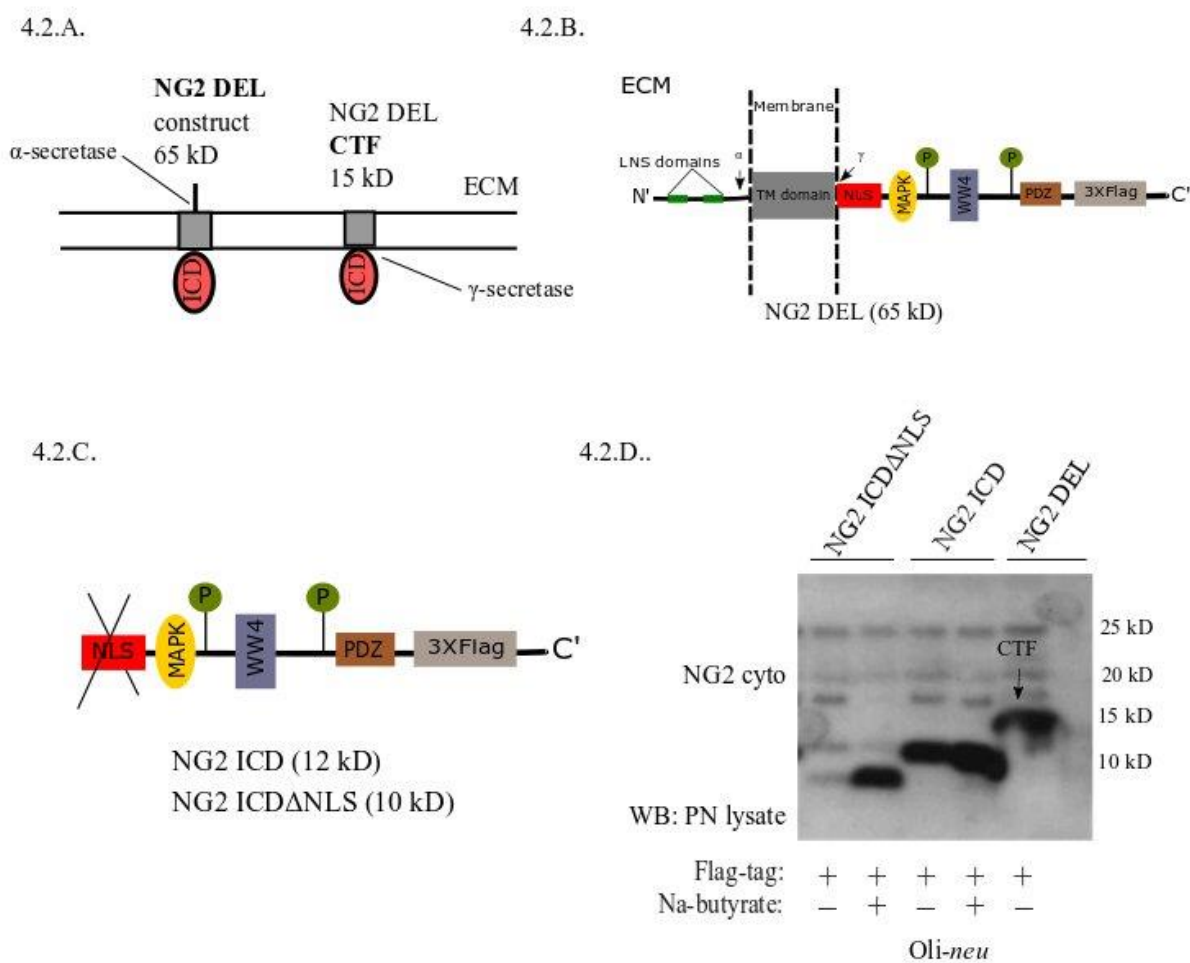


Fig.4.2. Diagram of used NG2 expression constructs and their expression. 4.2. (A) Schematic representation of NG2 protein undergoing Regulated Intramembrane Proteolysis (RIP) by the sequential action of α and γ -secretases. 4.2. (B, C) Schematic representation of the NG2 DEL, NG2 ICD and ICD Δ NLS expression constructs used in this study. All NG2 expression constructs were tagged with 3X-Flag (C-terminal). 4.2. (D) Western blot analysis of post-nuclear (PN) cell-lysates of the OPC cell-line, *Oli-neu* transfected with various NG2 expression constructs. Flag-tagged constructs revealed their size-based differences, NG2 ICD runs at 11 kD, and NG2 ICD Δ NLS (NLS was deleted) runs just below ICD at 10 kD. NG2 DEL (65kD) strongly shows processed membrane-bound CTF (15 kD) at the shown lower molecular masses. Na-butyrate was used only in this experiment to enhance the expression of ICD constructs. (Taken from Nayak T. et al., 2018)

4.1.2. Nuclear localization of NG2 ICD was detected by subcellular fractionation assay

To analyze the localization of cleaved NG2 ICD, subcellular fractionation assay was performed with *Oli-neu* cells overexpressing flag-tagged NG2 expression constructs.

The separated cytoplasmic and nuclear lysates were analyzed by western blot (WB) and probing the membrane with anti-flag antibody revealed the presence of NG2 ICD in both cytosolic and nuclear fraction with a higher level of ICD in the cytosol. NG2 ICD Δ NLS was used as an additional control here to check the function of the predicted NLS motifs. In contrast to NG2 ICD, ICD Δ NLS expression was only detected in the cytosolic but not in the nuclear fraction indicating the function of the NLS motifs in directing ICD to the nucleus. (Fig 4.3.) Lamin B and tubulin was used as a nuclear and cytosolic marker respectively, and the very low detection level of Lamin B in cytosolic fraction and undetected tubulin in nuclear fraction indicates about the purity of the performed fractionation.

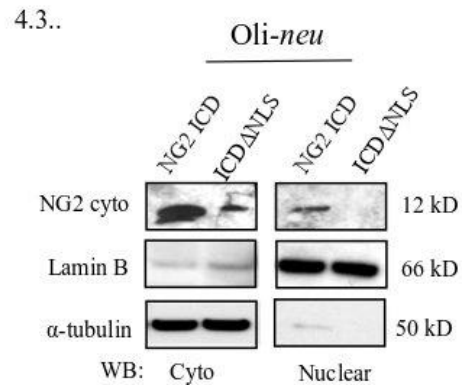


Fig.4.3. Sub-cellular fractionation assay. Fractionation assay was done from Oli-neu after overexpressing ICD or ICD Δ NLS for 48 hours. Lamin B and α -tubulin were used as nuclear and cytosolic markers respectively. NG2 ICD was found in nuclear fraction whereas NG2 ICD Δ NLS expression was limited to cytosolic fraction only. (Taken from Nayak T et al., 2018)

4.1.3 High-resolution Imaging confirmed the nuclear presence of cleaved NG2 ICD in cultured OPC

To confirm the specificity of the fractionation assay result, as a next approach, high-resolution confocal microscopy was used. NG2 ICD-flag or ICD Δ NLS-flag overexpressing Oli-neu cells were immunostained with anti-flag antibody (in red). H2B(green) was used as a nuclear marker, and DAPI (blue) was used to stain nuclei. Flag staining was detected as a homogeneous pattern over the cell including nuclei in

case of ICD, whereas ICD Δ NLS revealed extranuclear staining excluding nuclei. (Fig 4.4. A). For further validation, z-stack images of transfected cells were taken and analyzed by ImageJ, 3D viewer plugin where cells were represented as an orthogonal section and both the XY and YZ format of ICD-transfectants detected the presence of flag staining (red) inside the nucleus. In contrast to that, ICD Δ NLS showed no staining inside the nucleus. Tubulin (green) was used as a nuclear envelope marker. (Fig 4.4.B). Supporting the subcellular fractionation assay result, immunostaining also revealed that the expression of cleaved ICD was much higher in the cytosol than nucleus although ICD was detected in a low level in nucleus too in *Oli-neu* cells.

In a separate experiment, to assess whether nuclear import of cleaved NG2 ICD is an active process, *Oli-neu* cells were transfected only with ICD-flag constructs and treated with Ivermectin (Sigma). Ivermectin is a potent inhibitor of Imp α / β 1-dependent nuclear transport, and thus cells accumulate classical NLS-dependent active import of proteins when treated with Ivermectin. However, Ivermectin is cytotoxic and was used in this experiment at a very low concentration of 10 μ M after 24 hours of transfection. Ivermectin was added in the culture medium just 2-4 hours before fixing the cells. From Fig 4.4.C, it was evident that ICD expression was restricted in the peri-nuclear region only when treated with Ivermectin while Ivermectin-untreated ICD-expression was detected again in a homogeneous pattern including nuclei.

Altogether, these experiments support in favor of NLS-dependent active transport of cleaved NG2 ICD to the nucleus at a low level compared to its cytosolic expression.

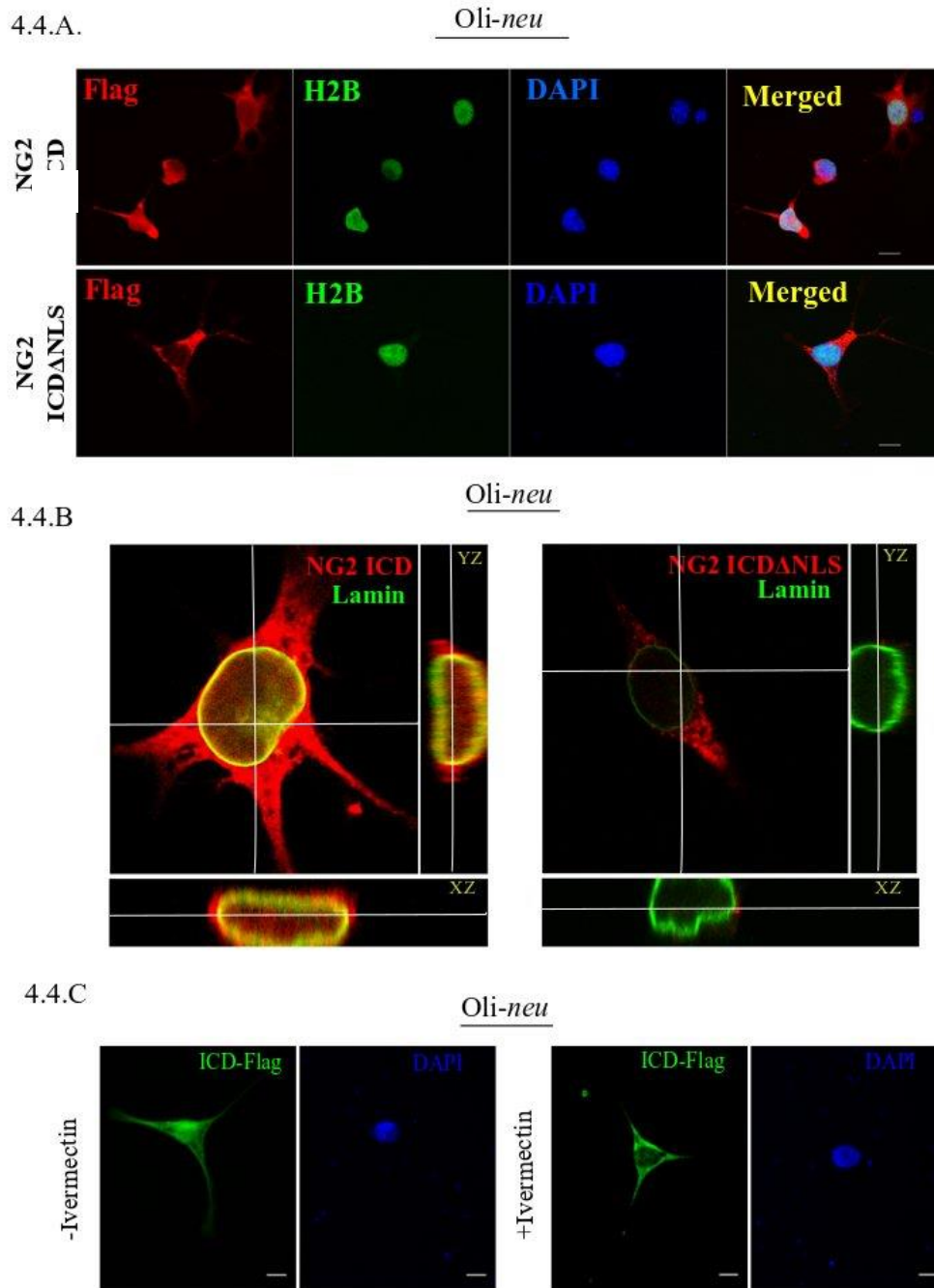


Fig.4.4. High-resolution imaging of NG2 expression constructs overexpressing Oli-neu cells. (A). Confocal laser scanning microscope images (z-stack, max. intensity projection) of Oli-neu expressing NG2 ICD or ICD Δ NLS (flag; red). Cells were immunostained with anti-flag antibody. NG2 ICD shows a distinguishable homogeneous staining pattern including nucleus where in case of ICD Δ NLS, expression remained cytosolic. H2B (green) and DAPI (blue) were used as nuclear markers. (B) Three-dimensional orthogonal view of a z-stack image of an Oli-neu cell showed the presence of NG2 ICD (red) within the nucleus, whereas ICD Δ NLS expression was limited to the cytosol and peri-nuclear area. Lamin B (green) was used as a nuclear envelope marker. (Scale bar= 10 μ m). (C) Oli-neu cells overexpressing ICD were treated with a nuclear import inhibitor, Ivermectin. Treatment with Ivermectin limited nuclear expression of ICD as shown in the confocal images (Scale bar= 10 μ m). (Taken and modified from Nayak T. et al., 2018)

4.2. Characterization of ICD-interactome

4.2.1 Investigation of ICD-interactome by IP-MS study

To elucidate the function of NG2 ICD, it was important to characterize its interactome. HEK293 cells were transfected with ICD-Flag or BAP-Flag (control) constructs and 48 hours post-transfection, cell lysate was prepared, and immunoprecipitated with pre-conjugated, magnetic anti-flag antibody beads. HEK cells were chosen to perform immunoprecipitation (IP) due to higher transfection efficiency. A schematic representation of the designed IP-MS experiment is given below. The IPed samples were subjected to Mass Spectrometry (MS) based analysis which was performed by IMB proteomics core facility, Mainz. Three independent experimental replicates were sent for MS analysis.

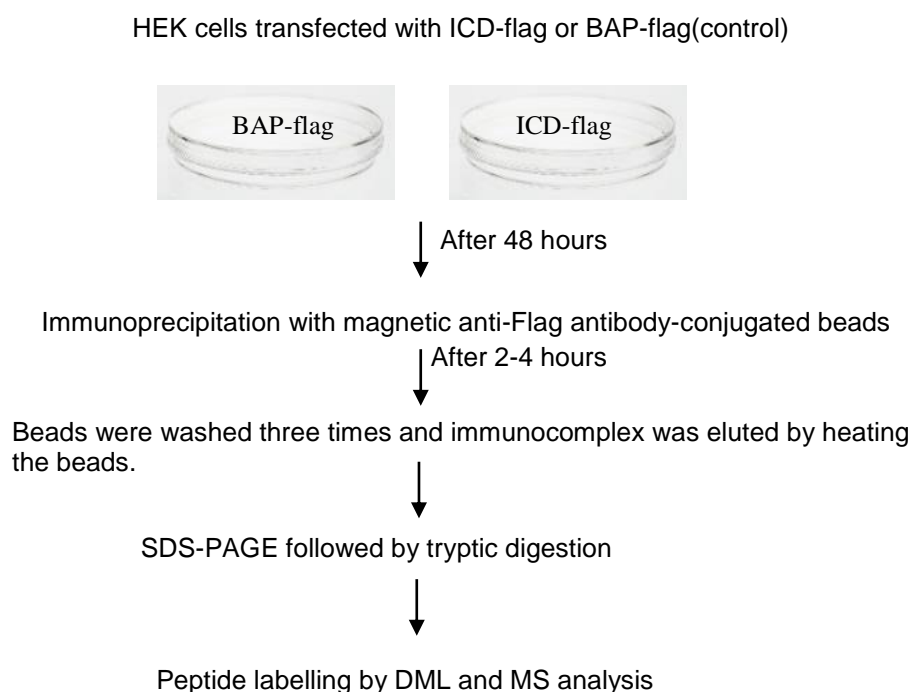


Fig.4.5. Schematic representation of IP-MS workflow.

The samples were analyzed by MaxQuant Software (www.Maxquant.org). The database, used for analysis, was restricted to peptides and the corresponding proteins derived from human species and served as the basis for the actual selection of potential candidates. As a first filtering method, only identified proteins with at least two peptides

were allowed. The second filtering contains an overview of identified protein groups present in forward and reverse experiment with at least one detected ratio.

The threshold was set to a default value of 2x enriched. The common contaminations, appearing regularly in MS analyses including keratins and IgG proteins were discarded from the provided lists of identified proteins.

4.2.2 Gene Ontology-based analysis of ICD-interactome.

Table 16 summarizes the top 25 candidates detected to be enriched in NG2-ICD_IP samples, passing the threshold of the selection criteria mentioned above and these candidates appeared at least twice in the three independent IP-MS analysis. Among the topmost candidates, several translation factors including ribosomal subunits were highly upregulated. The output also indicates precipitated proteins that are actively associated with DNA unwinding (XRCC5, XRCC6) and DNA replication process (MCM7, MCM3) and proteins that regulate the transcription machinery (CNBP, GTF II-I, PHF5A).

Table 16. List of top 25 putative interaction partners of cleaved NG2 ICD found by IP-MS study.

Gene ID	Protein Name	Average Fold-change (ICD/CNT)	Average Sequence Coverage (%)
EEF2	Elongation factor 2	5.88	57.5
HSPA1A	Heat shock 70 kDa protein 1A	5.35	58.5
PCMT1	Protein-L-isoaspartate O-methyltransferase	4.49	31.75
PRPS1	Ribose-phosphate pyrophosphokinase 1	3.6	34.15
EIF4B	Eukaryotic translation initiation factor 4B	3.58	20.1
KLHL9	Kelch-like protein 9	3.44	28.3
ERP44	Endoplasmic reticulum resident protein 44	3.36	22.56
EIF4A1	Eukaryotic initiation factor 4A-I	3.23	38.75
EEF1G	Elongation factor 1-gamma	3.2	32.85
XRCC6	X-ray repair cross-complementing	3.16	13.15

	protein 6		
XRCC5	X-ray repair cross-complementing protein 5	3.12	10.8
TCP1	T-complex protein 1 subunit alpha	3.04	25.25
PRDX1	Peroxiredoxin-1	2.95	53.5
MCM7	DNA replication licensing factor MCM7	2.95	11.55
GNB2L1	Guanine nucleotide-binding protein subunit beta-2-like 1	2.82	31.1
SERPINH1	Serpin H1	2.42	17.4
PCBP2	Poly(rC)-binding protein 2	2.41	23.15
MCM3	DNA replication licensing factor MCM3	2.2	12.5
RPS28	40S ribosomal protein S28	2.19	36.6
RPS12	40S ribosomal protein S12	1.96	30.7
CNBP	Cellular nucleic acid-binding protein	1.94	36.75
PHF5A	PHD finger-like domain-containing protein 5A	1.51	33.65
EIF3	Eukaryotic translation initiation factor 3	1.46	14.35
GTF2I	General transcription factor II-I	0.83	14.3
EWSR1	RNA-binding protein EWS	0.73	11.8

Table 16. Summarization of top 25 putative interaction partners of cleaved NG2 ICD identified by IP-MS. The candidates passed the threshold criteria set by MaxQuant analysis and were altered in the same ratio in both forward and reverse peptide labeling. The candidates were found in at least two independent IP-MS analysis performed in NG2 ICD-overexpressing HEK cells.

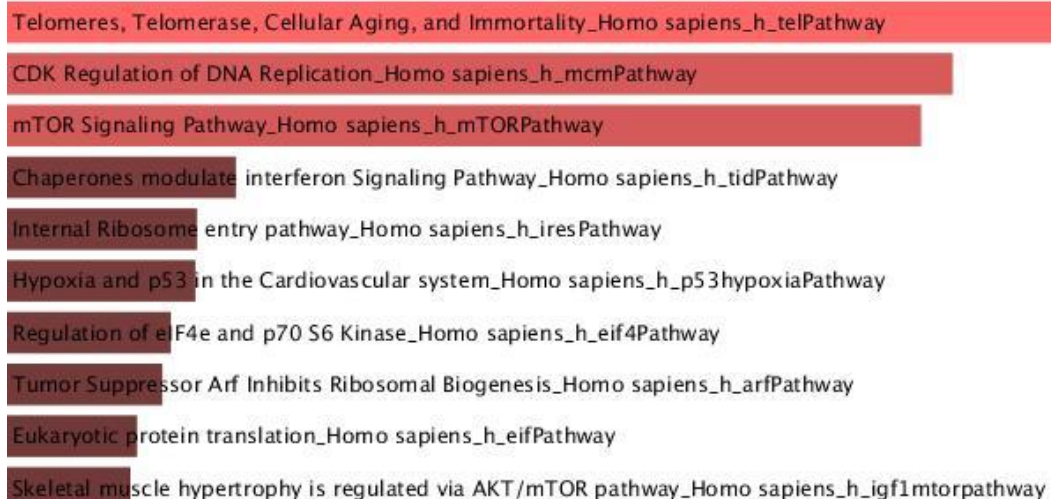
Table 17. List of enriched functional clusters of ICD-interactome by DAVID

Annotation Cluster 1	Enrichment Score: 3.3278				
Category	Term	Count	%	P-Value	Genes
Biological Process	cell-cell adhesion	5	21.73	3.85E-4	EEF1G, PCMT1, EEF2, HSPA1A, PRDX1
Molecular Function	poly(A) RNA binding	14	60.86	1.41E-10	XRCC5, CNBP, TCP1, XRCC6, EEF2, PRDX1, SERPINH1, EIF4B, RPS28, PCBP2, EIF4A1, RPS12, PHF5A, EWSR1
Annotation Cluster 2	Enrichment Score: 2.58				

Biological Process	DNA duplex unwinding	3	13.04	0.0014	XRCC5, XRCC6, MCM3
Molecular Function	DNA binding	7	30.43	0.0174	XRCC5, CNBP, MCM7, GTF2I, XRCC6, PHF5A, MCM3
Annotation Cluster 3	Enrichment Score: 1.804				
Biological Process	translational initiation	4	17.39	0.000/	EIF4B, RPS28, EIF4A1, RPS12
Molecular Function	cadherin binding involved in cell-cell adhesion	5	21.73	4.88E-4	EEF1G, PCMT1, EEF2, HSPA1A, PRDX1

Table 17. summarizes the overrepresented annotation clusters revealed by gene-ontology analysis of ICD-IP interactome by DAVID (NIH2.0). Every cluster is composed of two categories: altered biological process and molecular function. The genes associated with each cluster is also mentioned in the table.

Fig.4.6. Pathway analysis of the candidates by Enrichr database reveals the following over-regulated pathways in NG2 ICD-IP samples.



4.2.3 NG2 ICD co-precipitates with translation factors

In another experimental approach, the immunoprecipitated samples (ICD and BAP-flag IP) were run on a gradient gel, and the gel was stained by Coomassie Blue. After staining, the unique observed bands at 100 kD and 70 kD (indicated by the arrow in Fig 4.7.A) from ICD_IP lane was excised by a clean razor and sent for Mass-spectrometry based band-identification analysis. MS revealed that the two unique precipitated bands in ICD_IP lane were eEF2 (Elongation factor 2; 95 kD) and eIF4B (Initiation factor 4B; 70 kD) further confirming the data revealed in the whole IP sample analysis by MS.

To confirm that eEF2 and eIF4B co-associates with NG2 ICD, Co-IP was performed with IPed samples (HEK cells and flag pull down as previously mentioned) which were run on a gel and after transferring the separated proteins on a PVDF membrane, it was probed with anti-eEF2 and anti-eIF4B antibody. CoIP showed the co-precipitation of the translation factors (eEF2 and eIF4B) along with NG2 ICD showing the specificity of MS data. Cofilin was used as a negative control in the experiment to rule out the possibility of random pull-down of any high-abundant cytosolic proteins. Bacterial alkaline phosphatase (BAP) is a 51 kD protein and thus indistinguishable from the heavy antibody chain (55 kD) shown in the western blot (WB). The CoIP experiment was reproducibly repeated three times independently.

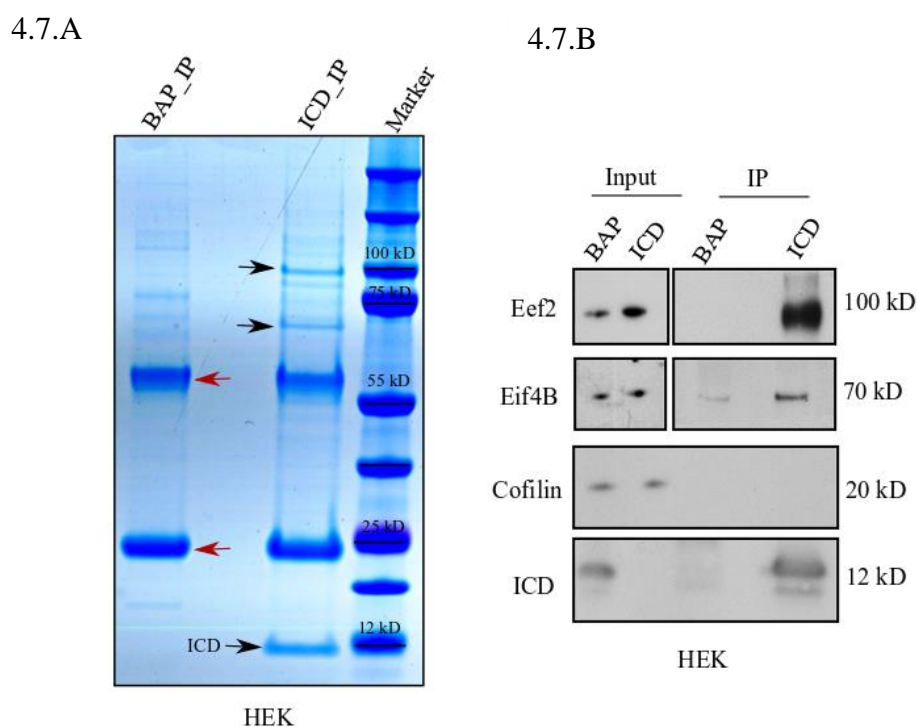


Fig.4.7. Validation of IP-MS targets by Co-Immunoprecipitation. (A) Representative Coomassie-stained gradient gel of NG2 ICD (ICD IP) and BAP-overexpressing samples (Control IP) after IP from HEK cells. Unique bands present in ICD-IP lane are indicated by black arrows, and red arrows indicate heavy and light chain (55 kD and 25 kD respectively) from anti-flag IgG used for IP. The unique bands were excised from gel between 70 and 100 kD and subjected to MS-based analysis. (B) Representative CoIP blot for validation of ICD_IP candidates (Eef2 and Eif4B) found by IP-MS screening and band-identification analysis. 10% input was loaded. Cofilin was used as negative control to check that ICD is not randomly pulling down highly abundant cytosolic control.

4.3. Translational regulation

4.3.1 NG2 ICD regulates translational rate in cultured cells

Translation was one of the highly regulated biological processes (based on Gene Ontology of NG2-ICD interactome, Fig 4.6) and co-precipitation of translation factors along with NG2 ICD was also shown. Next, it was addressed if the NG2 ICD exerts major influences on translation.

To address this, the SuNSET-WB technique was chosen. SuNSET assay was first described in the work of EK Schmidt et al., 2009 and termed as Surface Sensing of translation (SuNSET) where changes in global protein synthesis rate can be quantified

in a heterogeneous cell population *in vitro* (2009) and *in vivo* (Goodman et al., 2013). The technique relies on the incorporation of puromycin, which is a structural analogue of aminoacyl-transfer RNA (aminoacyl-tRNA; specifically, tyrosyl-tRNA) and thus when used in low concentration can be incorporated into elongating polypeptide chain by forming a peptide bond. (Fig 4.8)

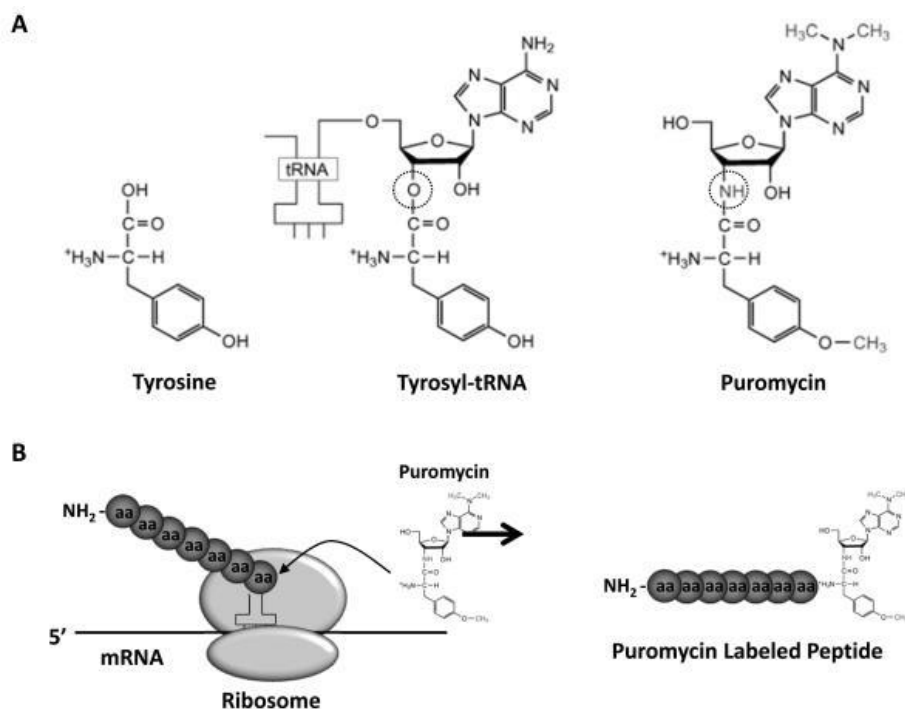


Fig 4.8. Working principle for SUnSET techniques. (Taken from CA Goodman et al., 2013)

Higher puromycin incorporation thus indicates a higher translation rate, which can be quantified using an anti-puromycin antibody.

Following this principle, HEK293 and Oli-*neu* cells, overexpressing ICD or control, were incubated with puromycin in the culture medium and lysed afterward for WB as described above. Anisomycin, a translation blocker, was used as a negative control to show that puromycin incorporation takes place only in active ongoing nascent polypeptide chains.

In addition to cell-lines, SuNSET assay was also performed with primary OPC (pOPC), obtained from the total brains of the Postnatal day (P) P6-9 of C57Bl/6N mice by magnetic isolation (MACS). At DIV1, pOPC were transfected with siCNT and siNG2, and after 24 hours of siRNA transfection, cells were incubated with puromycin as described above and subjected to WB analysis to determine active translation rate.

Since mTORC1 is the central regulator of translation, another experiment was deigned to investigate the specific involvement of mTORC1 on translation. Oli-neu cells, overexpressing control or ICD, were incubated with Temsirolimus (TM), a mTORC1 inhibitor, followed by puromycin treatment and were subjected to WB analysis.

ICD-transfectants showed increased puromycin incorporation by ~90% in HEK and ~70% in Oli-*neu* cells compared to controls, reflecting higher translation rate (Fig. 4.9.B). To validate that the observed increased translation rate is specific for cleaved NG2 ICD, NG2 DEL was used as an additional control. NG2 DEL mimics membrane-bound NG2 and undergoes cellular RIP yielding small amounts of ICD. NG2 DEL expression in Oli-*neu* resulted in a smaller increase in the puromycin signal compared to control (approximately 22%) which is likely to be mediated by endogenously cleaved NG2 ICD. Strikingly, treatment with temsirolimus (TM) abolished the NG2 ICD-driven upregulation in translation in Oli-*neu* (ICD + TM) compared to the control (TM) (Fig 4.9). Knock-down of endogenous NG2 (siNG2) in primary OPC by siRNA resulted in 40 % reduced NG2 levels, and total translation rate was also downregulated by ~30 % in pOPC transfected with siNG2 compared to control in accordance with the previous observation (Fig. 4.9).

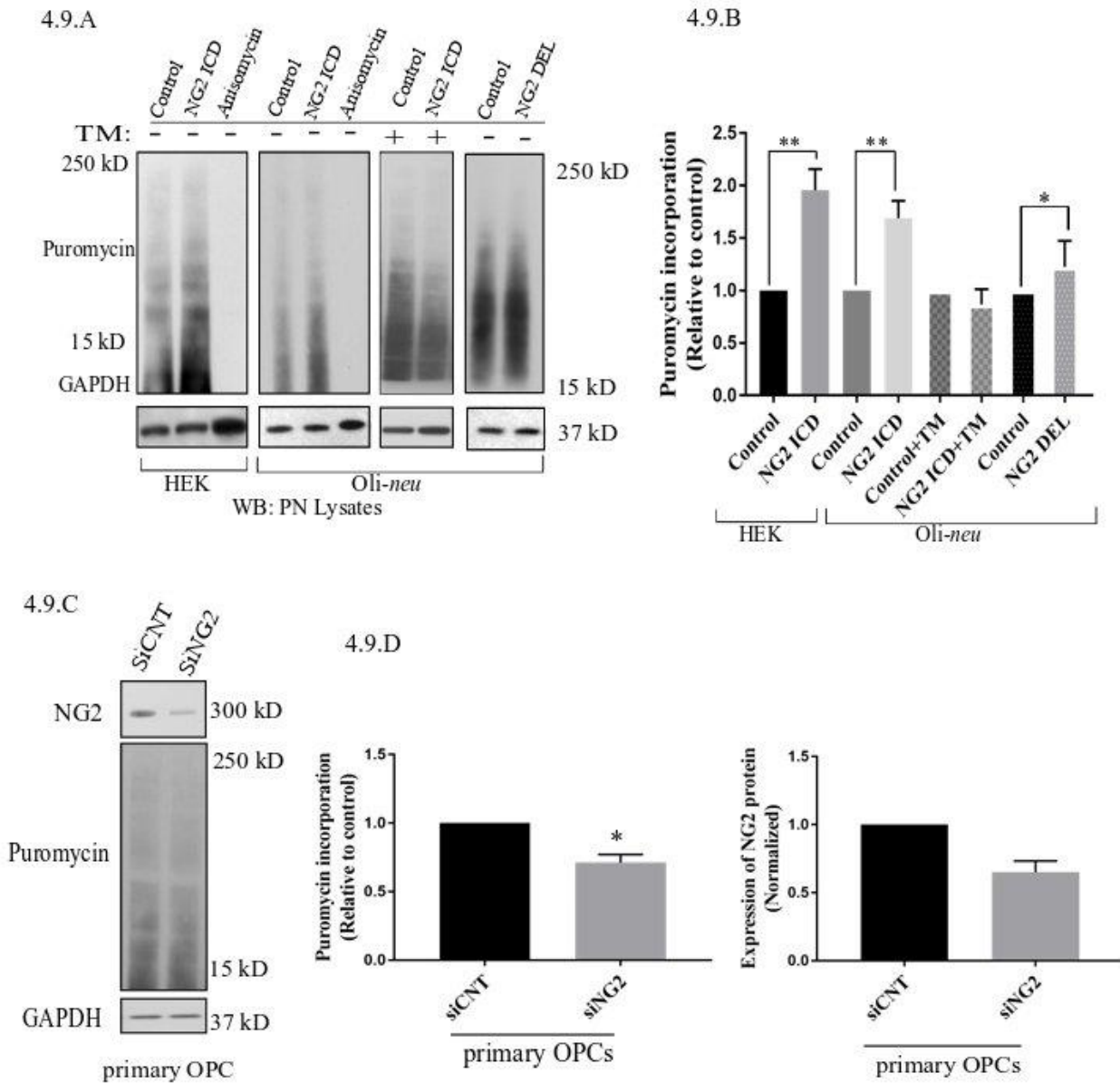


Fig.4.9. NG2 ICD upregulates translation rate. (A) HEK (n=5) and Oli-neu (n=4) cells were treated with 10 μ M puromycin after 48 hours of transient transfection with different NG2 expression constructs (DEL and ICD) or empty expression vector (control). Western blot analysis of PN cell-lysates after puromycin treatment was done with a specific antibody against puromycin, the translation blocker Anisomycin was used as a negative control. Additionally, a selective mTORC1 complex inhibitor, Temsirolimus (TM), was used (10 μ M) to investigate mTORC1 specific contribution to total translation rate between control (+TM) and ICD (+TM) (n=3). (B) Densitometric analysis was done for puromycin (from 15 kD to 250 kD) normalized to GAPDH. NG2 ICD showed an increase of puromycin incorporation (translation rate) by 70% in Oli-neu and by 90% in HEK cells compared to control. When treated with a mTORC1 inhibitor (TM), the ICD-mediated effect on translational is reduced slightly below control levels (control+TM vs. ICD+TM), indicating a mTORC1-dependent increase and a mTORC1-independent decrease of

translation by NG2 ICD overexpression. NG2 DEL mimics full-length NG2, and it predominantly expresses membrane-bound NG2 CTF but not cleaved ICD (Fig.1B&2A). NG2 DEL was used as an additional control to confer cleaved ICD-specificity in stimulating translation, and it shows only ~22% increase in translation rate compared to control (n=4). (C) Full-length NG2 knockdown (siRNA transfection) was performed in cultured primary OPC (pOPC) to check the effect on translation. (D) NG2 knockdown (siNG2) in pOPC revealed a knockdown efficiency of around 40% compared to control (siCNT), translation (puromycin level) was reduced by ~30% by NG2 knock-down. (Data represents mean \pm SEM. Statistical analysis was done by two-tailed paired *t*-test after checking the data is normally distributed by the Shapiro-Wilk normality test by PRISM (GraphPad)). (Taken and modified from Nayak T. et al., 2018)

4.3.2. NG2 ICD increases translation by modulating mTOR signaling components

After establishing ICD-mediated translational effects in HEK, Oli-neu, and pOPC, the molecular mechanism causing this effect was investigated. Gene ontology-based Pathway analysis (of ICD interactome) by DAVID already suggested involvement of mTOR signaling cascade in this regard and previous SUnSET experiments with mTORC1 specific inhibitor implied the possibility of mTOR-cascade involvement in ICD-mediated translational upregulation.

The mammalian target of rapamycin (mTOR) signaling pathway co-ordinates both intracellular and extracellular signals and plays a significant role in regulating translation, cell metabolism, growth, proliferation, and survival. mTOR is the principal component of two structurally and functionally separate enzyme complexes, mTORC1 and mTORC2, each having distinct downstream effectors. mTORC1 regulates translation by acting as a kinase for the downstream components involved in translation machinery, for example, 4E-BP1 and p70S6K1 whereas AKT, Serum and Glucocorticoid Kinase (SGK) and Protein-Kinase C (PKC) are downstream of mTORC2 (Jacinto et al., 2004, Ben-Sahra et al., 2017) and associated with cell survival and cellular metabolism (Sarbasov et al., 2005). The diagram given below represents a simple flow-chart of mTOR and the associated signaling components.

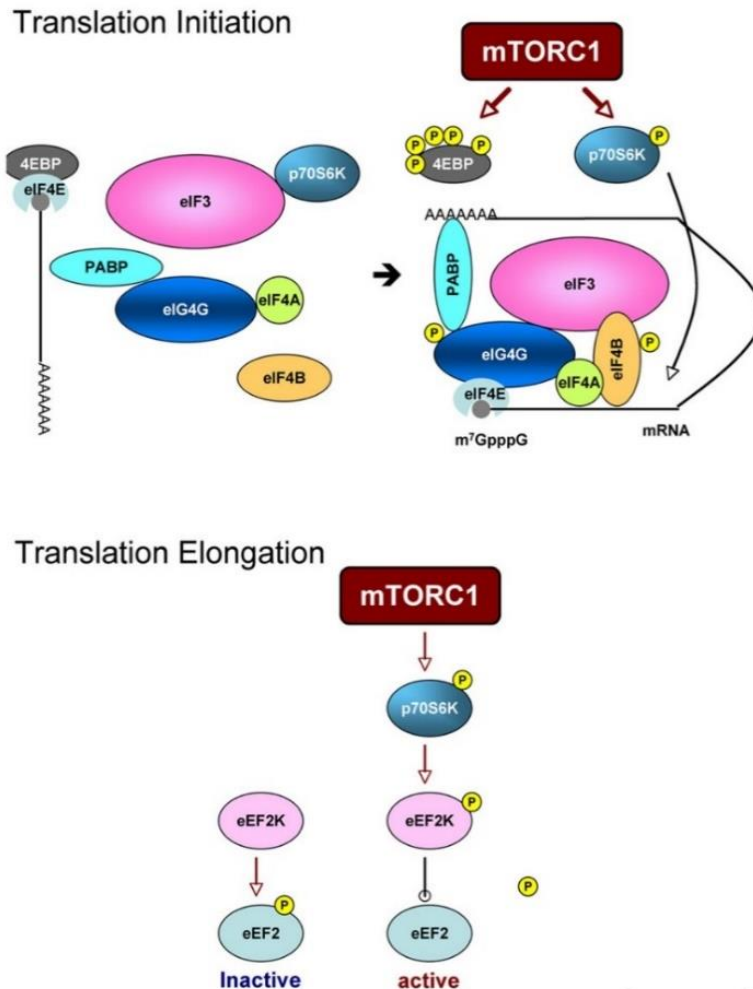


Fig 4.10. Overview of the mTORC1 signaling cascade in translation regulation (Taken from Nobuyuki Takei et al., 2014)

Given the context of ICD-mediated translational effect, the activity of mTORC1 was investigated. mTORC1 undergoes autophosphorylation at Ser2481 residue, and this phosphorylation stimulates its intrinsic catalytic activity. Phosphorylation at ser2481 is also increased upon mTORC1-activating stimulation (Soliman et al., 2010). In this study, the effect of cleaved ICD on p-mTORC1(Ser2481) was addressed. After transfection of ICD in both HEK and OPC, cells were lysed and subjected to immunoblot analysis. WB analysis revealed that ICD overexpression causes an upregulation of phosphorylated residue on an average of ~2.5 fold in both HEK and OPC. (Fig 4.11)

The ribosomal protein S6 kinase (S6K), a serine/threonine kinase that belongs to the AGC kinase family, is a well-established downstream target of mTORC1 and often used as a parameter to read out mTORC1 activity. mTOR kinase phosphorylates S6K1 at T389 which is the hydrophobic motif (HM) phosphorylation site (Pullen et al., Science, 1998, Ali et al., 2005). Usually, S6K1 is associated with eIF3 (Translation initiation factor 3) and prevents its binding to mRNAs. Phosphorylation of S6K1 at T389 causes dissociation from eIF3, and it then phosphorylates downstream components eIF4B and S6. Phosphorylation of eIF4B by S6K1 at S422 triggers its association with eIF3. (Holz et al., 2005, Shahbazian et al., 2006) and promotes translation initiation.

Following this already established signaling paradigm, phosphorylated levels of S6K1(Thr 389) and eIF4B (Ser 422) was investigated in ICD-overexpressing conditions. WB analysis revealed that ICD overexpression causes an increase of ~50% in both p-S6K1 (Thr389) and p-eIF4B (Ser 422) in HEK and OPC. (Fig 4.11)

In addition, *Oli-neu* cells were transfected with siRNA (siCNT/siNG2) to obtain endogenous NG2 knockdown and its effect on the mTOR cascade. siNG2-treated *Oli-neu* cells showed ~25-30% reduced mTOR and S6K1 phosphorylation in accordance with the previous observation. (Fig 4.12)

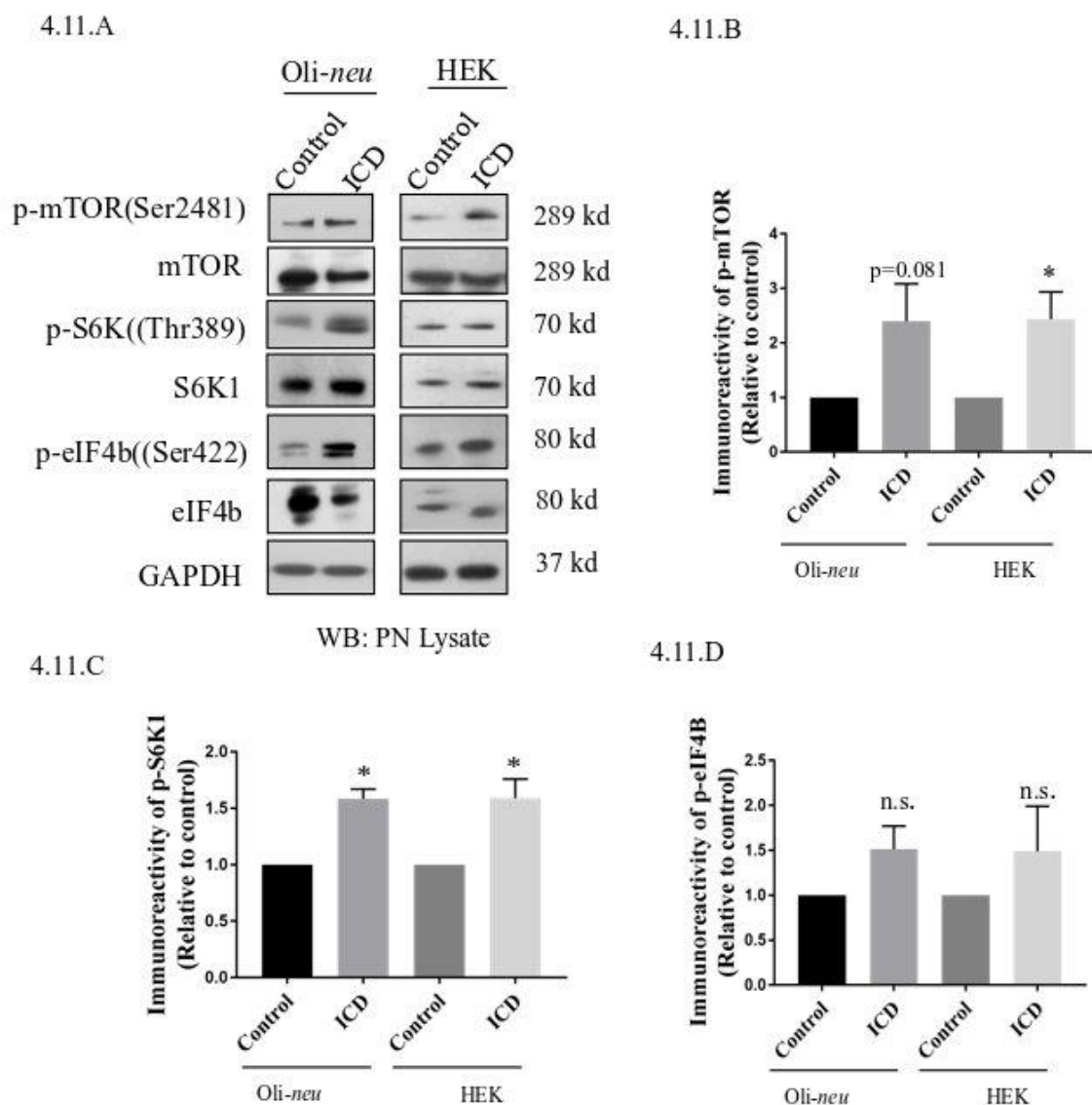
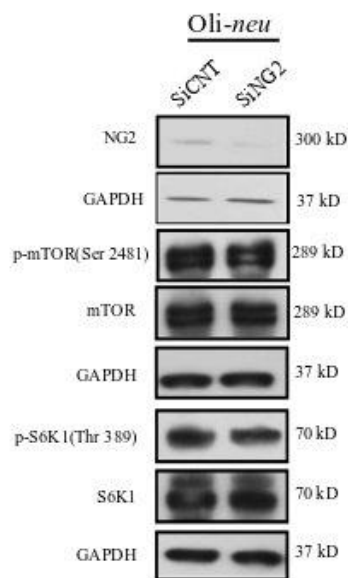


Figure 4.11. NG2 ICD overexpression increases phosphorylation of mTORC1 signaling components (A, C) Western blot analysis of post-nuclear (PN) lysate from NG2 ICD transfected HEK (n=3) and Oli-*neu* (n=4) cells compared to empty vector (control). (B, C, D) Quantification of western blot analysis. Phospho-specific expression of S6K1 (Thr389) is significantly upregulated in both cell lines and correlates with the increase of phospho-mTOR (Ser2481) levels. The downstream target of pS6K1, p-eIF4B was also increased in both cell lines. (Data represents mean \pm SEM. Statistical analysis was done by two-tailed paired *t*-test after checking the data is normally distributed by the Shapiro-Wilk normality test by PRISM (GraphPad). (Taken from Nayak T et al., 2018)

4.12.A.



4.12.B.

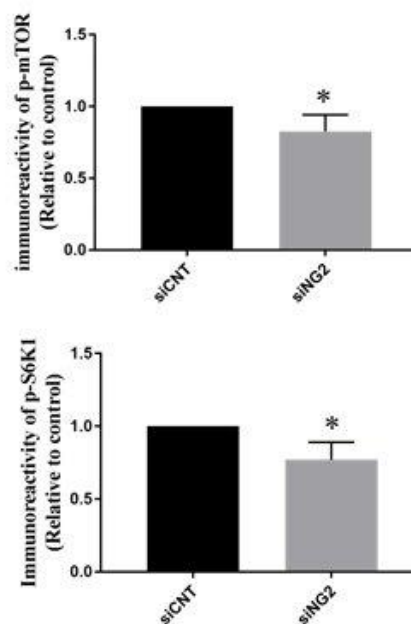


Figure 4.12. NG2 knockdown causes decreased phosphorylation of mTORC1 signaling components (A) WB analysis of mTOR cascade in NG2-knocked-down Oli-neu cells. (B) In the NG2-knockdown experiment, p-mTOR and p-S6K1 both were reduced (~20-25%) in NG2 knocked-down (efficacy 80%) Oli-neu samples compared to control. (Data represents mean \pm SEM. Statistical analysis was done by two-tailed paired *t*-test after checking the data is normally distributed by the Shapiro-Wilk normality test by PRISM (GraphPad) (Taken from Nayak T et al., 2018)

4.3.3. NG2 ICD modulates eef2/FMRP signaling pathway

Among the various targets of S6K1, eEF2K (elongation factor 2 kinase) regulates translation elongation. eEF2K is a kinase which inactivates by phosphorylation (at Thr 56 residue) its only known substrate, eEF2, causing a repressed translation elongation (Wang et al., 2001, 2014). Additionally, in the nervous system, S6K1 has been reported to phosphorylate the protein FMRP, which acts as a general repressor of translation (Narayanan et al., 2008). Mutation of FMRP is the causal link for the intellectual disorder; Fragile-X Mental Syndrome (Okray et al., 2015, Zalfa et al., 2003). FMRP is an RNA binding protein and has a wide range of substrates including dendritic mRNAs (Bassell et al., 2008) and thus play a key role in maintaining local translation and

neuronal development (Brown et al., 2001). In recent studies, eEF2 mRNA is recognized as another substrate of FMRP (Bagni et al., 2014, Richter et al., 2015) and FMRP/eEF2 signaling has been suggested to regulate dynamic translation of mRNAs involved in LTD in neurons (Park et al., 2008). Furthermore, FMRP-KO mice show exaggerated protein synthesis (Darnell et al., 2011) due to hyperactive S6K1 signaling (Bhattacharjee et al., 2012).

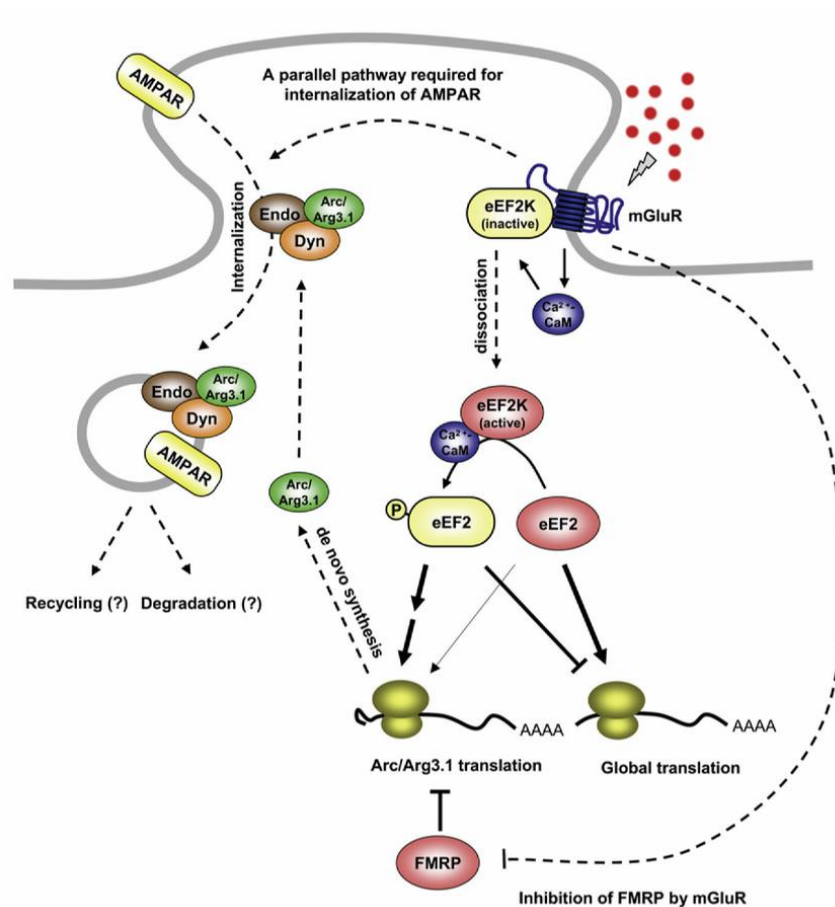


Fig 4.13. Role of FMRP/eEF2K/eEF2 pathway in mGluR-LTD regulation (Taken from Park et al., 2008)

Since the MS analysis of the ICD-interactome and independent band-identification analysis followed by CoIP validation confirmed the co-association of eEF2 with NG2 ICD, the effect of the ICD on eEF2 was investigated. As FMRP is one of the most important candidates influencing neuronal development, synaptic strength and neuronal translation regulation and a strong association between FMRP and eEF2 is shown, the total cellular level of FMRP in ICD-overexpressing cells was additionally checked.

WB analysis in an analogous manner as described above revealed a significant increase of total cellular levels of eEF2 (~50%) in ICD-transfectants (Fig 4.14.A) compared to control in both cell-types. Additionally, the level of eEF2 mRNA level was checked, and surprisingly it was ~30% less in ICD than control suggesting the occurrence of possible post-transcriptional regulation at this level (Fig 4.14.C). This result was particularly intriguing as several recent studies reported that FMRP binds eEF2 mRNA and post-transcriptionally repress its translation ((Darnell et al., 2013, Brown et al., 2001). Strikingly, WB analysis showed significant downregulation of FMRP (~70%) in ICD-overexpressing *Oli-neu* cells. Downregulation of FMRP was lower in HEK compared to OPC, as FMRP is predominantly a neuronal and developmentally regulated protein and the ICD-mediated FMRP downregulation is very likely to be cell type and developmental stage-specific. (Fig 4.14.A, B). FMRP protein is also reported to bind and stabilizes its own mRNA along with other target mRNAs and perturbation of intracellular protein level of FMRP regulates its mRNA binding and stabilization properties (Didiot et al., 2008). Hence in following experiments *Fmr1* total mRNA level was checked by qPCR analysis and the data revealed that *Fmr1* mRNA level was also ~35% reduced in ICD-overexpressing conditions compared to control (Fig 4.14.C). Several studies have reported that FMRP exerts stabilization effect on PSD95 and MBP (Giampetruzzi et al., 2013, Zalfa et al., 2007) mRNAs and hence an experiment was performed with a transcription blocker DRB (5,6 Dichlorobenzimidazole 1- β -D ribofuranoside) to study if ICD-mediated FMRP downregulation affects RNA stability of these above-mentioned mRNA candidates (Fig 4.14.D). Preliminary data revealed that both targets have reduced stability in ICD-overexpressing *Oli-neu* cells compared to control.

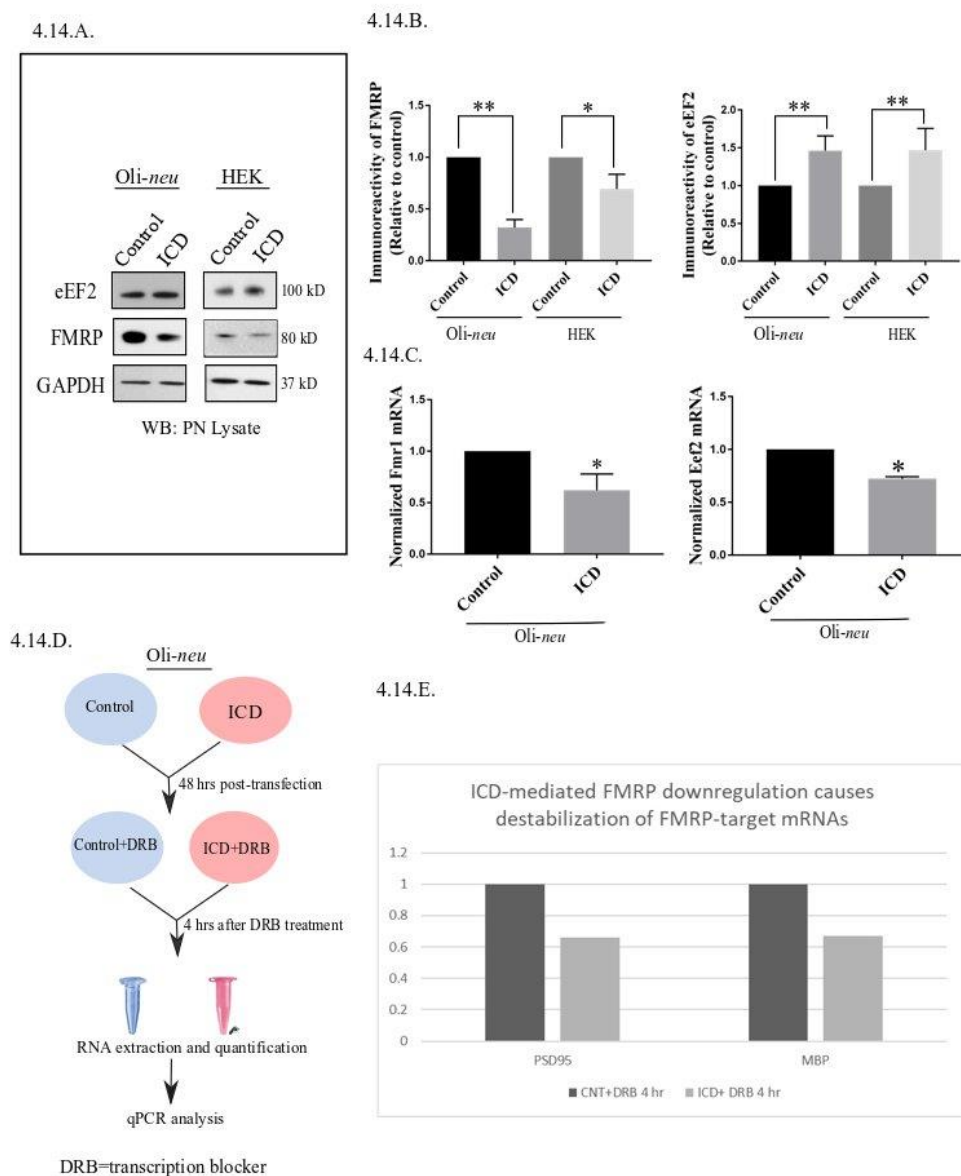


Figure 4.14. NG2 ICD regulates expression of eEF2 and FMRP

(A) Western blot analysis of post-nuclear (PN) lysate from NG2 ICD transfected HEK (n=6) and *Oli-neu* (n=7) cells compared to empty vector (control). PN lysates were prepared 48 hours after transfection. (B) Total protein levels (normalized against GAPDH) of eEF2 were increased in both cell-lines, while FMRP protein levels were significantly reduced after ICD-overexpression only in *Oli-neu*. (C) qPCR analysis of eEF2 and *Fmr1* mRNA showed that ICD-overexpression leads to 30% and 40% reduction respectively in *Oli-neu* samples. (D) Schematic representation of experimental design for studying ICD-mediated effect on stabilization of FMRP target mRNAs, taking DRB (5,6-Dichlorobenzimidazole 1- β -D-ribofuranoside) as a transcription blocker. (E) qPCR analysis of DRB-treated ICD/CNT overexpressing *Oli-neu* cells revealed that ICD overexpression causes destabilization of two FMRP targets; PSD95 and MBP. (Data represents mean \pm SEM. Statistical analysis was done by two-tailed paired *t*-test after checking the data is normally distributed by the Shapiro-Wilk normality test by PRISM (GraphPad). (Taken from Nayak T et al., 2018)

4.4. Characterization of ICD-mediated newly synthesized proteome

4.4.1. De novo proteome profiling of ICD-overexpressing population by pSILAC

After establishing the altered signaling cascade associated with NG2 ICD-driven translational upregulation, the characterization of newly synthesized proteome upon ICD overexpression was addressed.

One of the emerging, cutting-edge tools for studying the *de novo* proteome after a given stimulation or transfection is pulsed SILAC (pSILAC). pSILAC is a modified form of conventional SILAC where proteins are labeled by incorporation of two different isotopes of the same amino acid over a 3-5 generation of cultured cells. In contrast, pulsed SILAC can distinguish the newly synthesized proteome from the pre-existing protein pool by using three-channel labelling over a brief period. The procedure described in the publication by Björn Schwanhäusser et al, 2009, Proteomics, was followed in this study with some modifications for this experiment (Fig 4.15) (for details, see M&M).

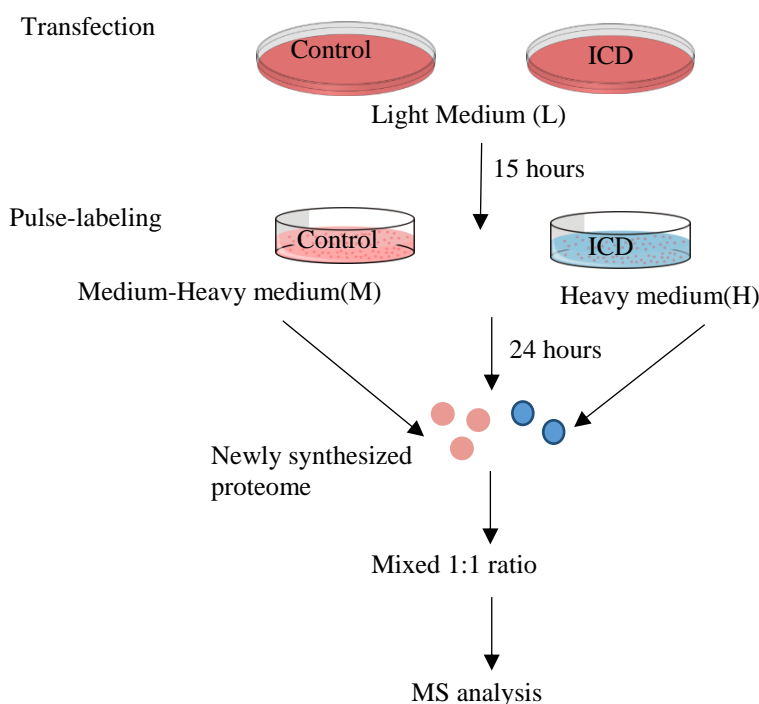


Fig 4.15. Schematic representation of the pSILAC workflow.

MS analysis of pSILAC samples from Oli-*neu* cells successfully characterized newly synthesized protein after ICD-overexpression. Gene-ontology based functional analysis of the enriched candidates suggested that many of the upregulated proteins are associated with DNA replication and repair, mTOR signaling pathways and proliferation (Fig 4.16). List of top 20 candidates from pSILAC analysis with their gene ID, fold-change and functions are summarized in the table below. (Table 18), These candidates were reproducibly found in both forward and reverse SILAC labelling.

Table 18. Summarization of upregulated candidates obtained from pSILAC-MS analysis

<i>Gene ID</i>	Protein name	Fold Change (ICD/CNT) (log₂ scale)	Function
<i>Hsd17b8</i>	Estradiol 17-beta-dehydrogenase 8	1.68	Estrogen metabolism, oxidation-reduction process
<i>Phldb1</i>	Pleckstrin homology-like domain family B member 1	1.17	Regulation of EMT transition, embryo morphogenesis
<i>Sdcbp</i>	Syntenin-1	1.39	Positive regulation of cell proliferation, migration, cell cycle, TGF-beta signalling pathway
<i>Adnp</i>	Activity-dependent neuroprotector homeobox protein	1.1	transcription factor, neuronal development, regulation of p53 pathway
<i>Lig3</i>	DNA ligase 3	0.88	DNA replication , base-excision repair, cell cycle
<i>Eefsec</i>	Selenocysteine-specific elongation factor	0.74	Translation elongation, protein biosynthesis.
<i>CDKn2aip</i>	CDKN2A-interacting protein	0.71	p53 binding, regulation of cell growth and DNA damage.
<i>Cox7a2l</i>	Cytochrome c oxidase subunit 7A-related protein	0.64	regulation of oxidative phosphorylation
<i>Exoc4</i>	Exocyst complex component 4	0.64	vesicle exocytosis, synaptic transmission, oligodendrocyte differentiation
<i>Lsm2</i>	U6 snRNA-associated Sm-like	0.61	mRNA splicing

	protein		
<i>Mon2</i>	Protein MON2 homolog	0.6	protein transport
<i>Rqcd1</i>	Cell differentiation protein RCD1 homolog	0.55	Transcription and translational regulation, cell differentiation
<i>Rae1</i>	mRNA export factor	0.52	Cell division , mitotic spindle formation, nucleocytoplasmic transport
<i>Wdr18</i>	WD repeat-containing protein 18	0.51	cellular development, migration
<i>Ethel1</i>	Persulfide dioxygenase ETHE1	0.49	suppress p53-induced apoptosis , metabolic activity
<i>Get4</i>	Golgi to ER traffic protein 4 homolog	0.48	maintenance of unfolded protein by ERAD pathway
<i>Fmnl</i>	Formin-like protein	0.42	cortical actin cytoskeletal organization, cell morphogenesis
<i>Fbxo22</i>	F-box only protein 22	0.41	positive regulation of protein ubiquitination, myotube differentiation
<i>Smrnb1</i>	SWI/SNF-related regulator of chromatin	0.4	cell cycle and differentiation regulator, p53 binding, DNA repair and chromatin remodeling
<i>Dnajb1</i>	DnaJ homolog subfamily B member 1	0.4	positive regulation of ATPase activity, chaperone co-factor
<i>Csk</i>	Tyrosine-protein kinase CSK	0.4	Oligodendrocyte differentiation, brain development, positive regulation of MAPK pathway

Table 18 summarizes the top 20 upregulated candidates in ICD over-expressing cells obtained by pSILAC-MS analysis with their gene ID, fold-change and functions. Many of the upregulated proteins are associated with DNA replication, cell growth, cell differentiation, and p53 binding while the downregulated candidates are mostly involved in ubiquitination and protein transport.

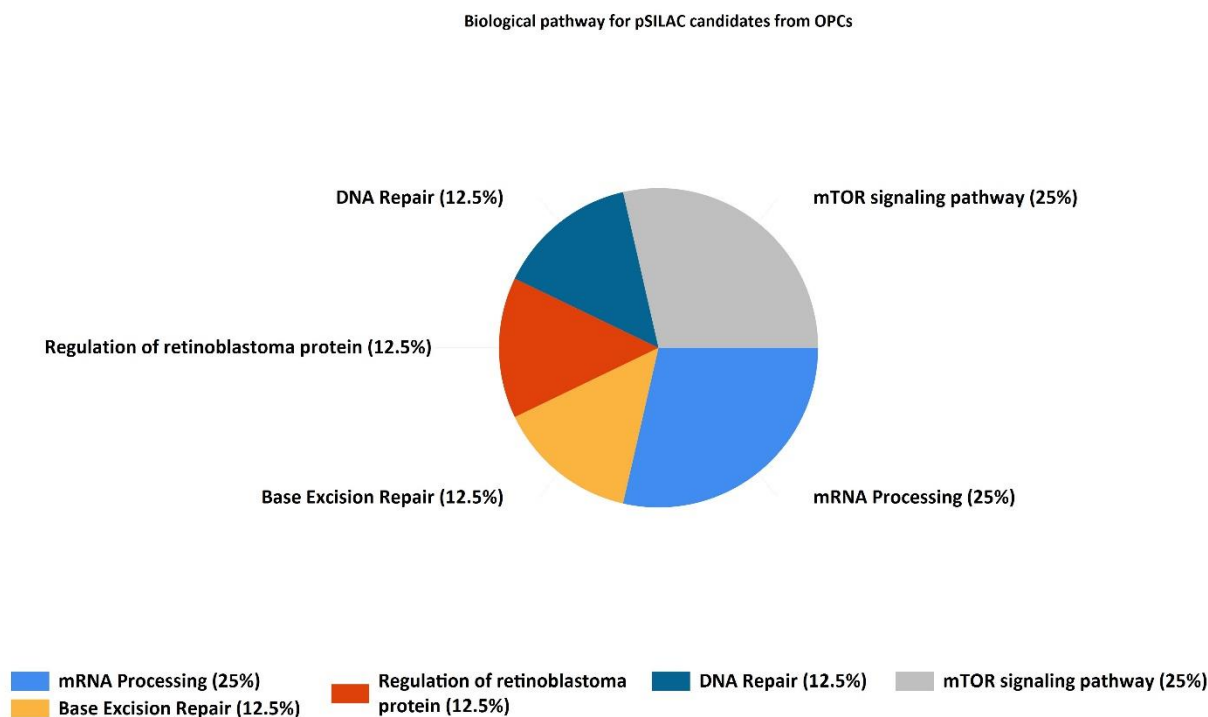


Fig.4.16. Gene-ontology based analysis of pSILAC-MS candidates. pSILAC-enriched putative upregulated proteins was analyzed by using FUNRICH analysis tool. Altered biological functional annotation based on gene ontology represented translation, DNA repair, and DNA replication to be significantly enriched.

4.4.2 Activity-dependent neuroprotective protein (ADNP) expression was regulated by cleaved NG2 ICD

For validating the pSILAC data, ADNP was chosen as one of the candidates as it was highly regulated both in forward and reverse SILAC experiments in an equal manner. Activity-dependent neuroprotector homeobox (ADNP) was initially identified in brain tissue with transcription factor activity (Zamostiano et al., 2001). ADNP has a high abundance in proliferative tissues, and inhibition of ADNP protein expression caused a significant reduction in metabolic activity in the target cells coupled with increases in the tumour suppressor p53 (Amson et al., 2000). In OPC, ICD-overexpressing cell population showed a significant increase of ADNP total protein expression (~40%) compared to control by WB analysis (Fig 4.17).

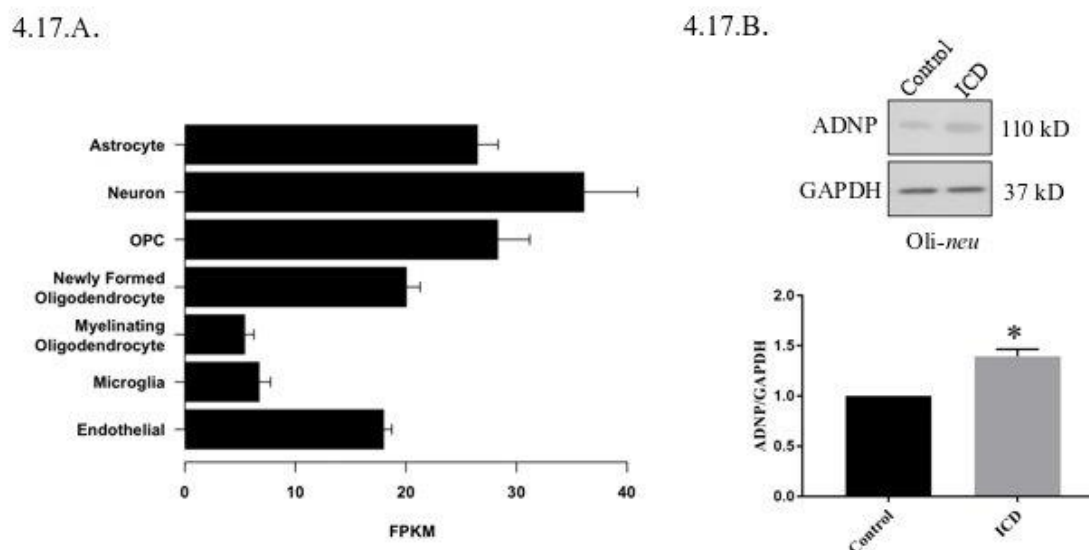


Fig.4.17. Validation of pSILAC-enriched candidate (A) RNA-Seq data for ADNP expression in different neuronal cells were obtained from www.brainrnaseq.org. ADNP is highly expressed in OPC, but its expression is downregulated as OPC matured into myelinating OLs. (B) ADNP protein expression was investigated in ICD-overexpressing *Oli-neu* cells, and the data revealed that ADNP was ~2-fold higher in ICD compared to control.

4.5. NG2 ICD alters the cell-cycle kinetics

4.5.1 NG2 ICD increases cell population in S-phase

Since the GO-based proteomics result suggested an enrichment of DNA repair and replication pathway, as a next approach, the cell-cycle kinetics after ICD-overexpression was studied. To study cell-cycle distribution, HEK cells overexpressing NG2 ICD or BAP-flag (control) were fixed 24 hours after transfection and intracellularly immunostained with anti-Flag-FITC conjugated antibody (details in M&M). The cell cycle distribution revealed that in the ICD overexpressing cells, 45.95% \pm 6.53% of the cells were in S-phase compared to 35.41% \pm 6.7% in control population giving a significant 10% S-phase shift mediated by ICD (Fig. 4.18).

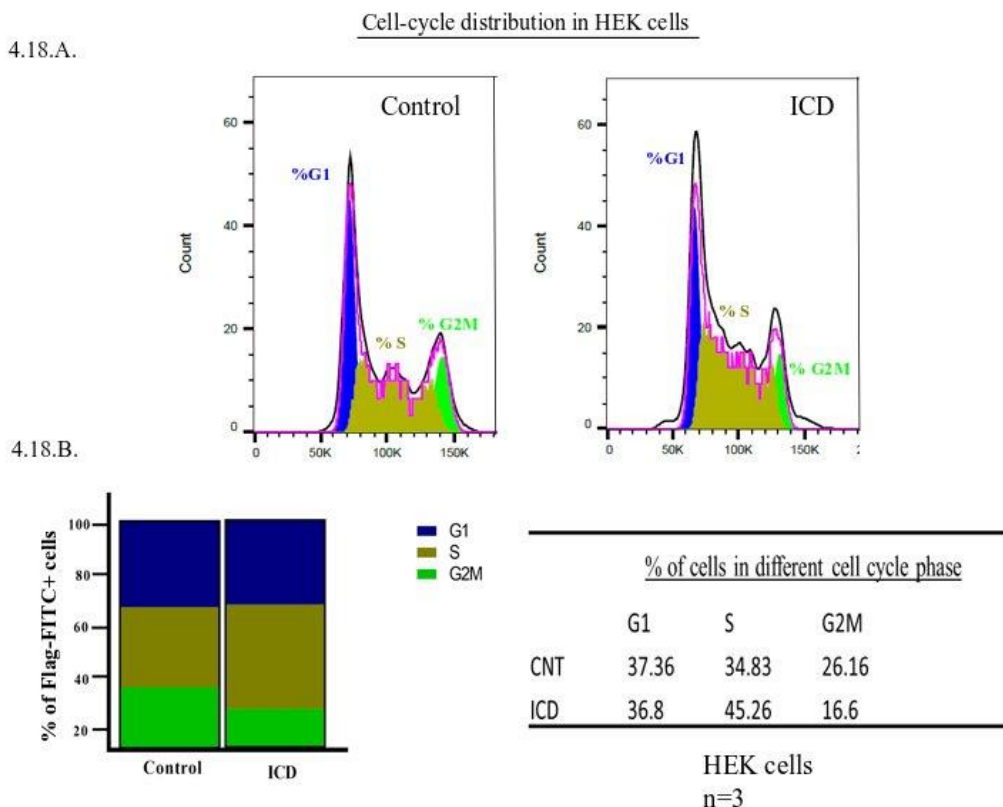


Fig 4.18. NG2 ICD shifts S-phase population in HEK cells. (A) Representative images of DNA histogram analysis for cell-cycle distribution in asynchronous HEK cells transfected with ICD-flag (ICD) or BAP-flag (control). Propidium iodide (PI) was used for DNA staining. Only flag-FITC+ cells were analyzed for PI quantification. (B) Quantification of FACS data from HEK cells represented in a stacked bar column shows that ICD promotes the cell population in S-phase by ~10%. Experiments were done in three independent sets (n=3) where 2000 events counted for each condition in each experiment. (Taken and modified from Nayak T et al., 2018)

FACS experiments were unsuccessful with *Oli-neu* cells owing to lower transfection efficiency compared to HEK cells. However, another experimental approach was taken to study S-phase effect in OPC. *Oli-neu* cells were immunostained for PCNA (Proliferating cell nuclear antigen) which is an S-phase specific marker as PCNA associates with active replisome (Mike O'Donnell and Huilin Li., 2016, Chagin et al., 2016). PCNA-staining showed that in ICD-overexpressing conditions, 21.04%± 1.26% *Oli-neu* cells were PCNA+ (out of total counted DAPI+ cells) whereas in the control

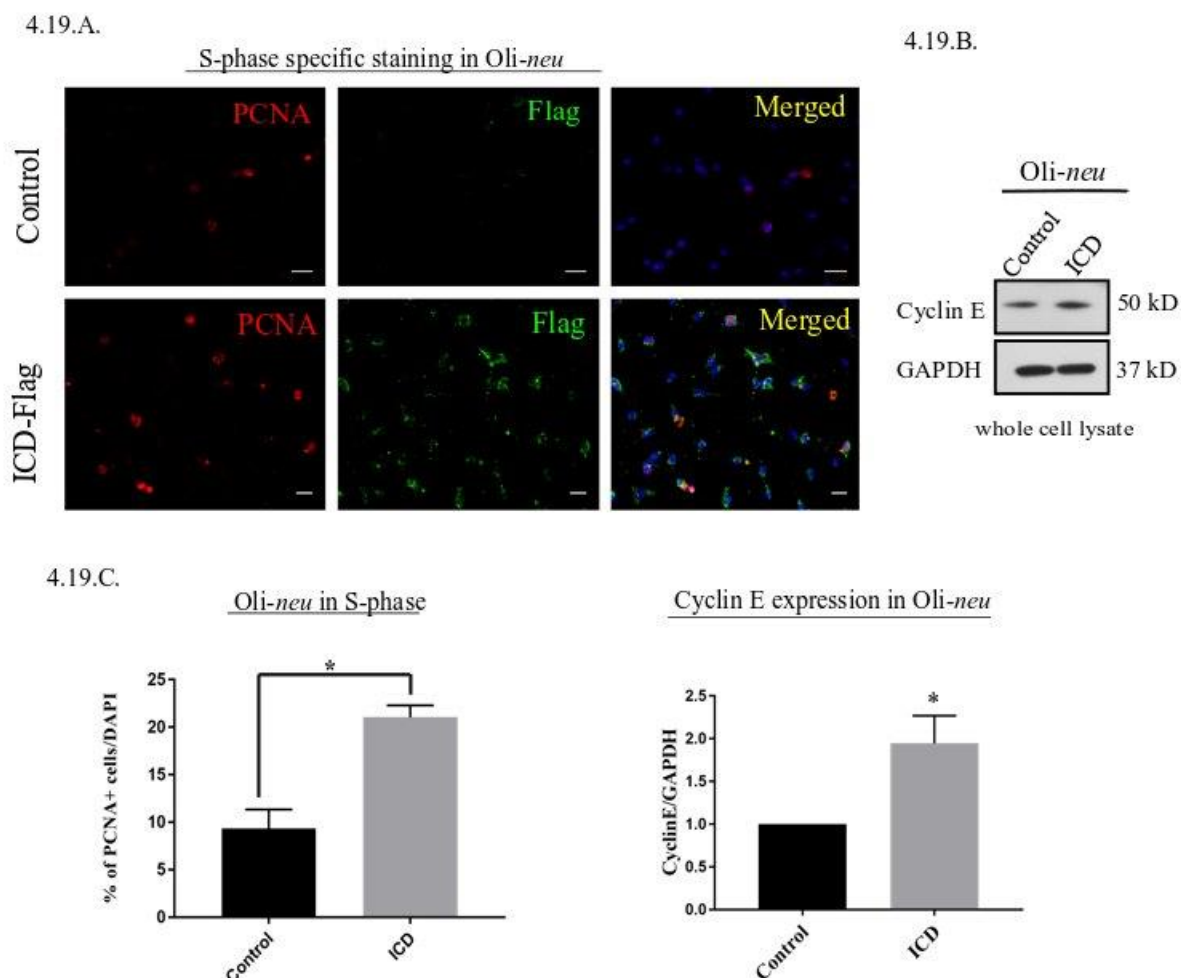


Figure 4.19. NG2 ICD overexpression increases PCNA+ cell numbers in Oli-neu cells (A) Oli-neu cells are immunostained with the S-phase marker, anti-PCNA antibody (red) and indicate increased PCNA-associated nuclear puncta when transfected with ICD (stained with anti-Flag antibody, green). Cell nuclei were stained with DAPI (blue). (C) Quantification of PCNA staining in Oli-neu reveals that the proportion of PCNA+ cells out of total cells (total counted DAPI+) is significantly increased in case of ICD overexpression (21.04%± 1.26%) compared to control (9.33± 2.03%), a total of ~250 cells were counted for quantification. (B, C) WB analysis of G1 to S-phase progression regulator, Cyclin E, revealed that Cyclin E was increased ~2 fold in ICD compared to control. (Data represents mean ±SEM. Statistical analysis was done by two-tailed paired *t*-test after checking the data is normally distributed by the Shapiro-Wilk normality test by PRISM (GraphPad). (Taken from Nayak T et al., 2018)

population 9.33%± 2.01% Oli-neu cells were PCNA+ (out of total DAPI+ cells) (Fig. 4.19). PCNA-staining quantification also revealed a significant 10% increase of Oli-neu cells in accordance with the previous observation found by FACS analysis in HEK cells.

Cyclin E is one of the principal regulators of G1 to S-phase progression in cell-cycle kinetics. Cyclin E expression is increased during the G1 phase and reaches its peak as cells enter into S-phase (Yang et al., 2012,). To address the ICD-mediated observed the S-phase effect on a molecular level, Cyclin E total cellular expression was checked by WB in ICD overexpression and control condition. The protein level of Cyclin E was found to be enriched in NG2 ICD-transfected Oli-neu cell population compared to control (~2 fold), in line with the previous observation (Fig 4.19).

4.5.2 NG2 ICD overexpression is associated with changed nuclear morphology in OPC

In their recent paper in 2016, Wang et al. demonstrated the tight coordination between nuclear shape and cell-cycle phases using high-resolution microscopy. Recent literature also support the notion that nuclear morphology changes with different phases of cell-cycle and it is reported that in G1 phase most of the cell nuclei appear round. After the synthesis and replication phase (late S-phase), the nuclear shape appears like more elongated or dumbbell-shaped as cells progress to mitosis (Wang et al., 2016). To strengthen the result of the newly found ICD-mediated effect on cell-cycle progression, investigation on the nuclear morphology in ICD-transfectants using two parameters; nuclear area and roundness was performed. Data quantification revealed that nuclear roundness was significantly reduced in ICD overexpressing OPC while nuclear area was increased around 1.6 fold in ICD overexpressing cells, suggesting a cell-cycle progression specific changes brought upon by cleaved NG2 ICD (Fig 4.20).

4.20.A.

4.20.B.

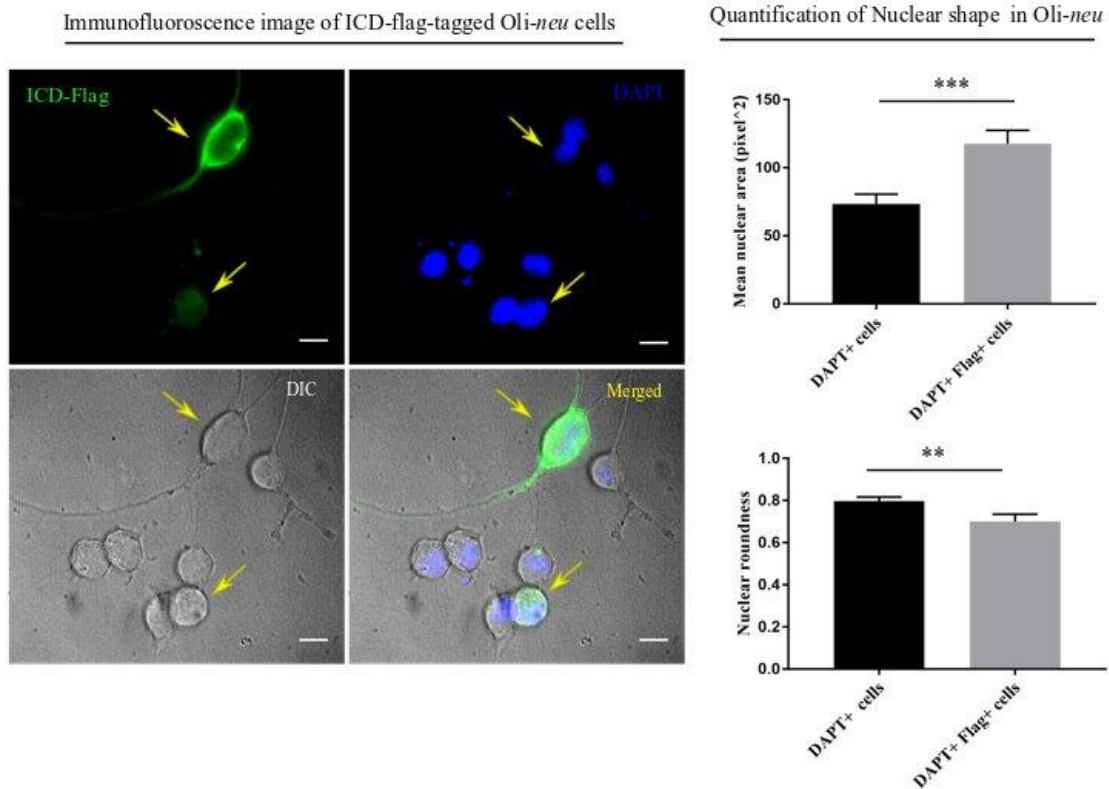


Figure 4.20. Altered nuclear morphology in ICD-overexpressing cells (A) Immunofluorescent images of *Oli-neu* cells expressing ICD-flag (green). The arrows indicate ICD-transfected cells. (B) Quantification of nuclear shape based on two indices (ImageJ); nuclear area (unit for area) and roundness (0.0-1.0), revealed that nuclei of ICD-transfected *Oli-neu* were ~1.6 times larger (area) and less round (roundness) than *Oli-neu* from control (Mean values \pm SEM was shown in the data. Total 50 cells were counted from three independent experiments (n=3) for each condition. Statistical test was carried out by Mann-Whitney-rank based test.) (Taken from Nayak T et al., 2018)

Discussion

5. Discussion

5.1. Sub-cellular localization of the NG2 ICD

Previous findings on ICDs of type-1 transmembrane proteins shed a major focus on nuclear signaling and gene regulation (for example ICDs of Notch or APP protein exert a transcriptional role). An initial study by our group also observed the nuclear presence of ICD in a preliminary study. Sakry et al., in 2015, found that after transfection, most of the protein was localized in the cytoplasm with a lower nuclear level (Sakry et al., 2015). Here, in this study, the same localization pattern was observed, and previous results were validated. However, immunofluorescent staining of cells expressing an NLS-truncated ICD construct showed only cytoplasmic and no nuclear localization. Therefore, it is likely that there is an NLS-dependent transport of the NG2 ICD into the cell nucleus. To validate whether NLS-dependent ICD translocation is an active process, treatment with an importin inhibitor, Ivermectin, was carried out and the observed results indicate an active nuclear targeting of NG2 ICD.

However, unlike Notch ICD, NG2 ICD does not contain any DNA-binding domain (DBD) or transcription factor (TF)-binding/regulatory domain, making it an unlikely event that NG2 ICD plays a direct role in transcription regulation by direct binding to DNA or TF. IP-MS study was performed from ICD-overexpressing samples to determine if any putative candidates could be found in ICD-interactome to explain the nuclear presence of the NG2 ICD. Strikingly, ICD-interactome by determined IP-MS revealed that mainly cytoplasmic proteins (translation factors, cell-cycle factors) are associated with NG2 ICD and GO-based analysis of IP-MS candidates suggest an alteration in translation and cell-cycle kinetics. Interaction analysis did not provide any conclusive information on coprecipitation of cleaved NG2 ICD with nuclear proteins or any such protein complex that is known to exhibit nuclear translocation; rather it strongly suggested the involvement of translation regulatory pathways which could be a convincing explanation for the predominant cytosolic expression of the ICD.

5.2. A novel role of NG2 ICD as a regulator of translation and cell-cycle progression via modulation of mTOR-signaling cascade

Based on the results from the ontology analysis of proteomics data, the effect of the NG2 ICD on mRNA translation and cell-cycle kinetics was investigated.

Interestingly, ICD was shown to co-precipitate with translation factors and total translation was increased by ~70% by NG2 ICD overexpression, but only slightly and not significantly by NG2 DEL expression in OPC and HEK cells. Results from previous (Sakry et al., 2015) and the present study has shown that the membrane-bound NG2 CTF, but not the ICD, is the major fragment generated after NG2 DEL expression. While investigating the molecular mechanism behind the ICD-mediated translation regulation, at first the involvement of the global translator regulator mTORC1 was demonstrated by treating the cells with a specific mTORC1-inhibitor, and then mTOR-signaling cascade upon ICD overexpression was studied in both cell line. Increased phosphorylation of the mTOR-signaling components was found in ICD-overexpressing cells compared to control, confirming an active mTORC1-cascade.

NG2 ICD has also been found to play a role in regulating cell-cycle kinetics. Cell cycle analysis of FACS-sorted ICD-transfectants from HEK cells demonstrated a 10% shift towards S-phase, reflecting increased DNA replication in the HEK cell population. Immunofluorescent staining of *Oli-neu* cells using a specific S-phase protein marker (PCNA) also revealed an increase of PCNA+ cells in the ICD-overexpressing population (21.04%) compared to control (9.33%), thus establishing a novel role for NG2 ICD in cell-cycle progression. Changes in nuclear morphology of ICD-transfected OPC were also detected in line with the observed alterations in nuclear shape reported in S-phase cells (Wang et al., 2016) and many recent literatures provide information on interconnection between cell-cycle progression and altered nuclear morphology (Xue et al., 2013, Schlaitz et al., 2013).

Progression through different stages of the cell-cycle requires that a proliferating cell gains sufficient energy and cell mass and emerging reports have demonstrated that genes involved in regulating protein biosynthesis, DNA repair, replication, nucleocytoplasmic transport are upregulated as cells progress from G1 to S-phase

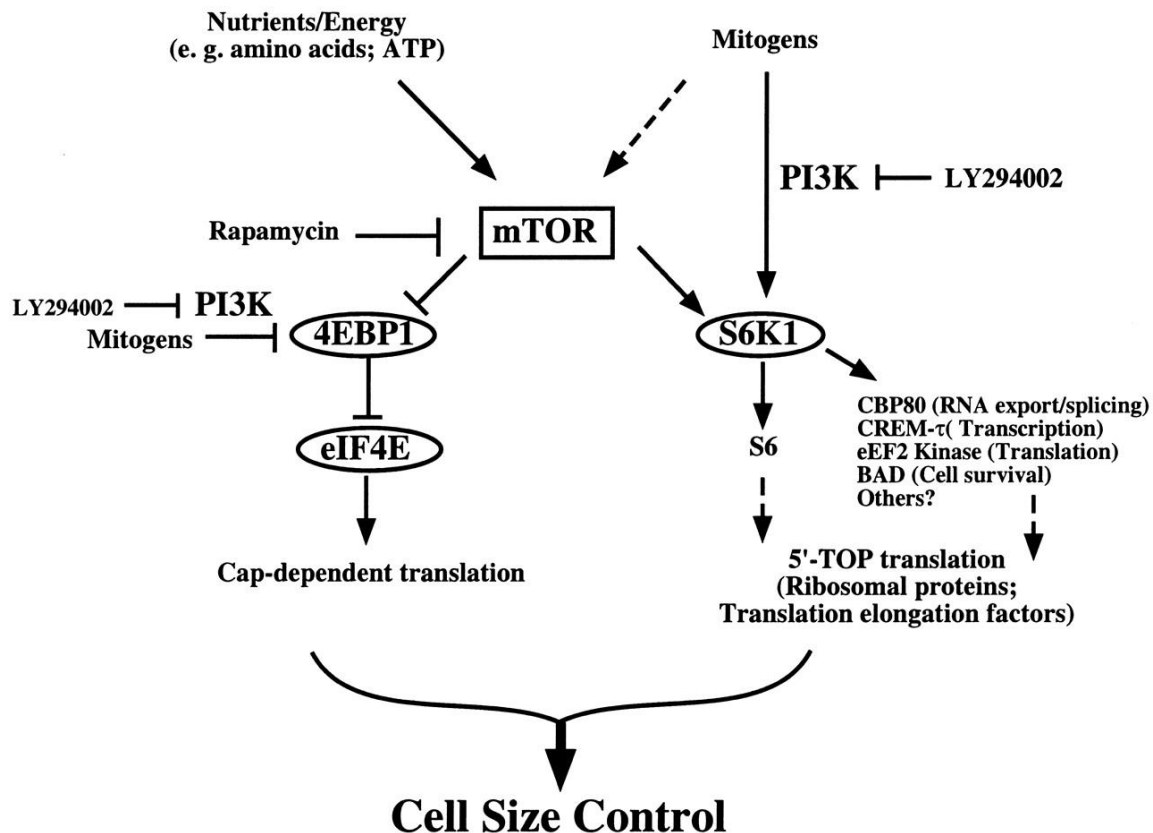


Fig 5.1. Role of mTOR signaling in controlling cellular growth (Taken from Fingar et al., 2002)

(Stumph et al., 2014, Aviner, et al., 2015). It has been shown that nutrients, growth factors and mTOR, in an orchestrated action, mediate specific checkpoints during G1-phase (R-point and late G1-phase metabolic checkpoint) where it is decided whether the cell contains optimal size and nutrients to accomplish replication phase (S-phase) (Foster et al., 2010, Saqcena et al., 2013). The downstream components of mTOR, S6K1 and eIF4B, are also tightly linked with G1 to S-phase progression as their increased phosphorylation is correlated with accelerated cellular growth and proliferation (Fingar et al. 2004., Gingras et al., 2001) (Fig 5.1). mTOR-S6K1 signaling has also been found to control transcription of CHK1 via Rb-E2F pathway by upregulating Cyclin D and Cyclin E (Zhou et al., 2017), and inhibition of active mTOR-signaling causes slower S-phase progression of cells following DNA-damage. Interestingly, we found increased Cyclin E1 expression in ICD-overexpressing *Oli-neu*

cells. Therefore, it is very likely that ICD-mediated translational upregulation is coupled with the increased G1 to S-phase progression and mTORC1, upon activated by released NG2 ICD, plays a pivotal role in regulating these phenomena.

These results are particularly promising because so far, NG2 has not been reported to have direct effects on translation, and this study for the first time shows that NG2 ICD, specifically, alters translation and cell-cycle kinetics and thus displays a unique functional property. However, cell proliferation has been associated with NG2 expression, since OPC are the only proliferating cell population in the adult unlesioned mammalian CNS, apart from stem cells (Simon et al., 2011, Dimou et al., 2014). The ICD-mediated drive towards S-phase progression in OPC is striking as recent literature found that stimulation of neuronal circuits causes an increase in adjacent neuronal progenitor proliferation, including NG2+ OPC (Gibson et al.; 2014, Reviewed in Forbes and Gallo, 2017). Since neuronal activity stimulates NG2 cleavage leading to the increased cytoplasmic release of NG2 ICD (Sakry et al., 2014), the observation of ICD-mediated cell-cycle progression is of interest in this context.

5.3. NG2 ICD regulates FMRP, an activity-dependent, a neuronal protein involved in local translation

As discussed in detail in the Results Section, Fragile X protein (FMRP) is an RNA binding protein with demonstrated roles in mRNA transport, localization, stability, and translation. FMRP is a neuronal protein which exerts its regulatory effect upon receiving neuronal stimuli. To date, the targets of FMRP and its role in translation are well-established in neurons only, where it plays a pivotal role in regulating local translation, via its role as a translation repressor. Investigation on how FMRP loss is related to elevated translation revealed that FMRP controls the expression of two key components of the phosphoinositide 3-kinase (PI3K) signaling cascade: the catalytic subunit, p110 β , and PI3K enhancer (PIKE) (Fig 5.2). The translation and expression of both are elevated in the brains of Fmr1-KO mice (Sharma et al., 2010, Gross C et al., 2010). PI3K lies as an upstream activator of the mTOR-signaling pathway, and mTOR-signaling cascade has also been reported to be hyperactive in the absence of FMRP (Sharma et al., 2010, Rehnitz et al., 2017). The translation factor, eEF2, is a reported

target of FMRP (Darnell et al., 2013) and in FMRP knockout mice, total eEF2 protein and levels of p-eIF4B were higher than in wild-type mice (Bhattacharjee et al., 2012) in hippocampal cells. Although the characterization of FMRP has been extensively done in neurons, the role of FMRP in glial cells is still in its early days and awaits further research. Expression profile of FMRP in glial cells revealed that FMRP expression is abundant at post-natal day 0 (PND 0) in astrocytes, OPC and microglia with a gradual decline during the developmental course and finally with a low/undetectable level in the adult brain in different brain regions (Gholizadeh et al., 2014, Zhang et al., 2014).

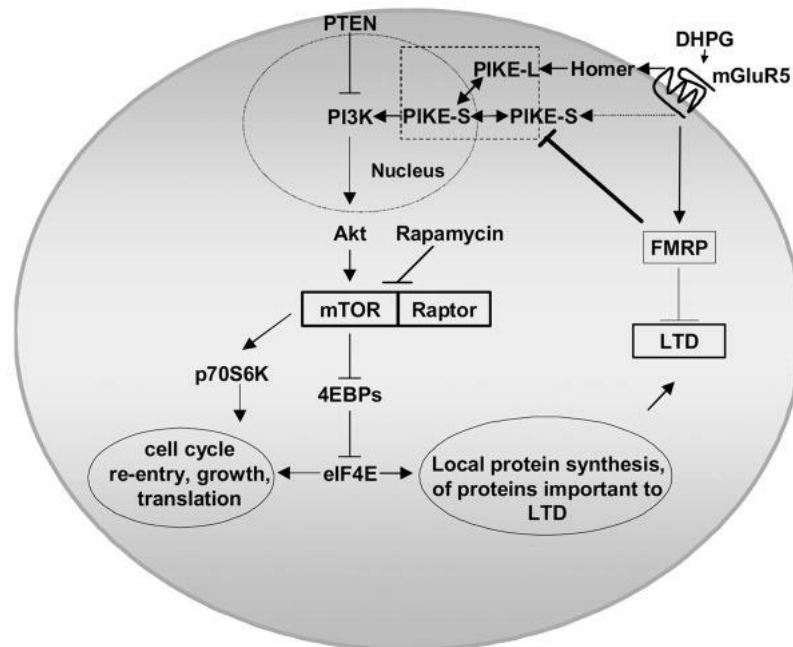


Fig 5.2. Crosstalk between FMRP and mTOR signaling pathways. (Taken from Sharma A et al., 2010)

FMRP has been found in the soma and distal processes of OPC and immature OLs in neonatal brain, in oligodendrocyte cell line and in primary oligodendrocyte cell culture (Wang et al., 2004, Pacey et al., 2013). Like in other glial cells, FMRP expression is reduced as OPC differentiate into matured OLs, although Giampetruzzi et al., in 2013, showed that FMRP expression is detected in matured MBP+ OLs of rodents and human OLs. Interestingly, MBP is one known target of FMRP (Darnell et al., 2013) and FMRP has been shown to bind MBP and inhibit its translation in vitro (Wang et al., 2004)

FMRP-KO mice showed delayed myelination and reduced number of OPCs found in deep cerebellar white matter (Pacey et al., 2013).

Interestingly, we found significant downregulation of FMRP protein levels of 70% compared to the normal protein levels in NG2 ICD-overexpressing OPC, but in HEK cells overexpressing the NG2 ICD, this regulation was much lower implicating a cell-specific effect of ICD on FMRP. Since we found reduced FMRP levels and increased translation after NG2 ICD overexpression in OPC, it is likely that FMRP also acts as a translational repressor in OPC, as well as in neurons. Moreover, eEF2 protein level was also higher (~40%) after ICD-overexpression with a reduced eef2 mRNA level, implying a potential involvement of post-transcriptional regulation by FMRP.

5.4. Role of FMRP/eEF2 in synaptic signaling and myelination

The molecular interplay between FMRP/eEF2/NG2 ICD could have a crucial effect on a broader aspect of activity-dependent local translation. FMRP is known to bind and repress translation of several dendritic and synaptic mRNAs among which some are immediate early genes (IEG) such as CamKII, MAP1B and Arc/Arg 3.1. Upon receiving stimulus, translational repression of Arc, exerted by FMRP is relieved, and optimal expression level of Arc is attained which is required for AMPAR trafficking and internalization (Chowdhury et al., 2006). In 2008, Park et al. showed that eEF2K/eEF2 and FMRP-dependent translation pathway acts in a coordinated fashion upon receiving stimuli and controls the rapid and transient switch of translation factors that are required for mGluR-LTD (Park et al., 2008).

In this context, interestingly, it has been shown that neuronal activity-mediated NG2 shedding has a significant impact on the neuronal glutamate receptor currents and synaptic strength in somatosensory cortex (Sakry et al., 2014), further showing the importance of precise control of synaptic receptors and the optimal expression of their pivotal regulatory proteins in a timely manner.

In addition to controlling local translation, FMRP is also known to bind and exerts stabilization factor on its mRNA targets. Among many identified FMRP-mRNA targets, two of the most relevant candidates are PSD95 and MBP mRNA. For PSD-95, It has

been shown that FMRP binds to its 3'-UTR and stabilizes the mRNA and a loss of FMRP results in a reduction of this essential synaptic protein (Zalfa et al., 2007).

MBP and the control of myelination by FMRP is still a topic of debate. Several groups reported that FMRP binds MBP mRNA *in vitro* and *in vivo* and inhibits MBP protein expression *in vitro* (Li et al., 2001, Wang et al., 2004, Darnell et al., 2011, Giampetruzzi et al., 2013). As FMRP expression gradually declines as OPC mature into OLs, it is likely that FMRP-mediated translational repression of MBP mRNA is relieved in mature OLs, allowing abundant expression of MBP protein. Massive reduction of MBP protein and thinner myelination is observed at postnatal day (PND) 7 in cerebellum of FMRP-KO mice compared to wildtype (Giampetruzzi et al., 2013, Pacey et al., 2013) and this altered expression returned to normal levels by PND-30, suggesting that impaired development of OPC caused a delayed myelination in this context.

A mRNA-stabilization study in ICD-overexpressing *Oli-neu* cells has been done, and strikingly, the data revealed reduced stability of both PSD-95 and MBP mRNA in cultured OPC (*Oli-neu*). This observation could be explained by ICD-mediated downregulation of FMRP which eventually leads to less stabilization effect on the target mRNA. Thus, the control of FMRP by NG2 ICD is of great importance as FMRP plays a potential role in OPC maturation and myelination.

In this study, two translation-related pathways are found to be affected by the NG2 ICD. One is responsible for general translation regulation in cells (mTOR/S6K1 signaling cascade), and the other one is important for regulating local translation and synaptic strength including LTD (FMRP-eEF2) in neurons (Park et al., 2008). Recent studies have shown that FMRP also activates the mTOR-signaling pathway in neurons (Bhattacharjee et al., Sharma et al., J neuro, 2010), combining these two signaling cascades. (Fig 5.3)

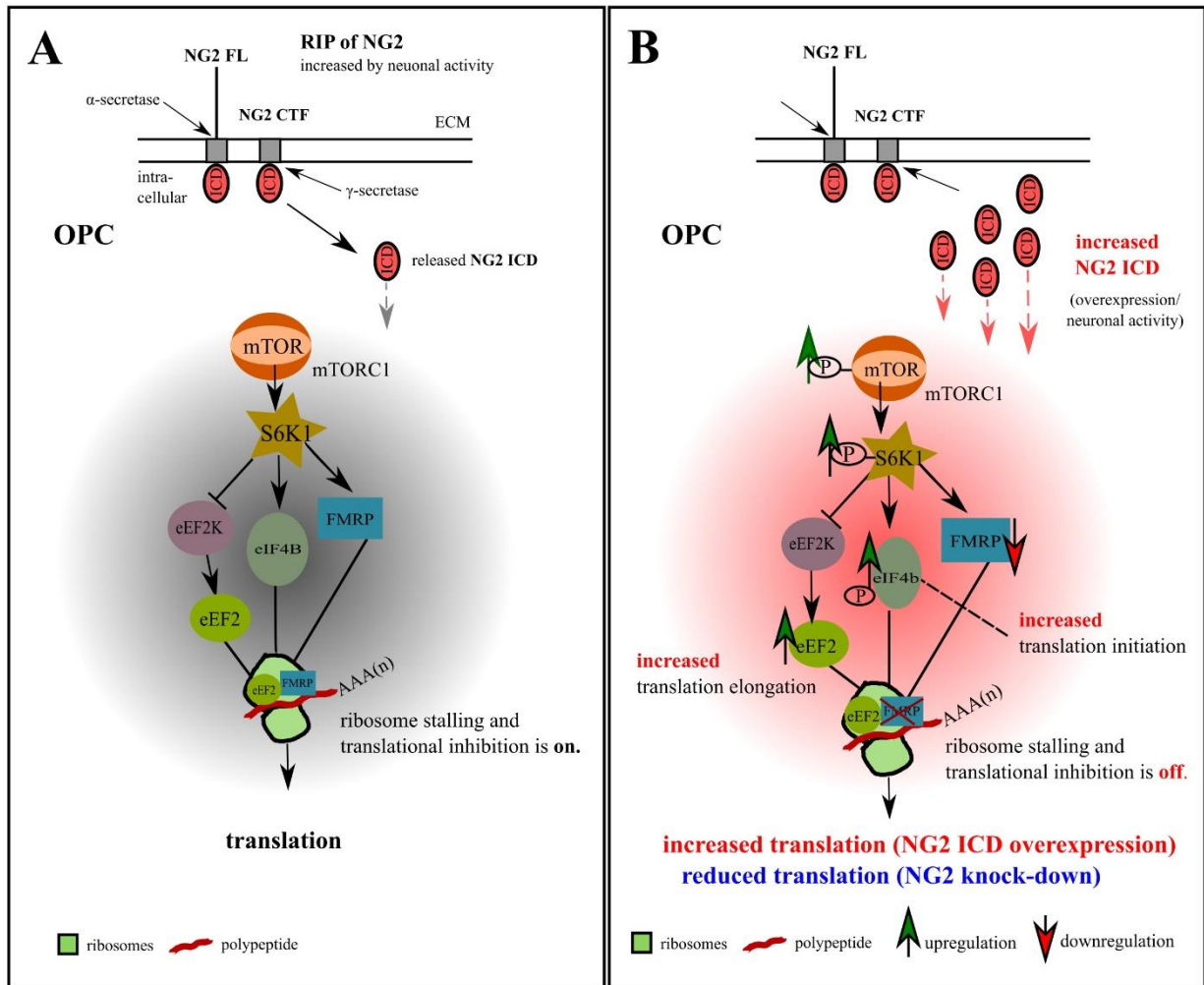


Fig 5.3. Model depicting altered signaling pathways by cleaved NG2 ICD (Taken from Nayak T et al., 2018)

5.5. NG2 ICD causes upregulation of proteins involved in cellular differentiation and tumorigenesis

Interestingly, KEGG pathway analysis of pSILAC data revealed that the set of proteins involved in cell cycle regulation ($p = 2.6E-1$) and transcriptional regulation ($p = 7.5E-1$) was highly enriched among the up-regulated proteins. Among them, syntenin1 is already a known binding partner of ICD (Chatterjee et al., 2008) and known to regulate G1 to S-phase progression (Kashyap et al.; 2015). Several transcription factors were enriched in pSILAC, among which Phldb1, Sdcbp, and Adnp are involved in cell

differentiation. Recent evidence suggests *phldb1* is one of the top regulated genes in glioma and Knockdown of *phldb1* in U87MG cells had a significant impact on cell viability due to increased cell death (Baskin et al.; 2015). Phldb1 also facilitates insulin-dependent Akt phosphorylation and is involved in adipocyte differentiation.

Activity-dependent neuroprotector homeobox protein (ADNP) was initially identified in brain tissue with transcription factor activity and is essential for proper neuronal development and cranial neural tube closure (Pinhasov A et al., 2003). To date, ADNP is known to repress expression of genes involved in transcriptional regulation, neurogenesis and organogenesis and evidence supports that ADNP directly interacts with chromatin-remodeling complex associated with cellular differentiation (Mandel S et al., 2007). Studies have also shown that ADNP has a high abundance in proliferative tissues and promotes tumourigenesis and cancer cell survival (Zamostiano et al., 2001, Bassan M et al., 1999) and inhibition of ADNP protein expression caused a significant reduction in metabolic activity in the target cells coupled with increases in the tumour suppressor p53 (Amson R; 2000).

Interestingly, RNA-Seq data obtained from www.brainrnaseq.org showed that ADNP has the highest expression in OPC amongst all glial cells and its expression is reduced as OPC progress towards the maturation stage. In addition, ADNP was one of the most consistently found, top-regulated proteins altered upon ICD-overexpression. Hence, we studied ADNP total protein expression and found a significantly higher level (~40%) of ADNP in ICD-overexpressing OPC, further opening new avenues for studying cellular differentiation and gene regulation.

5.6. NG2 ICD signaling in Tumours

Interestingly, dysregulation of the FMRP/Akt/mTOR pathway has been reported to promote tumourigenesis (Luca et al., 2013, Rajasekhar et al., 2003) and impaired mTOR cascade has especially been linked with Glioblastoma, the most common form of primary brain tumour. (Akhavan et al., 2010, Hu et al., 2005). NG2 has been shown to be abundantly expressed by high proliferative tumour cells in melanomas and gliomas (Al-Mayhany et al., 2011; Chekenya et al., 2008; Persson et al., 2010). The migration-promoting function of NG2 (Biname et al., 2013), as well as the binding to OMI/HtrA2

(Maus et al., 2015), features favoring NG2 expression by tumour cells promoting invasion and increasing resistance to oxidative stress. NG2 is included in a pool of several antigens used in a vaccine therapy against glioblastoma multiform, which reduces tumour growth (Poli A, 2013). Additionally, OPC are discussed as the major cells of origin for gliomas (Liu et al., 2012). NG2 is also involved in regulating symmetric versus asymmetric cell-division of OPC, the mode of division influences the likelihood of an OPC to become a tumour cell (Sugiarto et al., 2011). The findings of increased translation and DNA-synthesis (S-phase) by NG2 ICD correlates with the high proliferation and expression rates of these NG2-expressing tumours. These data also matches with the molecular signature of NG2+ GBMs which revealed that genes associated with proliferation and cell-cycle (MCCM, DNA replication and repair, E2F, MELK, nucleotide metabolism) were overrepresented in those tumour cells (Al-Mayhany et al., 2011), and ICD-mediated effects are therefore likely to be contributing factors to increased translation and DNA-synthesis within these tumours.

5.7. Physiological Impact of NG2 cleavage

NG2 cleavage has a multimodal effect in OPC biology. NG2, being a type-1 transmembrane protein is subjected to intramembrane proteolysis and generates an extracellular domain, CTF and intracellular domain (ICD).

This study, for the first time, revealed distinct roles of the NG2 intracellular region and provided evidence for cleaved NG2 ICD as a functional domain which adds new insights on the impact of NG2 cleavage in OPC and tumour signaling pathways (altered mTOR/FMRP). In addition to effects of the released NG2 ectodomain on the glutamatergic properties of neurons (Sakry et al., 2014), it has been shown here that the released NG2 ICD affects translation and cell-cycle kinetics and regulates expression of proteins specific to the p53 regulatory pathway and cell differentiation. These effects are important both for normal OPC as well as NG2 expressing tumours. Importantly, NG2 cleavage also could take place at the Neuron-OPC synapse where mRNAs are localized and stored (including MBP mRNA) and FMRP is likely to play a translation

repressor role in OPC as evident from this study. It would be interesting to investigate how ICD-mediated effect on FMRP downregulation alters the dynamics of local translation upon receiving stimuli. Moreover, these newly identified, altered (by NG2 ICD) signaling pathways in OPC can be influenced by the neuronal network and play an enormous role in controlling synaptic strength (Fig 5.4). It has also been shown that activity stimulates NG2 cleavage and influences OPC proliferation (Mangin et al., 2012), which could be explained by ICD-mediated drive for cell-cycle progression found in this study.

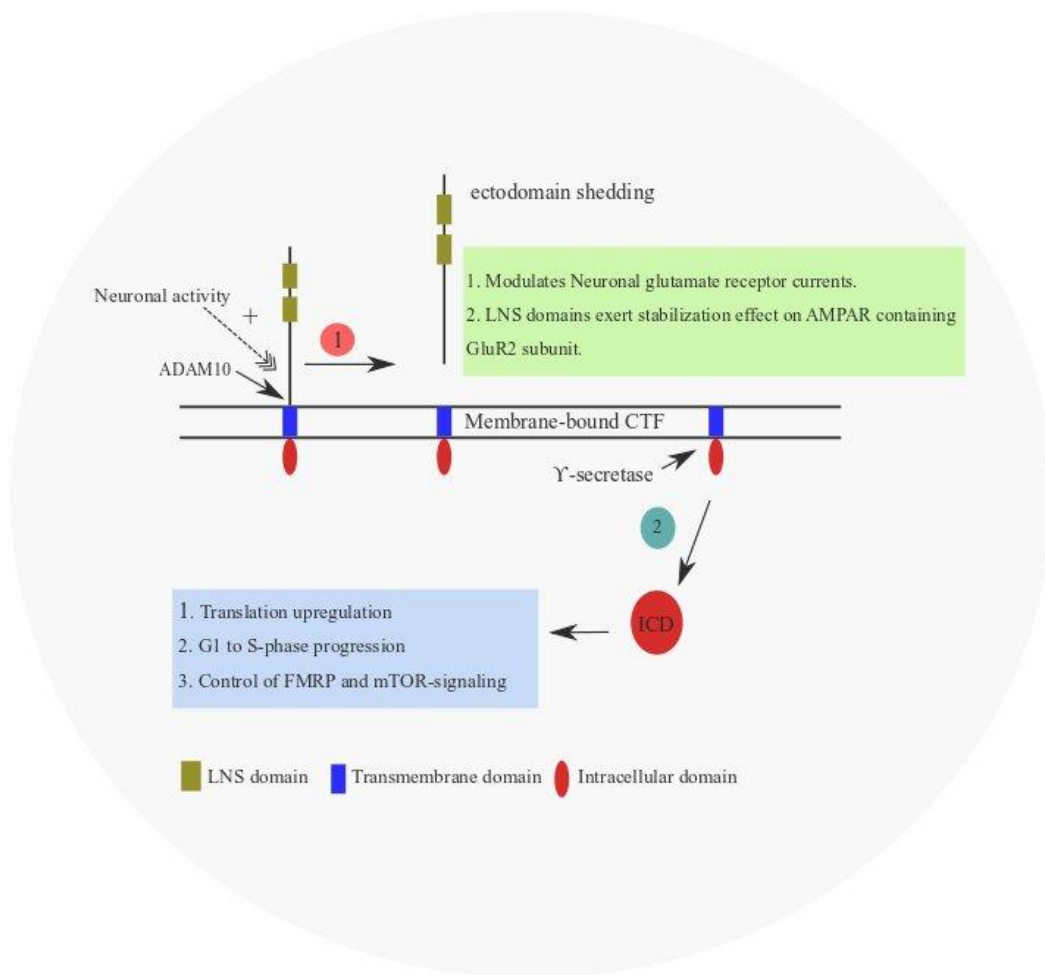


Fig 5.4. Model depicting NG2 cleavage and the main functions of the cleaved NG2 products in OPC

5.8. Future directions

This study demonstrated the functional properties of the cleaved NG2 ICD. These findings provide new insights for further research on NG2+OPC biology. Future studies should address the role of nuclear ICD (although proven to have a lower nuclear expression) in more detail. Since ICD significantly downregulates FMRP expression in OPC, the mechanism behind this downregulation needs to be investigated. This is especially important as FMRP has been shown to translocate to nucleus owing to its NLS domains and actively participates in chromatin remodeling and p53-induced DNA-damage response. As discussed above, ICD-mediated de novo proteome also represents a large fraction of DNA replication and p53- regulatory proteins and the molecular interrelation between ICD and FMRP could have a significant effect on OPC chromatin-remodeling and gene expression that has not been addressed in this study.

Moreover, cleaved NG2 ICD and FMRP are colocalized at OPC processes. It has been shown in this study that FMRP also acts as a translation repressor in NG2+ OPC, which serve as a post-synaptic compartment, and FMRP plays an important role in controlling local translation upon receiving stimuli. Therefore, the negative regulation of ICD on FMRP protein levels could exert an aberrant and impaired local translation in NG2+ OPC, which would be intriguing to investigate. The effect of FMRP downregulation on its target MBP mRNA in OPC could play a crucial role in OPC maturation. Preliminary data in this study already has shown an ICD-dependent effect on MBP mRNA stabilization and awaits further research.

It would be intriguing to investigate effects of cleaved ICD in NG2-expressing tumours and if ICD promotes or inhibits tumorigenesis in these cells which hold great potential for future NG2 therapeutic approaches to treat NG2+ GBMs.

References

References

- Akhavan, D., Cloughesy, T.F., and Mischel, P.S. (2010). mTOR signaling in glioblastoma: lessons learned from bench to bedside. *Neuro Oncol* 12(8), 882-889. doi: 10.1093/neuonc/noq052.
- Al-Mayhani, M.T., Grenfell, R., Narita, M., Piccirillo, S., Kenney-Herbert, E., Fawcett, J.W., et al. (2011). NG2 expression in glioblastoma identifies an actively proliferating population with an aggressive molecular signature. *Neuro Oncol* 13(8), 830-845. doi: 10.1093/neuonc/nor088.
- Albrecht, S., Hagemeyer, K., Ehrlich, M., Kemming, C., Trotter, J., and Kuhlmann, T. (2016). Recovery from Toxic-Induced Demyelination Does Not Require the NG2 Proteoglycan. *PLoS One* 11(10), e0163841. doi: 10.1371/journal.pone.0163841.
- Ali, S.M., and Sabatini, D.M. (2005). Structure of S6 kinase 1 determines whether raptor-mTOR or rictor-mTOR phosphorylates its hydrophobic motif site. *J Biol Chem* 280(20), 19445-19448. doi: 10.1074/jbc.C500125200.
- Allen, N.J., Bennett, M.L., Foo, L.C., Wang, G.X., Chakraborty, C., Smith, S.J., et al. (2012). Astrocyte glypicans 4 and 6 promote formation of excitatory synapses via GluA1 AMPA receptors. *Nature* 486(7403), 410-414. doi: 10.1038/nature11059.
- Alpatov, R., Lesch, B.J., Nakamoto-Kinoshita, M., Blanco, A., Chen, S., Stutzer, A., et al. (2014). A chromatin-dependent role of the fragile X mental retardation protein FMRP in the DNA damage response. *Cell* 157(4), 869-881. doi: 10.1016/j.cell.2014.03.040.
- Amson, R., Lassalle, J.M., Halley, H., Prieur, S., Lethrosne, F., Roperch, J.P., et al. (2000). Behavioral alterations associated with apoptosis and down-regulation of presenilin 1 in the brains of p53-deficient mice. *Proc Natl Acad Sci U S A* 97(10), 5346-5350.
- Andersson, E.R., Sandberg, R., and Lendahl, U. (2011). Notch signaling: simplicity in design, versatility in function. *Development* 138(17), 3593-3612. doi: 10.1242/dev.063610.
- Araque, A., Parpura, V., Sanzgiri, R.P., and Haydon, P.G. (1999). Tripartite synapses: glia, the unacknowledged partner. *Trends Neurosci* 22(5), 208-215.
- Attwell, D., Mishra, A., Hall, C.N., O'Farrell, F.M., and Dalkara, T. (2016). What is a pericyte? *J Cereb Blood Flow Metab* 36(2), 451-455. doi: 10.1177/0271678X15610340.
- Aviner, R., Shenoy, A., Elroy-Stein, O., and Geiger, T. (2015). Uncovering Hidden Layers of Cell Cycle Regulation through Integrative Multi-omic Analysis. *PLoS Genet* 11(10), e1005554. doi: 10.1371/journal.pgen.1005554.
- Bansal, R., Warrington, A.E., Gard, A.L., Ranscht, B., and Pfeiffer, S.E. (1989). Multiple and novel specificities of monoclonal antibodies O1, O4, and R-mAb used in the analysis of oligodendrocyte development. *J Neurosci Res* 24(4), 548-557. doi: 10.1002/jnr.490240413.

- Bao, J., Wolpowitz, D., Role, L.W., and Talmage, D.A. (2003). Back signaling by the Nrg-1 intracellular domain. *J Cell Biol* 161(6), 1133-1141. doi: 10.1083/jcb.200212085.
- Barres, B.A., and Raff, M.C. (1999). Axonal control of oligodendrocyte development. *J Cell Biol* 147(6), 1123-1128.
- Barritt, D.S., Pearn, M.T., Zisch, A.H., Lee, S.S., Javier, R.T., Pasquale, E.B., et al. (2000). The multi-PDZ domain protein MUPP1 is a cytoplasmic ligand for the membrane-spanning proteoglycan NG2. *J Cell Biochem* 79(2), 213-224.
- Baskin, R., Woods, N.T., Mendoza-Fandino, G., Forsyth, P., Egan, K.M., and Monteiro, A.N. (2015). Functional analysis of the 11q23.3 glioma susceptibility locus implicates PHLDB1 and DDX6 in glioma susceptibility. *Sci Rep* 5, 17367. doi: 10.1038/srep17367.
- Bassan, M., Zamostiano, R., Davidson, A., Pinhasov, A., Giladi, E., Perl, O., et al. (1999). Complete sequence of a novel protein containing a femtomolar-activity-dependent neuroprotective peptide. *J Neurochem* 72(3), 1283-1293.
- Bassell, G.J., and Warren, S.T. (2008). Fragile X syndrome: loss of local mRNA regulation alters synaptic development and function. *Neuron* 60(2), 201-214. doi: 10.1016/j.neuron.2008.10.004.
- Bayraktar, O.A., Fuentealba, L.C., Alvarez-Buylla, A., and Rowitch, D.H. (2014). Astrocyte development and heterogeneity. *Cold Spring Harb Perspect Biol* 7(1), a020362. doi: 10.1101/cshperspect.a020362.
- Ben-Sahra, I., and Manning, B.D. (2017). mTORC1 signaling and the metabolic control of cell growth. *Curr Opin Cell Biol* 45, 72-82. doi: 10.1016/j.ceb.2017.02.012.
- Bergles, D.E., Roberts, J.D., Somogyi, P., and Jahr, C.E. (2000). Glutamatergic synapses on oligodendrocyte precursor cells in the hippocampus. *Nature* 405(6783), 187-191. doi: 10.1038/35012083.
- Bhattacharya, A., Kaphzan, H., Alvarez-Dieppa, A.C., Murphy, J.P., Pierre, P., and Klann, E. (2012). Genetic removal of p70 S6 kinase 1 corrects molecular, synaptic, and behavioral phenotypes in fragile X syndrome mice. *Neuron* 76(2), 325-337. doi: 10.1016/j.neuron.2012.07.022.
- Biname, F., Sakry, D., Dimou, L., Jolivel, V., and Trotter, J. (2013). NG2 regulates directional migration of oligodendrocyte precursor cells via Rho GTPases and polarity complex proteins. *J Neurosci* 33(26), 10858-10874. doi: 10.1523/JNEUROSCI.5010-12.2013.
- Bouvier, C., Bartoli, C., Aguirre-Cruz, L., Virard, I., Colin, C., Fernandez, C., et al. (2003). Shared oligodendrocyte lineage gene expression in gliomas and oligodendrocyte progenitor cells. *J Neurosurg* 99(2), 344-350. doi: 10.3171/jns.2003.99.2.0344.

- Brown, M.S., Ye, J., Rawson, R.B., and Goldstein, J.L. (2000). Regulated intramembrane proteolysis: a control mechanism conserved from bacteria to humans. *Cell* 100(4), 391-398.
- Browne, G.J., and Proud, C.G. (2004). A Novel mTOR-Regulated Phosphorylation Site in Elongation Factor 2 Kinase Modulates the Activity of the Kinase and Its Binding to Calmodulin. *Molecular and Cellular Biology* 24(7), 2986-2997. doi: 10.1128/mcb.24.7.2986-2997.2004.
- Bujalka, H., Koenning, M., Jackson, S., Perreau, V.M., Pope, B., Hay, C.M., et al. (2013). MYRF is a membrane-associated transcription factor that autoproteolytically cleaves to directly activate myelin genes. *PLoS Biol* 11(8), e1001625. doi: 10.1371/journal.pbio.1001625.
- Burg, M.A., Grako, K.A., and Stallcup, W.B. (1998). Expression of the NG2 proteoglycan enhances the growth and metastatic properties of melanoma cells. *J Cell Physiol* 177(2), 299-312. doi: 10.1002/(SICI)1097-4652(199811)177:2<299::AID-JCP12>3.0.CO;2-5.
- Ceni, C., Kommaddi, R.P., Thomas, R., Vereker, E., Liu, X., McPherson, P.S., et al. (2010). The p75NTR intracellular domain generated by neurotrophin-induced receptor cleavage potentiates Trk signaling. *J Cell Sci* 123(Pt 13), 2299-2307. doi: 10.1242/jcs.062612.
- Chatterjee, N., Stegmuller, J., Schatzle, P., Karram, K., Koroll, M., Werner, H.B., et al. (2008). Interaction of syntenin-1 and the NG2 proteoglycan in migratory oligodendrocyte precursor cells. *J Biol Chem* 283(13), 8310-8317. doi: 10.1074/jbc.M706074200.
- Chekenya, M., Enger, P.O., Thorsen, F., Tysnes, B.B., Al-Sarraj, S., Read, T.A., et al. (2002). The glial precursor proteoglycan, NG2, is expressed on tumour neovasculature by vascular pericytes in human malignant brain tumours. *Neuropathol Appl Neurobiol* 28(5), 367-380.
- Chekenya, M., Krakstad, C., Svendsen, A., Netland, I.A., Staalesen, V., Tysnes, B.B., et al. (2008). The progenitor cell marker NG2/MPG promotes chemoresistance by activation of integrin-dependent PI3K/Akt signaling. *Oncogene* 27(39), 5182-5194. doi: 10.1038/onc.2008.157.
- Chekenya, M., and Pilkington, G.J. (2002). NG2 precursor cells in neoplasia: functional, histogenesis and therapeutic implications for malignant brain tumours. *J Neurocytol* 31(6-7), 507-521.
- Christopherson, K.S., Ullian, E.M., Stokes, C.C., Mullaney, C.E., Hell, J.W., Agah, A., et al. (2005). Thrombospondins are astrocyte-secreted proteins that promote CNS synaptogenesis. *Cell* 120(3), 421-433. doi: 10.1016/j.cell.2004.12.020.

- Darnell, J.C., and Klann, E. (2013). The translation of translational control by FMRP: therapeutic targets for FXS. *Nat Neurosci* 16(11), 1530-1536. doi: 10.1038/nn.3379.
- Darnell, J.C., Mostovetsky, O., and Darnell, R.B. (2005). FMRP RNA targets: identification and validation. *Genes Brain Behav* 4(6), 341-349. doi: 10.1111/j.1601-183X.2005.00144.x.
- Darnell, J.C., Van Driesche, S.J., Zhang, C., Hung, K.Y., Mele, A., Fraser, C.E., et al. (2011). FMRP stalls ribosomal translocation on mRNAs linked to synaptic function and autism. *Cell* 146(2), 247-261. doi: 10.1016/j.cell.2011.06.013.
- Dawson, M.R., Polito, A., Levine, J.M., and Reynolds, R. (2003). NG2-expressing glial progenitor cells: an abundant and widespread population of cycling cells in the adult rat CNS. *Mol Cell Neurosci* 24(2), 476-488.
- De Biase, L.M., Nishiyama, A., and Bergles, D.E. (2010). Excitability and synaptic communication within the oligodendrocyte lineage. *J Neurosci* 30(10), 3600-3611. doi: 10.1523/JNEUROSCI.6000-09.2010.
- de Hoz, L., and Simons, M. (2015). The emerging functions of oligodendrocytes in regulating neuronal network behaviour. *Bioessays* 37(1), 60-69. doi: 10.1002/bies.201400127.
- De Strooper, B., Annaert, W., Cupers, P., Saftig, P., Craessaerts, K., Mumm, J.S., et al. (1999). A presenilin-1-dependent gamma-secretase-like protease mediates release of Notch intracellular domain. *Nature* 398(6727), 518-522. doi: 10.1038/19083.
- Dicthenberg, J.B., Swanger, S.A., Antar, L.N., Singer, R.H., and Bassell, G.J. (2008). A direct role for FMRP in activity-dependent dendritic mRNA transport links filopodial-spine morphogenesis to fragile X syndrome. *Dev Cell* 14(6), 926-939. doi: 10.1016/j.devcel.2008.04.003.
- Didiot, M.C., Tian, Z., Schaeffer, C., Subramanian, M., Mandel, J.L., and Moine, H. (2008). The G-quartet containing FMRP binding site in FMR1 mRNA is a potent exonic splicing enhancer. *Nucleic Acids Res* 36(15), 4902-4912. doi: 10.1093/nar/gkn472.
- Diers-Fenger, M., Kirchhoff, F., Kettenmann, H., Levine, J.M., and Trotter, J. (2001). AN2/NG2 protein-expressing glial progenitor cells in the murine CNS: isolation, differentiation, and association with radial glia. *Glia* 34(3), 213-228.
- Dimou, L., and Gotz, M. (2014). Glial cells as progenitors and stem cells: new roles in the healthy and diseased brain. *Physiol Rev* 94(3), 709-737. doi: 10.1152/physrev.00036.2013.
- Edbauer, D., Winkler, E., Regula, J.T., Pesold, B., Steiner, H., and Haass, C. (2003). Reconstitution of gamma-secretase activity. *Nat Cell Biol* 5(5), 486-488. doi: 10.1038/ncb960.
- Eroglu, C., and Barres, B.A. (2010). Regulation of synaptic connectivity by glia. *Nature* 468(7321), 223-231. doi: 10.1038/nature09612.

- Estrada, B., Gisselbrecht, S.S., and Michelson, A.M. (2007). The transmembrane protein Perdido interacts with Grip and integrins to mediate myotube projection and attachment in the *Drosophila* embryo. *Development* 134(24), 4469-4478. doi: 10.1242/dev.014027.
- Etxeberria, A., Hokanson, K.C., Dao, D.Q., Mayoral, S.R., Mei, F., Redmond, S.A., et al. (2016). Dynamic Modulation of Myelination in Response to Visual Stimuli Alters Optic Nerve Conduction Velocity. *J Neurosci* 36(26), 6937-6948. doi: 10.1523/JNEUROSCI.0908-16.2016.
- Fingar, D.C., and Blenis, J. (2004). Target of rapamycin (TOR): an integrator of nutrient and growth factor signals and coordinator of cell growth and cell cycle progression. *Oncogene* 23(18), 3151-3171. doi: 10.1038/sj.onc.1207542.
- Fingar, D.C., Richardson, C.J., Tee, A.R., Cheatham, L., Tsou, C., and Blenis, J. (2003). mTOR Controls Cell Cycle Progression through Its Cell Growth Effectors S6K1 and 4E-BP1/Eukaryotic Translation Initiation Factor 4E. *Molecular and Cellular Biology* 24(1), 200-216. doi: 10.1128/mcb.24.1.200-216.2004.
- Forbes, T.A., and Gallo, V. (2017). All Wrapped Up: Environmental Effects on Myelination. *Trends Neurosci* 40(9), 572-587. doi: 10.1016/j.tins.2017.06.009.
- Forsyth, P.A., Krishna, N., Lawn, S., Valadez, J.G., Qu, X., Fenstermacher, D.A., et al. (2014). p75 neurotrophin receptor cleavage by alpha- and gamma-secretases is required for neurotrophin-mediated proliferation of brain tumor-initiating cells. *J Biol Chem* 289(12), 8067-8085. doi: 10.1074/jbc.M113.513762.
- Foster, D.A., Yellen, P., Xu, L., and Saqcena, M. (2010). Regulation of G1 Cell Cycle Progression: Distinguishing the Restriction Point from a Nutrient-Sensing Cell Growth Checkpoint(s). *Genes Cancer* 1(11), 1124-1131. doi: 10.1177/1947601910392989.
- Fruhbeis, C., Frohlich, D., Kuo, W.P., Amphornrat, J., Thilemann, S., Saab, A.S., et al. (2013). Neurotransmitter-triggered transfer of exosomes mediates oligodendrocyte-neuron communication. *PLoS Biol* 11(7), e1001604. doi: 10.1371/journal.pbio.1001604.
- Fu, H., Cai, J., Clevers, H., Fast, E., Gray, S., Greenberg, R., et al. (2009). A genome-wide screen for spatially restricted expression patterns identifies transcription factors that regulate glial development. *J Neurosci* 29(36), 11399-11408. doi: 10.1523/JNEUROSCI.0160-09.2009.
- Fukushi, J., Inatani, M., Yamaguchi, Y., and Stallcup, W.B. (2003). Expression of NG2 proteoglycan during endochondral and intramembranous ossification. *Dev Dyn* 228(1), 143-148. doi: 10.1002/dvdy.10359.

- Fukushi, J., Makagiansar, I.T., and Stallcup, W.B. (2004). NG2 proteoglycan promotes endothelial cell motility and angiogenesis via engagement of galectin-3 and alpha3beta1 integrin. *Mol Biol Cell* 15(8), 3580-3590. doi: 10.1091/mbc.e04-03-0236.
- Funfschilling, U., Supplie, L.M., Mahad, D., Boretius, S., Saab, A.S., Edgar, J., et al. (2012). Glycolytic oligodendrocytes maintain myelin and long-term axonal integrity. *Nature* 485(7399), 517-521. doi: 10.1038/nature11007.
- Gallo, V., and Armstrong, R.C. (2008). Myelin repair strategies: a cellular view. *Curr Opin Neurol* 21(3), 278-283. doi: 10.1097/WCO.0b013e3282fd1875.
- Garrett, A.M., and Weiner, J.A. (2009). Control of CNS synapse development by {gamma}-protocadherin-mediated astrocyte-neuron contact. *J Neurosci* 29(38), 11723-11731. doi: 10.1523/JNEUROSCI.2818-09.2009.
- Ghali, L., Wong, S.T., Tidman, N., Quinn, A., Philpott, M.P., and Leigh, I.M. (2004). Epidermal and hair follicle progenitor cells express melanoma-associated chondroitin sulfate proteoglycan core protein. *J Invest Dermatol* 122(2), 433-442. doi: 10.1046/j.0022-202X.2004.22207.x.
- Giampetruzzi, A., Carson, J.H., and Barbarese, E. (2013). FMRP and myelin protein expression in oligodendrocytes. *Mol Cell Neurosci* 56, 333-341. doi: 10.1016/j.mcn.2013.07.009.
- Gibson, E.M., Purger, D., Mount, C.W., Goldstein, A.K., Lin, G.L., Wood, L.S., et al. (2014). Neuronal activity promotes oligodendrogenesis and adaptive myelination in the mammalian brain. *Science* 344(6183), 1252304. doi: 10.1126/science.1252304.
- Girolamo, F., Ferrara, G., Strippoli, M., Rizzi, M., Errede, M., Trojano, M., et al. (2011). Cerebral cortex demyelination and oligodendrocyte precursor response to experimental autoimmune encephalomyelitis. *Neurobiol Dis* 43(3), 678-689. doi: 10.1016/j.nbd.2011.05.021.
- Goldman, S. (2005). Stem and progenitor cell-based therapy of the human central nervous system. *Nat Biotechnol* 23(7), 862-871. doi: 10.1038/nbt1119.
- Goodman, C.A., Pierre, P., and Hornberger, T.A. (2012). Imaging of protein synthesis with puromycin. *Proc Natl Acad Sci U S A* 109(17), E989; author reply E990. doi: 10.1073/pnas.1202000109.
- Goretzki, L., Burg, M.A., Grako, K.A., and Stallcup, W.B. (1999). High-affinity binding of basic fibroblast growth factor and platelet-derived growth factor-AA to the core protein of the NG2 proteoglycan. *J Biol Chem* 274(24), 16831-16837.
- Goritz, C., Mauch, D.H., and Pfrieger, F.W. (2005). Multiple mechanisms mediate cholesterol-induced synaptogenesis in a CNS neuron. *Mol Cell Neurosci* 29(2), 190-201. doi: 10.1016/j.mcn.2005.02.006.

- Goutte, C., Tsunozaki, M., Hale, V.A., and Priess, J.R. (2002). APH-1 is a multipass membrane protein essential for the Notch signaling pathway in *Caenorhabditis elegans* embryos. *Proc Natl Acad Sci U S A* 99(2), 775-779. doi: 10.1073/pnas.022523499.
- Grako, K.A., and Stallcup, W.B. (1995). Participation of the NG2 proteoglycan in rat aortic smooth muscle cell responses to platelet-derived growth factor. *Exp Cell Res* 221(1), 231-240. doi: 10.1006/excr.1995.1371.
- Gross, C., Nakamoto, M., Yao, X., Chan, C.B., Yim, S.Y., Ye, K., et al. (2010). Excess phosphoinositide 3-kinase subunit synthesis and activity as a novel therapeutic target in fragile X syndrome. *J Neurosci* 30(32), 10624-10638. doi: 10.1523/JNEUROSCI.0402-10.2010.
- Haas, B.W., Barnea-Goraly, N., Lightbody, A.A., Patnaik, S.S., Hoeft, F., Hazlett, H., et al. (2009). Early white-matter abnormalities of the ventral frontostriatal pathway in fragile X syndrome. *Dev Med Child Neurol* 51(8), 593-599. doi: 10.1111/j.1469-8749.2009.03295.x.
- He, Y., Dupree, J., Wang, J., Sandoval, J., Li, J., Liu, H., et al. (2007). The transcription factor Yin Yang 1 is essential for oligodendrocyte progenitor differentiation. *Neuron* 55(2), 217-230. doi: 10.1016/j.neuron.2007.06.029.
- Hill, R.A., Patel, K.D., Medved, J., Reiss, A.M., and Nishiyama, A. (2013). NG2 cells in white matter but not gray matter proliferate in response to PDGF. *J Neurosci* 33(36), 14558-14566. doi: 10.1523/JNEUROSCI.2001-12.2013.
- Hoeft, F., Carter, J.C., Lightbody, A.A., Cody Hazlett, H., Piven, J., and Reiss, A.L. (2010). Region-specific alterations in brain development in one- to three-year-old boys with fragile X syndrome. *Proc Natl Acad Sci U S A* 107(20), 9335-9339. doi: 10.1073/pnas.1002762107.
- Holz, M.K., Ballif, B.A., Gygi, S.P., and Blenis, J. (2005). mTOR and S6K1 mediate assembly of the translation preinitiation complex through dynamic protein interchange and ordered phosphorylation events. *Cell* 123(4), 569-580. doi: 10.1016/j.cell.2005.10.024.
- Hu, X., Pandolfi, P.P., Li, Y., Koutcher, J.A., Rosenblum, M., and Holland, E.C. (2005). mTOR promotes survival and astrocytic characteristics induced by Pten/AKT signaling in glioblastoma. *Neoplasia* 7(4), 356-368.
- Huang, W., Zhao, N., Bai, X., Karram, K., Trotter, J., Goebbels, S., et al. (2014). Novel NG2-CreERT2 knock-in mice demonstrate heterogeneous differentiation potential of NG2 glia during development. *Glia* 62(6), 896-913. doi: 10.1002/glia.22648.

- Jacinto, E., Loewith, R., Schmidt, A., Lin, S., Ruegg, M.A., Hall, A., et al. (2004). Mammalian TOR complex 2 controls the actin cytoskeleton and is rapamycin insensitive. *Nat Cell Biol* 6(11), 1122-1128. doi: 10.1038/ncb1183.
- Joy, A.M., Beaudry, C.E., Tran, N.L., Ponce, F.A., Holz, D.R., Demuth, T., et al. (2003). Migrating glioma cells activate the PI3-K pathway and display decreased susceptibility to apoptosis. *J Cell Sci* 116(Pt 21), 4409-4417. doi: 10.1242/jcs.00712.
- Jung, M., Kramer, E., Grzenkowski, M., Tang, K., Blakemore, W., Aguzzi, A., et al. (1995). Lines of murine oligodendroglial precursor cells immortalized by an activated neu tyrosine kinase show distinct degrees of interaction with axons in vitro and in vivo. *Eur J Neurosci* 7(6), 1245-1265.
- Kadoya, K., Fukushi, J., Matsumoto, Y., Yamaguchi, Y., and Stallcup, W.B. (2008). NG2 proteoglycan expression in mouse skin: altered postnatal skin development in the NG2 null mouse. *J Histochem Cytochem* 56(3), 295-303. doi: 10.1369/jhc.7A7349.2007.
- Kang, S.H., Fukaya, M., Yang, J.K., Rothstein, J.D., and Bergles, D.E. (2010). NG2+ CNS glial progenitors remain committed to the oligodendrocyte lineage in postnatal life and following neurodegeneration. *Neuron* 68(4), 668-681. doi: 10.1016/j.neuron.2010.09.009.
- Kashyap, R., Roucourt, B., Lembo, F., Fares, J., Carcavilla, A.M., Restouin, A., et al. (2015). Syntenin controls migration, growth, proliferation, and cell cycle progression in cancer cells. *Front Pharmacol* 6, 241. doi: 10.3389/fphar.2015.00241.
- Kawasumi, M., Matsuda, S., Matsuoka, M., and Nishimoto, I. (2004). Cytoplasmic tail adaptors of Alzheimer's amyloid-beta protein precursor. *Mol Neurobiol* 30(2), 185-200. doi: 10.1385/MN:30:2:185.
- Kettenmann, H., Hanisch, U.K., Noda, M., and Verkhratsky, A. (2011). Physiology of microglia. *Physiol Rev* 91(2), 461-553. doi: 10.1152/physrev.00011.2010.
- Kimberly, W.T., LaVoie, M.J., Ostaszewski, B.L., Ye, W., Wolfe, M.S., and Selkoe, D.J. (2003). Gamma-secretase is a membrane protein complex comprised of presenilin, nicastrin, Aph-1, and Pen-2. *Proc Natl Acad Sci U S A* 100(11), 6382-6387. doi: 10.1073/pnas.1037392100.
- Kopec, C.D., Real, E., Kessels, H.W., and Malinow, R. (2007). GluR1 links structural and functional plasticity at excitatory synapses. *J Neurosci* 27(50), 13706-13718. doi: 10.1523/JNEUROSCI.3503-07.2007.
- Kucukdereli, H., Allen, N.J., Lee, A.T., Feng, A., Ozlu, M.I., Conatser, L.M., et al. (2011). Control of excitatory CNS synaptogenesis by astrocyte-secreted proteins Hevin and SPARC. *Proc Natl Acad Sci U S A* 108(32), E440-449. doi: 10.1073/pnas.1104977108.

- Lal, M., and Caplan, M. (2011). Regulated intramembrane proteolysis: signaling pathways and biological functions. *Physiology (Bethesda)* 26(1), 34-44. doi: 10.1152/physiol.00028.2010.
- Laplante, M., and Sabatini, D.M. (2012). mTOR signaling in growth control and disease. *Cell* 149(2), 274-293. doi: 10.1016/j.cell.2012.03.017.
- Lee, Y., Morrison, B.M., Li, Y., Lengacher, S., Farah, M.H., Hoffman, P.N., et al. (2012). Oligodendroglia metabolically support axons and contribute to neurodegeneration. *Nature* 487(7408), 443-448. doi: 10.1038/nature11314.
- Legg, J., Jensen, U.B., Broad, S., Leigh, I., and Watt, F.M. (2003). Role of melanoma chondroitin sulphate proteoglycan in patterning stem cells in human interfollicular epidermis. *Development* 130(24), 6049-6063. doi: 10.1242/dev.00837.
- Levine, J.M., and Nishiyama, A. (1996). The NG2 chondroitin sulfate proteoglycan: a multifunctional proteoglycan associated with immature cells. *Perspect Dev Neurobiol* 3(4), 245-259.
- Li, X., Wu, C., Chen, N., Gu, H., Yen, A., Cao, L., et al. (2016). PI3K/Akt/mTOR signaling pathway and targeted therapy for glioblastoma. *Oncotarget* 7(22), 33440-33450. doi: 10.18632/oncotarget.7961.
- Li, Y., and Zhao, X. (2014). Concise review: Fragile X proteins in stem cell maintenance and differentiation. *Stem Cells* 32(7), 1724-1733. doi: 10.1002/stem.1698.
- Lichtenthaler, S.F., Haass, C., and Steiner, H. (2011). Regulated intramembrane proteolysis-lessons from amyloid precursor protein processing. *J Neurochem* 117(5), 779-796. doi: 10.1111/j.1471-4159.2011.07248.x.
- Lin, S.C., Huck, J.H., Roberts, J.D., Macklin, W.B., Somogyi, P., and Bergles, D.E. (2005). Climbing fiber innervation of NG2-expressing glia in the mammalian cerebellum. *Neuron* 46(5), 773-785. doi: 10.1016/j.neuron.2005.04.025.
- Lin, X.H., Dahlin-Huppe, K., and Stallcup, W.B. (1996a). Interaction of the NG2 proteoglycan with the actin cytoskeleton. *J Cell Biochem* 63(4), 463-477. doi: 10.1002/(SICI)1097-4644(19961215)63:4<463::AID-JCB8>3.0.CO;2-R.
- Lin, X.H., Grako, K.A., Burg, M.A., and Stallcup, W.B. (1996b). NG2 proteoglycan and the actin-binding protein fascin define separate populations of actin-containing filopodia and lamellipodia during cell spreading and migration. *Mol Biol Cell* 7(12), 1977-1993.
- Liu, C., and Zong, H. (2012). Developmental origins of brain tumors. *Curr Opin Neurobiol* 22(5), 844-849. doi: 10.1016/j.conb.2012.04.012.
- Liu, W., Jiang, F., Bi, X., and Zhang, Y.Q. (2012). Drosophila FMRP participates in the DNA damage response by regulating G2/M cell cycle checkpoint and apoptosis. *Hum Mol Genet* 21(21), 4655-4668. doi: 10.1093/hmg/dds307.

- Loeb, K.R., Kostner, H., Firpo, E., Norwood, T., K, D.T., Clurman, B.E., et al. (2005). A mouse model for cyclin E-dependent genetic instability and tumorigenesis. *Cancer Cell* 8(1), 35-47. doi: 10.1016/j.ccr.2005.06.010.
- Lu, Q.R., Sun, T., Zhu, Z., Ma, N., Garcia, M., Stiles, C.D., et al. (2002). Common developmental requirement for Olig function indicates a motor neuron/oligodendrocyte connection. *Cell* 109(1), 75-86.
- Luca, R., Averna, M., Zalfa, F., Vecchi, M., Bianchi, F., La Fata, G., et al. (2013). The fragile X protein binds mRNAs involved in cancer progression and modulates metastasis formation. *EMBO Mol Med* 5(10), 1523-1536. doi: 10.1002/emmm.201302847.
- Lyons, D.A., Naylor, S.G., Scholze, A., and Talbot, W.S. (2009). Kif1b is essential for mRNA localization in oligodendrocytes and development of myelinated axons. *Nat Genet* 41(7), 854-858. doi: 10.1038/ng.376.
- Makagiansar, I.T., Williams, S., Dahlin-Huppe, K., Fukushi, J., Mustelin, T., and Stallcup, W.B. (2004). Phosphorylation of NG2 proteoglycan by protein kinase C-alpha regulates polarized membrane distribution and cell motility. *J Biol Chem* 279(53), 55262-55270. doi: 10.1074/jbc.M411045200.
- Makagiansar, I.T., Williams, S., Mustelin, T., and Stallcup, W.B. (2007). Differential phosphorylation of NG2 proteoglycan by ERK and PKCalpha helps balance cell proliferation and migration. *J Cell Biol* 178(1), 155-165. doi: 10.1083/jcb.200612084.
- Maldonado, P.P., Velez-Fort, M., and Angulo, M.C. (2011). Is neuronal communication with NG2 cells synaptic or extrasynaptic? *J Anat* 219(1), 8-17. doi: 10.1111/j.1469-7580.2011.01350.x.
- Malinverno, M., Carta, M., Epis, R., Marcello, E., Verpelli, C., Cattabeni, F., et al. (2010). Synaptic localization and activity of ADAM10 regulate excitatory synapses through N-cadherin cleavage. *J Neurosci* 30(48), 16343-16355. doi: 10.1523/JNEUROSCI.1984-10.2010.
- Mallon, B.S., Shick, H.E., Kidd, G.J., and Macklin, W.B. (2002). Proteolipid promoter activity distinguishes two populations of NG2-positive cells throughout neonatal cortical development. *J Neurosci* 22(3), 876-885.
- Mandel, S., and Gozes, I. (2007). Activity-dependent neuroprotective protein constitutes a novel element in the SWI/SNF chromatin remodeling complex. *J Biol Chem* 282(47), 34448-34456. doi: 10.1074/jbc.M704756200.
- Mangin, J.M., and Gallo, V. (2011). The curious case of NG2 cells: transient trend or game changer? *ASN Neuro* 3(1), e00052. doi: 10.1042/AN20110001.
- Marambaud, P., Wen, P.H., Dutt, A., Shioi, J., Takashima, A., Siman, R., et al. (2003). A CBP binding transcriptional repressor produced by the PS1/epsilon-cleavage of N-cadherin is inhibited by PS1 FAD mutations. *Cell* 114(5), 635-645.

- Marques, S., van Bruggen, D., Vanichkina, D.P., Floriddia, E.M., Munguba, H., Varemo, L., et al. (2018). Transcriptional Convergence of Oligodendrocyte Lineage Progenitors during Development. *Dev Cell* 46(4), 504-517 e507. doi: 10.1016/j.devcel.2018.07.005.
- Martin, L.J., Oh, G.H., and Orser, B.A. (2009). Etomidate targets alpha5 gamma-aminobutyric acid subtype A receptors to regulate synaptic plasticity and memory blockade. *Anesthesiology* 111(5), 1025-1035. doi: 10.1097/ALN.0b013e3181bbc961.
- Matsuno, K., Diederich, R.J., Go, M.J., Blaumueller, C.M., and Artavanis-Tsakonas, S. (1995). Deltex acts as a positive regulator of Notch signaling through interactions with the Notch ankyrin repeats. *Development* 121(8), 2633-2644.
- Matthias, K., Kirchhoff, F., Seifert, G., Huttmann, K., Matyash, M., Kettenmann, H., et al. (2003). Segregated expression of AMPA-type glutamate receptors and glutamate transporters defines distinct astrocyte populations in the mouse hippocampus. *J Neurosci* 23(5), 1750-1758.
- Maus, F., Sakry, D., Biname, F., Karram, K., Rajalingam, K., Watts, C., et al. (2015). The NG2 Proteoglycan Protects Oligodendrocyte Precursor Cells against Oxidative Stress via Interaction with OMI/HtrA2. *PLoS One* 10(9), e0137311. doi: 10.1371/journal.pone.0137311.
- McKenzie, I.A., Ohayon, D., Li, H., de Faria, J.P., Emery, B., Tohyama, K., et al. (2014). Motor skill learning requires active central myelination. *Science* 346(6207), 318-322. doi: 10.1126/science.1254960.
- Mensch, S., Baraban, M., Almeida, R., Czopka, T., Ausborn, J., El Manira, A., et al. (2015). Synaptic vesicle release regulates myelin sheath number of individual oligodendrocytes in vivo. *Nat Neurosci* 18(5), 628-630. doi: 10.1038/nn.3991.
- Micu, I., Plemel, J.R., Lachance, C., Proft, J., Jansen, A.J., Cummins, K., et al. (2016). The molecular physiology of the axo-myelinic synapse. *Exp Neurol* 276, 41-50. doi: 10.1016/j.expneurol.2015.10.006.
- Miller, R.H. (1996). Oligodendrocyte origins. *Trends Neurosci* 19(3), 92-96.
- Milner, R., Anderson, H.J., Rippon, R.F., McKay, J.S., Franklin, R.J., Marchionni, M.A., et al. (1997). Contrasting effects of mitogenic growth factors on oligodendrocyte precursor cell migration. *Glia* 19(1), 85-90.
- Muller, T., Meyer, H.E., Egensperger, R., and Marcus, K. (2008). The amyloid precursor protein intracellular domain (AICD) as modulator of gene expression, apoptosis, and cytoskeletal dynamics-relevance for Alzheimer's disease. *Prog Neurobiol* 85(4), 393-406. doi: 10.1016/j.pneurobio.2008.05.002.
- Narayanan, U., Nalavadi, V., Nakamoto, M., Thomas, G., Ceman, S., Bassell, G.J., et al. (2008). S6K1 phosphorylates and regulates fragile X mental retardation protein

- (FMRP) with the neuronal protein synthesis-dependent mammalian target of rapamycin (mTOR) signaling cascade. *J Biol Chem* 283(27), 18478-18482. doi: 10.1074/jbc.C800055200.
- Nave, K.A. (2010a). Myelination and support of axonal integrity by glia. *Nature* 468(7321), 244-252. doi: 10.1038/nature09614.
- Nave, K.A. (2010b). Myelination and the trophic support of long axons. *Nat Rev Neurosci* 11(4), 275-283. doi: 10.1038/nrn2797.
- Nayak, T., Trotter, J., and Sakry, D. (2018). The Intracellular Cleavage Product of the NG2 Proteoglycan Modulates Translation and Cell-Cycle Kinetics via Effects on mTORC1/FMRP Signaling. *Front Cell Neurosci* 12, 231. doi: 10.3389/fncel.2018.00231.
- Niehaus, A., Stegmüller, J., Diers-Fenger, M., and Trotter, J. (1999). Cell-surface glycoprotein of oligodendrocyte progenitors involved in migration. *J Neurosci* 19(12), 4948-4961.
- Nishiyama, A., Komitova, M., Suzuki, R., and Zhu, X. (2009). Polydendrocytes (NG2 cells): multifunctional cells with lineage plasticity. *Nat Rev Neurosci* 10(1), 9-22. doi: 10.1038/nrn2495.
- Nishiyama, A., Lin, X.H., Giese, N., Heldin, C.H., and Stallcup, W.B. (1996a). Co-localization of NG2 proteoglycan and PDGF alpha-receptor on O2A progenitor cells in the developing rat brain. *J Neurosci Res* 43(3), 299-314. doi: 10.1002/(SICI)1097-4547(19960201)43:3<299::AID-JNR5>3.0.CO;2-E.
- Nishiyama, A., Lin, X.H., Giese, N., Heldin, C.H., and Stallcup, W.B. (1996b). Interaction between NG2 proteoglycan and PDGF alpha-receptor on O2A progenitor cells is required for optimal response to PDGF. *J Neurosci Res* 43(3), 315-330. doi: 10.1002/(SICI)1097-4547(19960201)43:3<315::AID-JNR6>3.0.CO;2-M.
- Nishiyama, A., Lin, X.H., and Stallcup, W.B. (1995). Generation of truncated forms of the NG2 proteoglycan by cell surface proteolysis. *Mol Biol Cell* 6(12), 1819-1832.
- Okray, Z., de Esch, C.E., Van Esch, H., Devriendt, K., Claeys, A., Yan, J., et al. (2015). A novel fragile X syndrome mutation reveals a conserved role for the carboxy-terminus in FMRP localization and function. *EMBO Mol Med* 7(4), 423-437. doi: 10.15252/emmm.201404576.
- Ozerdem, U., Monosov, E., and Stallcup, W.B. (2002). NG2 proteoglycan expression by pericytes in pathological microvasculature. *Microvasc Res* 63(1), 129-134. doi: 10.1006/mvre.2001.2376.
- Pacey, L.K., Xuan, I.C., Guan, S., Sussman, D., Henkelman, R.M., Chen, Y., et al. (2013). Delayed myelination in a mouse model of fragile X syndrome. *Hum Mol Genet* 22(19), 3920-3930. doi: 10.1093/hmg/ddt246.

- Paolicelli, R.C., Bolasco, G., Pagani, F., Maggi, L., Scianni, M., Panzanelli, P., et al. (2011). Synaptic pruning by microglia is necessary for normal brain development. *Science* 333(6048), 1456-1458. doi: 10.1126/science.1202529.
- Park, S., Park, J.M., Kim, S., Kim, J.A., Shepherd, J.D., Smith-Hicks, C.L., et al. (2008). Elongation factor 2 and fragile X mental retardation protein control the dynamic translation of Arc/Arg3.1 essential for mGluR-LTD. *Neuron* 59(1), 70-83. doi: 10.1016/j.neuron.2008.05.023.
- Pasciuto, E., Ahmed, T., Wahle, T., Gardoni, F., D'Andrea, L., Pacini, L., et al. (2015). Dysregulated ADAM10-Mediated Processing of APP during a Critical Time Window Leads to Synaptic Deficits in Fragile X Syndrome. *Neuron* 87(2), 382-398. doi: 10.1016/j.neuron.2015.06.032.
- Pasciuto, E., and Bagni, C. (2014). SnapShot: FMRP mRNA targets and diseases. *Cell* 158(6), 1446-1446 e1441. doi: 10.1016/j.cell.2014.08.035.
- Pinhasov, A., Mandel, S., Torchinsky, A., Giladi, E., Pittel, Z., Goldsweig, A.M., et al. (2003). Activity-dependent neuroprotective protein: a novel gene essential for brain formation. *Brain Res Dev Brain Res* 144(1), 83-90.
- Pluschke, G., Vanek, M., Evans, A., Dittmar, T., Schmid, P., Itin, P., et al. (1996). Molecular cloning of a human melanoma-associated chondroitin sulfate proteoglycan. *Proc Natl Acad Sci U S A* 93(18), 9710-9715.
- Poli, A., Wang, J., Domingues, O., Planaguma, J., Yan, T., Rygh, C.B., et al. (2013). Targeting glioblastoma with NK cells and mAb against NG2/CSPG4 prolongs animal survival. *Oncotarget* 4(9), 1527-1546. doi: 10.18632/oncotarget.1291.
- Polito, A., and Reynolds, R. (2005). NG2-expressing cells as oligodendrocyte progenitors in the normal and demyelinated adult central nervous system. *J Anat* 207(6), 707-716. doi: 10.1111/j.1469-7580.2005.00454.x.
- Poskanzer, K.E., and Molofsky, A.V. (2018). Dynamism of an Astrocyte In Vivo: Perspectives on Identity and Function. *Annu Rev Physiol* 80, 143-157. doi: 10.1146/annurev-physiol-021317-121125.
- Pringle, N.P., Mudhar, H.S., Collarini, E.J., and Richardson, W.D. (1992). PDGF receptors in the rat CNS: during late neurogenesis, PDGF alpha-receptor expression appears to be restricted to glial cells of the oligodendrocyte lineage. *Development* 115(2), 535-551.
- Pringle, N.P., Nadon, N.L., Rhode, D.M., Richardson, W.D., and Duncan, I.D. (1997). Normal temporal and spatial distribution of oligodendrocyte progenitors in the myelin-deficient (md) rat. *J Neurosci Res* 47(3), 264-270.

- Pringle, N.P., and Richardson, W.D. (1993). A singularity of PDGF alpha-receptor expression in the dorsoventral axis of the neural tube may define the origin of the oligodendrocyte lineage. *Development* 117(2), 525-533.
- Pullen, N., Dennis, P.B., Andjelkovic, M., Dufner, A., Kozma, S.C., Hemmings, B.A., et al. (1998). Phosphorylation and activation of p70s6k by PDK1. *Science* 279(5351), 707-710.
- Raff, M.C., Miller, R.H., and Noble, M. (1983). A glial progenitor cell that develops in vitro into an astrocyte or an oligodendrocyte depending on culture medium. *Nature* 303(5916), 390-396.
- Rajasekhar, V.K., Viale, A., Socci, N.D., Wiedmann, M., Hu, X., and Holland, E.C. (2003). Oncogenic Ras and Akt signaling contribute to glioblastoma formation by differential recruitment of existing mRNAs to polysomes. *Mol Cell* 12(4), 889-901.
- Rangroo Thrane, V., Thrane, A.S., Wang, F., Cotrina, M.L., Smith, N.A., Chen, M., et al. (2013). Ammonia triggers neuronal disinhibition and seizures by impairing astrocyte potassium buffering. *Nat Med* 19(12), 1643-1648. doi: 10.1038/nm.3400.
- Ransohoff, R.M., and Perry, V.H. (2009). Microglial physiology: unique stimuli, specialized responses. *Annu Rev Immunol* 27, 119-145. doi: 10.1146/annurev.immunol.021908.132528.
- Rao, V.R., and Finkbeiner, S. (2003). Secrets of a secretase: N-cadherin proteolysis regulates CBP function. *Cell* 114(5), 533-535.
- Raychaudhuri, M., and Mukhopadhyay, D. (2007). AICD and its adaptors - in search of new players. *J Alzheimers Dis* 11(3), 343-358.
- Reiss, K., Maretzky, T., Ludwig, A., Tousseyn, T., de Strooper, B., Hartmann, D., et al. (2005). ADAM10 cleavage of N-cadherin and regulation of cell-cell adhesion and beta-catenin nuclear signalling. *EMBO J* 24(4), 742-752. doi: 10.1038/sj.emboj.7600548.
- Richardson, W.D., Kessaris, N., and Pringle, N. (2006). Oligodendrocyte wars. *Nat Rev Neurosci* 7(1), 11-18. doi: 10.1038/nrn1826.
- Richardson, W.D., Pringle, N.P., Yu, W.P., and Hall, A.C. (1997). Origins of spinal cord oligodendrocytes: possible developmental and evolutionary relationships with motor neurons. *Dev Neurosci* 19(1), 58-68. doi: 10.1159/000111186.
- Richter, J.D., Bassell, G.J., and Klann, E. (2015). Dysregulation and restoration of translational homeostasis in fragile X syndrome. *Nat Rev Neurosci* 16(10), 595-605. doi: 10.1038/nrn4001.
- Richter, J.D., and Collier, J. (2015). Pausing on Polyribosomes: Make Way for Elongation in Translational Control. *Cell* 163(2), 292-300. doi: 10.1016/j.cell.2015.09.041.

- Riedle, S., Kiefel, H., Gast, D., Bondong, S., Wolterink, S., Gutwein, P., et al. (2009). Nuclear translocation and signalling of L1-CAM in human carcinoma cells requires ADAM10 and presenilin/gamma-secretase activity. *Biochem J* 420(3), 391-402. doi: 10.1042/BJ20081625.
- Rivers, L.E., Young, K.M., Rizzi, M., Jamen, F., Psachoulia, K., Wade, A., et al. (2008). PDGFRA/NG2 glia generate myelinating oligodendrocytes and piriform projection neurons in adult mice. *Nat Neurosci* 11(12), 1392-1401. doi: 10.1038/nn.2220.
- Saftig, P., and Lichtenthaler, S.F. (2015). The alpha secretase ADAM10: A metalloprotease with multiple functions in the brain. *Prog Neurobiol* 135, 1-20. doi: 10.1016/j.pneurobio.2015.10.003.
- Saitoh, M., Pullen, N., Brennan, P., Cantrell, D., Dennis, P.B., and Thomas, G. (2002). Regulation of an activated S6 kinase 1 variant reveals a novel mammalian target of rapamycin phosphorylation site. *J Biol Chem* 277(22), 20104-20112. doi: 10.1074/jbc.M201745200.
- Sakry, D., Karram, K., and Trotter, J. (2011). Synapses between NG2 glia and neurons. *J Anat* 219(1), 2-7. doi: 10.1111/j.1469-7580.2011.01359.x.
- Sakry, D., Neitz, A., Singh, J., Frischknecht, R., Marongiu, D., Biname, F., et al. (2014). Oligodendrocyte precursor cells modulate the neuronal network by activity-dependent ectodomain cleavage of glial NG2. *PLoS Biol* 12(11), e1001993. doi: 10.1371/journal.pbio.1001993.
- Sakry, D., and Trotter, J. (2016). The role of the NG2 proteoglycan in OPC and CNS network function. *Brain Res* 1638(Pt B), 161-166. doi: 10.1016/j.brainres.2015.06.003.
- Sakry, D., Yigit, H., Dimou, L., and Trotter, J. (2015). Oligodendrocyte precursor cells synthesize neuromodulatory factors. *PLoS One* 10(5), e0127222. doi: 10.1371/journal.pone.0127222.
- Saqcena, M., Menon, D., Patel, D., Mukhopadhyay, S., Chow, V., and Foster, D.A. (2013). Amino acids and mTOR mediate distinct metabolic checkpoints in mammalian G1 cell cycle. *PLoS One* 8(8), e74157. doi: 10.1371/journal.pone.0074157.
- Sarbasov, D.D., Guertin, D.A., Ali, S.M., and Sabatini, D.M. (2005). Phosphorylation and regulation of Akt/PKB by the rictor-mTOR complex. *Science* 307(5712), 1098-1101. doi: 10.1126/science.1106148.
- Sardi, S.P., Murtie, J., Koirala, S., Patten, B.A., and Corfas, G. (2006). Presenilin-dependent ErbB4 nuclear signaling regulates the timing of astrogenesis in the developing brain. *Cell* 127(1), 185-197. doi: 10.1016/j.cell.2006.07.037.
- Schafer, D.P., Lehrman, E.K., Kautzman, A.G., Koyama, R., Mardinly, A.R., Yamasaki, R., et al. (2012). Microglia sculpt postnatal neural circuits in an activity and complement-dependent manner. *Neuron* 74(4), 691-705. doi: 10.1016/j.neuron.2012.03.026.

- Schlaitz, A.L., Thompson, J., Wong, C.C., Yates, J.R., 3rd, and Heald, R. (2013). REEP3/4 ensure endoplasmic reticulum clearance from metaphase chromatin and proper nuclear envelope architecture. *Dev Cell* 26(3), 315-323. doi: 10.1016/j.devcel.2013.06.016.
- Schlegel, A.A., Rudelson, J.J., and Tse, P.U. (2012). White matter structure changes as adults learn a second language. *J Cogn Neurosci* 24(8), 1664-1670. doi: 10.1162/jocn_a_00240.
- Schlingemann, R.O., Rietveld, F.J., Kwaspens, F., van de Kerkhof, P.C., de Waal, R.M., and Ruiten, D.J. (1991). Differential expression of markers for endothelial cells, pericytes, and basal lamina in the microvasculature of tumors and granulation tissue. *Am J Pathol* 138(6), 1335-1347.
- Schmidt, E.K., Clavarino, G., Ceppi, M., and Pierre, P. (2009). SUnSET, a nonradioactive method to monitor protein synthesis. *Nat Methods* 6(4), 275-277. doi: 10.1038/nmeth.1314.
- Schnadelbach, O., Blaschuk, O.W., Symonds, M., Gour, B.J., Doherty, P., and Fawcett, J.W. (2000). N-cadherin influences migration of oligodendrocytes on astrocyte monolayers. *Mol Cell Neurosci* 15(3), 288-302. doi: 10.1006/mcne.1999.0819.
- Schneider, S., Bosse, F., D'Urso, D., Muller, H., Sereda, M.W., Nave, K., et al. (2001). The AN2 protein is a novel marker for the Schwann cell lineage expressed by immature and nonmyelinating Schwann cells. *J Neurosci* 21(3), 920-933.
- Schnorrer, F., Kalchauer, I., and Dickson, B.J. (2007). The transmembrane protein Kon-tiki couples to Dgrip to mediate myotube targeting in *Drosophila*. *Dev Cell* 12(5), 751-766. doi: 10.1016/j.devcel.2007.02.017.
- Scholz, J., Klein, M.C., Behrens, T.E., and Johansen-Berg, H. (2009). Training induces changes in white-matter architecture. *Nat Neurosci* 12(11), 1370-1371. doi: 10.1038/nn.2412.
- Schrappe, M., Klier, F.G., Spiro, R.C., Waltz, T.A., Reisfeld, R.A., and Gladson, C.L. (1991). Correlation of chondroitin sulfate proteoglycan expression on proliferating brain capillary endothelial cells with the malignant phenotype of astroglial cells. *Cancer Res* 51(18), 4986-4993.
- Schwanhausser, B., Gossen, M., Dittmar, G., and Selbach, M. (2009). Global analysis of cellular protein translation by pulsed SILAC. *Proteomics* 9(1), 205-209. doi: 10.1002/pmic.200800275.
- Sgambato, A., Camerini, A., Pani, G., Cangiano, R., Faraglia, B., Bianchino, G., et al. (2003). Increased expression of cyclin E is associated with an increased resistance to doxorubicin in rat fibroblasts. *Br J Cancer* 88(12), 1956-1962. doi: 10.1038/sj.bjc.6600970.

- Shahbazian, D., Roux, P.P., Mieulet, V., Cohen, M.S., Raught, B., Taunton, J., et al. (2006). The mTOR/PI3K and MAPK pathways converge on eIF4B to control its phosphorylation and activity. *EMBO J* 25(12), 2781-2791. doi: 10.1038/sj.emboj.7601166.
- Sharma, A., Hoeffler, C.A., Takayasu, Y., Miyawaki, T., McBride, S.M., Klann, E., et al. (2010). Dysregulation of mTOR signaling in fragile X syndrome. *J Neurosci* 30(2), 694-702. doi: 10.1523/JNEUROSCI.3696-09.2010.
- Shibata, T., Yamada, K., Watanabe, M., Ikenaka, K., Wada, K., Tanaka, K., et al. (1997). Glutamate transporter GLAST is expressed in the radial glia-astrocyte lineage of developing mouse spinal cord. *J Neurosci* 17(23), 9212-9219.
- Shoshan, Y., Nishiyama, A., Chang, A., Mork, S., Barnett, G.H., Cowell, J.K., et al. (1999). Expression of oligodendrocyte progenitor cell antigens by gliomas: implications for the histogenesis of brain tumors. *Proc Natl Acad Sci U S A* 96(18), 10361-10366.
- Shrager, P., and Novakovic, S.D. (1995). Control of myelination, axonal growth, and synapse formation in spinal cord explants by ion channels and electrical activity. *Brain Res Dev Brain Res* 88(1), 68-78.
- Simon, C., Gotz, M., and Dimou, L. (2011). Progenitors in the adult cerebral cortex: cell cycle properties and regulation by physiological stimuli and injury. *Glia* 59(6), 869-881. doi: 10.1002/glia.21156.
- Soliman, G.A., Acosta-Jaquez, H.A., Dunlop, E.A., Ekim, B., Maj, N.E., Tee, A.R., et al. (2010). mTOR Ser-2481 autophosphorylation monitors mTORC-specific catalytic activity and clarifies rapamycin mechanism of action. *J Biol Chem* 285(11), 7866-7879. doi: 10.1074/jbc.M109.096222.
- Sommer, I., and Schachner, M. (1981). Monoclonal antibodies (O1 to O4) to oligodendrocyte cell surfaces: an immunocytological study in the central nervous system. *Dev Biol* 83(2), 311-327.
- Spassky, N., de Castro, F., Le Bras, B., Heydon, K., Queraud-LeSaux, F., Bloch-Gallego, E., et al. (2002). Directional guidance of oligodendroglial migration by class 3 semaphorins and netrin-1. *J Neurosci* 22(14), 5992-6004. doi: 20026573.
- Stallcup, W.B. (1977a). Nerve and glial-specific antigens on cloned neural cell lines. *Prog Clin Biol Res* 15, 165-178.
- Stallcup, W.B. (1977b). Specificity of adhesion between cloned neural cell lines. *Brain Res* 126(3), 475-486.
- Stallcup, W.B. (2017). NG2 Proteoglycan Enhances Brain Tumor Progression by Promoting Beta-1 Integrin Activation in both Cis and Trans Orientations. *Cancers (Basel)* 9(4). doi: 10.3390/cancers9040031.

- Stallcup, W.B., and Huang, F.J. (2008). A role for the NG2 proteoglycan in glioma progression. *Cell Adh Migr* 2(3), 192-201.
- Stegmuller, J., Schneider, S., Hellwig, A., Garwood, J., and Trotter, J. (2002). AN2, the mouse homologue of NG2, is a surface antigen on glial precursor cells implicated in control of cell migration. *J Neurocytol* 31(6-7), 497-505.
- Stegmuller, J., Werner, H., Nave, K.A., and Trotter, J. (2003). The proteoglycan NG2 is complexed with alpha-amino-3-hydroxy-5-methyl-4-isoxazolepropionic acid (AMPA) receptors by the PDZ glutamate receptor interaction protein (GRIP) in glial progenitor cells. Implications for glial-neuronal signaling. *J Biol Chem* 278(6), 3590-3598. doi: 10.1074/jbc.M210010200.
- Stellwagen, D., and Malenka, R.C. (2006). Synaptic scaling mediated by glial TNF-alpha. *Nature* 440(7087), 1054-1059. doi: 10.1038/nature04671.
- Stevens, B., Allen, N.J., Vazquez, L.E., Howell, G.R., Christopherson, K.S., Nouri, N., et al. (2007). The classical complement cascade mediates CNS synapse elimination. *Cell* 131(6), 1164-1178. doi: 10.1016/j.cell.2007.10.036.
- Stevens, B., and Fields, R.D. (2000). Response of Schwann cells to action potentials in development. *Science* 287(5461), 2267-2271.
- Stevens, B., Tanner, S., and Fields, R.D. (1998). Control of myelination by specific patterns of neural impulses. *J Neurosci* 18(22), 9303-9311.
- Stolt, C.C., Lommes, P., Friedrich, R.P., and Wegner, M. (2004). Transcription factors Sox8 and Sox10 perform non-equivalent roles during oligodendrocyte development despite functional redundancy. *Development* 131(10), 2349-2358. doi: 10.1242/dev.01114.
- Stumpf, C.R., Moreno, M.V., Olshen, A.B., Taylor, B.S., and Ruggero, D. (2013). The translational landscape of the mammalian cell cycle. *Mol Cell* 52(4), 574-582. doi: 10.1016/j.molcel.2013.09.018.
- Stupp, R., Mason, W.P., van den Bent, M.J., Weller, M., Fisher, B., Taphoorn, M.J., et al. (2005). Radiotherapy plus concomitant and adjuvant temozolomide for glioblastoma. *N Engl J Med* 352(10), 987-996. doi: 10.1056/NEJMoa043330.
- Sugiarto, S., Persson, A.I., Munoz, E.G., Waldhuber, M., Lamagna, C., Andor, N., et al. (2011). Asymmetry-defective oligodendrocyte progenitors are glioma precursors. *Cancer Cell* 20(3), 328-340. doi: 10.1016/j.ccr.2011.08.011.
- Sutton, M.A., and Schuman, E.M. (2006). Dendritic protein synthesis, synaptic plasticity, and memory. *Cell* 127(1), 49-58. doi: 10.1016/j.cell.2006.09.014.
- Takei, N., and Nawa, H. (2014). mTOR signaling and its roles in normal and abnormal brain development. *Front Mol Neurosci* 7, 28. doi: 10.3389/fnmol.2014.00028.

- Tanaka, J., Horiike, Y., Matsuzaki, M., Miyazaki, T., Ellis-Davies, G.C., and Kasai, H. (2008). Protein synthesis and neurotrophin-dependent structural plasticity of single dendritic spines. *Science* 319(5870), 1683-1687. doi: 10.1126/science.1152864.
- Tillet, E., Ruggiero, F., Nishiyama, A., and Stallcup, W.B. (1997). The membrane-spanning proteoglycan NG2 binds to collagens V and VI through the central nonglobular domain of its core protein. *J Biol Chem* 272(16), 10769-10776.
- Tremblay, M.E., Lowery, R.L., and Majewska, A.K. (2010). Microglial interactions with synapses are modulated by visual experience. *PLoS Biol* 8(11), e1000527. doi: 10.1371/journal.pbio.1000527.
- Trinidad, J.C., Thalhammer, A., Burlingame, A.L., and Schoepfer, R. (2013). Activity-dependent protein dynamics define interconnected cores of co-regulated postsynaptic proteins. *Mol Cell Proteomics* 12(1), 29-41. doi: 10.1074/mcp.M112.019976.
- Tsai, H.H., Niu, J., Munji, R., Davalos, D., Chang, J., Zhang, H., et al. (2016). Oligodendrocyte precursors migrate along vasculature in the developing nervous system. *Science* 351(6271), 379-384. doi: 10.1126/science.aad3839.
- Ullian, E.M., Sapperstein, S.K., Christopherson, K.S., and Barres, B.A. (2001). Control of synapse number by glia. *Science* 291(5504), 657-661. doi: 10.1126/science.291.5504.657.
- Wake, H., Lee, P.R., and Fields, R.D. (2011). Control of local protein synthesis and initial events in myelination by action potentials. *Science* 333(6049), 1647-1651. doi: 10.1126/science.1206998.
- Wang, J., Svendsen, A., Kmiecik, J., Immervoll, H., Skaftnesmo, K.O., Planaguma, J., et al. (2011). Targeting the NG2/CSPG4 proteoglycan retards tumour growth and angiogenesis in preclinical models of GBM and melanoma. *PLoS One* 6(7), e23062. doi: 10.1371/journal.pone.0023062.
- Wang, Q., Rowan, M.J., and Anwyl, R. (2004). Beta-amyloid-mediated inhibition of NMDA receptor-dependent long-term potentiation induction involves activation of microglia and stimulation of inducible nitric oxide synthase and superoxide. *J Neurosci* 24(27), 6049-6056. doi: 10.1523/JNEUROSCI.0233-04.2004.
- Wang, R., Kamgoue, A., Normand, C., Leger-Silvestre, I., Mangeat, T., and Gadal, O. (2016). High resolution microscopy reveals the nuclear shape of budding yeast during cell cycle and in various biological states. *J Cell Sci* 129(24), 4480-4495. doi: 10.1242/jcs.188250.
- Wang, X., Li, W., Williams, M., Terada, N., Alessi, D.R., and Proud, C.G. (2001). Regulation of elongation factor 2 kinase by p90(RSK1) and p70 S6 kinase. *EMBO J* 20(16), 4370-4379. doi: 10.1093/emboj/20.16.4370.

- Wang, X., Osada, T., Wang, Y., Yu, L., Sakakura, K., Katayama, A., et al. (2010a). CSPG4 protein as a new target for the antibody-based immunotherapy of triple-negative breast cancer. *J Natl Cancer Inst* 102(19), 1496-1512. doi: 10.1093/jnci/djq343.
- Wang, X., Wang, Y., Yu, L., Sakakura, K., Visus, C., Schwab, J.H., et al. (2010b). CSPG4 in cancer: multiple roles. *Curr Mol Med* 10(4), 419-429.
- Wang, Y., and Schachner, M. (2015). The intracellular domain of L1CAM binds to casein kinase 2alpha and is neuroprotective via inhibition of the tumor suppressors PTEN and p53. *J Neurochem* 133(6), 828-843. doi: 10.1111/jnc.13083.
- Weiler, I.J., Spangler, C.C., Klintsova, A.Y., Grossman, A.W., Kim, S.H., Bertaina-Anglade, V., et al. (2004). Fragile X mental retardation protein is necessary for neurotransmitter-activated protein translation at synapses. *Proc Natl Acad Sci U S A* 101(50), 17504-17509. doi: 10.1073/pnas.0407533101.
- Weiss, E.M., Gschaidbauer, B., Kaufmann, L., Fink, A., Schuler, G., Mittenecker, E., et al. (2017). Age-related differences in inhibitory control and memory updating in boys with Asperger syndrome. *Eur Arch Psychiatry Clin Neurosci* 267(7), 651-659. doi: 10.1007/s00406-016-0756-8.
- Wolpowitz, D., Mason, T.B., Dietrich, P., Mendelsohn, M., Talmage, D.A., and Role, L.W. (2000). Cysteine-rich domain isoforms of the neuregulin-1 gene are required for maintenance of peripheral synapses. *Neuron* 25(1), 79-91.
- Woodruff, R.H., Tekki-Kessarlis, N., Stiles, C.D., Rowitch, D.H., and Richardson, W.D. (2001). Oligodendrocyte development in the spinal cord and telencephalon: common themes and new perspectives. *Int J Dev Neurosci* 19(4), 379-385.
- Wu, H., Xu, J., Pang, Z.P., Ge, W., Kim, K.J., Bianchi, B., et al. (2007). Integrative genomic and functional analyses reveal neuronal subtype differentiation bias in human embryonic stem cell lines. *Proc Natl Acad Sci U S A* 104(34), 13821-13826. doi: 10.1073/pnas.0706199104.
- Wyss-Coray, T., and Rogers, J. (2012). Inflammation in Alzheimer disease—a brief review of the basic science and clinical literature. *Cold Spring Harb Perspect Med* 2(1), a006346. doi: 10.1101/cshperspect.a006346.
- Xue, J.Z., Woo, E.M., Postow, L., Chait, B.T., and Funabiki, H. (2013). Chromatin-bound *Xenopus* Dppa2 shapes the nucleus by locally inhibiting microtubule assembly. *Dev Cell* 27(1), 47-59. doi: 10.1016/j.devcel.2013.08.002.
- Yang, Q.K., Xiong, J.X., and Yao, Z.X. (2013). Neuron-NG2 cell synapses: novel functions for regulating NG2 cell proliferation and differentiation. *Biomed Res Int* 2013, 402843. doi: 10.1155/2013/402843.

- Yang, Y., Wang, X.B., Frerking, M., and Zhou, Q. (2008). Spine expansion and stabilization associated with long-term potentiation. *J Neurosci* 28(22), 5740-5751. doi: 10.1523/JNEUROSCI.3998-07.2008.
- Zalfa, F., Giorgi, M., Primerano, B., Moro, A., Di Penta, A., Reis, S., et al. (2003). The fragile X syndrome protein FMRP associates with BC1 RNA and regulates the translation of specific mRNAs at synapses. *Cell* 112(3), 317-327.
- Zamostiano, R., Pinhasov, A., Gelber, E., Steingart, R.A., Seroussi, E., Giladi, E., et al. (2001). Cloning and characterization of the human activity-dependent neuroprotective protein. *J Biol Chem* 276(1), 708-714. doi: 10.1074/jbc.M007416200.
- Zhang, H., Vutskits, L., Calaora, V., Durbec, P., and Kiss, J.Z. (2004). A role for the polysialic acid-neural cell adhesion molecule in PDGF-induced chemotaxis of oligodendrocyte precursor cells. *J Cell Sci* 117(Pt 1), 93-103. doi: 10.1242/jcs.00827.
- Zhang, Y.V., Ormerod, K.G., and Littleton, J.T. (2017). Astrocyte Ca(2+) Influx Negatively Regulates Neuronal Activity. *eNeuro* 4(2). doi: 10.1523/ENEURO.0340-16.2017.
- Zhou, Q., and Anderson, D.J. (2002). The bHLH transcription factors OLIG2 and OLIG1 couple neuronal and glial subtype specification. *Cell* 109(1), 61-73.
- Zhou, Z.D., Kumari, U., Xiao, Z.C., and Tan, E.K. (2010). Notch as a molecular switch in neural stem cells. *IUBMB Life* 62(8), 618-623. doi: 10.1002/iub.362.
- Zhu, X., Bergles, D.E., and Nishiyama, A. (2008a). NG2 cells generate both oligodendrocytes and gray matter astrocytes. *Development* 135(1), 145-157. doi: 10.1242/dev.004895.
- Zhu, X., Hill, R.A., and Nishiyama, A. (2008b). NG2 cells generate oligodendrocytes and gray matter astrocytes in the spinal cord. *Neuron Glia Biol* 4(1), 19-26. doi: 10.1017/S1740925X09000015.
- Zou, Y., Jiang, W., Wang, J., Li, Z., Zhang, J., Bu, J., et al. (2014). Oligodendrocyte precursor cell-intrinsic effect of Rheb1 controls differentiation and mediates mTORC1-dependent myelination in brain. *J Neurosci* 34(47), 15764-15778. doi: 10.1523/JNEUROSCI.2267-14.2014.

Acknowledgment

The enthusiasm to contribute to the field of research, however insignificant it might be, was growing inside me when I was studying Molecular Genetics in my master's degree in University of Calcutta, India. Coming to Germany with an exciting research project to work on, would have been a distant dream unless my supervisor provided the opportunity to take part in the International Ph.D. Program in Mainz. I am immensely grateful to her for the support, supervision and the encouraging (not restricted to research only) thoughts that helped me develop both as a young researcher and a better individual throughout my PhD journey.

My sincerest gratitude goes to the postdoc, who, in the initial days, literally taught the wide-eyed naïve learner not only the research techniques but also helped in building a critical and logical mind that were the prerequisites for a successful PhD. Starting from guidance on experimental procedures to writing a manuscript together and finally proofreading this thesis, I could not thank him enough for his continuous and motivated support, even from 300 km away.

I would like to thank my second supervisor, who always raised constructive and critical questions during lab seminars and TAC meetings that eventually shaped the thesis better. I could not think of a single moment of hesitation from her whenever I asked for her help.

I would like to thank all my colleagues for their support in this journey.

Curriculum Vitae

Tanmoyita Nayak

Auf Der Borg 2B, 59494, Soest, Germany.

Contact: +4917672995849

tanmoyitan@gmail.com

Date of Birth: 17.10.1990

Nationality: Indian

Research experiences:

Research scholar (PhD) at Institute of Molecular Biology (IMB), Mainz in affiliation with Johannes-Gutenberg Universität, Mainz. (2014-current)

- Successfully completed project entitled '*NG2; a translation regulator in OPCs by transducing FMRP-Akt-mTOR signaling pathway*'.
- Responsible for design and development of analytical biochemical methods, primary cell isolation by MACS, FACS and cell sorting, protein analytical method coupled with Mass-Spectrometry and High-resolution microscopy.
- Presented data in international platforms and submitted manuscript as a single first author.
- Credited Certification in Basic project management by IPMA.

Research assistant in National Brain Research Centre, India. (07/2013-05/2014)

- Contributed in a project '*Imprinting of UbE3a gene in Angelman Syndrome using Drosophila as model.*' and developed a novel role for an enzyme in Angelman syndrome, a cognitive learning disorder.

Internship at Indian Institute of Chemical Biology (05/2012- 09/2012)

- Contributed in project '*SNP and their significance in speech disorder*'
- Interaction with patients and documentation of survey reports, sample collection and experiments.

Education:

- **PhD in Molecular biology**, 2014-18, Johannes-Gutenberg-Universität, Mainz, Germany.
- **M.Sc. in Biotechnology** (specializing in Genetics), 2013-2011, University of Calcutta.
Ranked 1st class 2nd position.
- **B.Sc. in Physiology**, 2008-2011, University of Calcutta, 1st Class

Publications:

- Nayak T, Trotter J, Sakry D. The intracellular domain of NG2 protein modulates translation and cell-cycle kinetics via effects on mTOR/FMRP signaling. *Frontiers in Cellular Neuroscience*. 2018.
- Chakraborty M, Paul BK, Nayak T, Das A, Bhutani S, Jana NR. The E3 ligase ube3a is required for learning in *Drosophila melanogaster*. *Biochem Biophys Research Commun*. 2015.

Workshops and training:

- Participated in practical course on proteomics sample preparation and measurement on LC-MS/MS system.
- Completed training on RNA quality control and NGS library preparation by core facility at IMB, Mainz.
- Participated in Leica organized workshop on Light and Confocal microscopy.
- Attended practical training on Flow cytometry analysis by core facility at IMB, Mainz.

Hobbies, Interest and personal achievements:

- Awarded Full time PhD Scholarship funded by Boehringer-Ingelheim Foundation.
- Completion and certified by GPM for basic Project management course.
- Received 2nd place in poster presentation at Euroglia meeting.
- Ranked among top ten students in bachelor's degree in University of Calcutta.
- Hobbies: Travelling, music and reading.

Eidesstattliche Erklärung

Hiermit erkläre ich, Tanmoyita Nayak, geboren am 17.10.1990 in India, dass ich meine Dissertation selbständig und nur unter Verwendung der angegebenen Hilfsmittel angefertigt habe. Ich habe keinen anderen Promotionsversuch unternommen.

Tanmoyita Nayak

Mainz, 30.10.2018